Simulation of an OFDM System for a Wireless Battery Management System

Master's thesis

by

Fernando Gaitán Gutiérrez,

at

Institute of Industrial Information Technology

Time period:	15/04/2014 – 15/10/2014
Supervisor:	Prof. Dr.-Ing. habil. Klaus Dostert
Advisor:	Dipl.-Ing. Damián Alonso

Declaration

I hereby declare that I wrote my Master's thesis on my own and that I have followed the regulations relating to good scientific practice of the Karlsruhe Institute of Technology (KIT) in its latest form. I did not use any unacknowledged sources or means and I marked all references I used literally or by content.

Karlsruhe, 15 October 2014

Dedicated to my family

who always have helped me unconditionally
and without their support it could not have been possible

Abstract

With the aim of innovating a new physical layer that can be used as an alternative to the standard of the Battery Management System (BMS, CAN-Bus), wireless approach proposes a new BMS communication system to transmit information between the Battery Control Unit (BCU) and the Cell Sensor Units (CSU). Multi-carrier modulation techniques are appropriated when the transmission occurs over frequency selective channels such as the channel within the battery pack, one of these techniques is Orthogonal Frequency Division Multiplexing (OFDM).

OFDM can provide large data rate in environments with several channel conditions, like narrowband interference or multipath fading. Countless number of applications are studied to improve OFDM system and adapt it as a solution. The Institute of Industrial and Information Technology (IIIT) in Karlsruhe Institute of Technology (KIT) helps to give a new purpose to a project called IntLIon. The IntLion project aims at controlling and monitoring each cell found in a battery pack individually, without extra cabling and with a higher bandwidth than the current systems typically based on CAN-Bus standard.

The work of the group involves the investigation of wireless channels inside the battery and their viability as a new BMS alternative.

The purpose of this thesis is to provide a simulation of an OFDM system, employing the vector network analyzer (VNA) to measure the transfer function between antennas inside the battery prototype which will be used as a communication channel. The performance of the OFDM system is evaluated by varying parameter such as modulation, constellation, cyclic prefix, etc. Applying frequency diversity technique in conjunction with a channel coding, the system acquires more robustness against the distorting effects.

Zusammenfassung

Mit dem Ziel eine neue physikalische Schicht zu entwickeln, die als Alternative zu dem Battery Management System (BMS, CAN-BUS) angesehen werden kann, bietet der hier simulierte ”kabellose Ansatz” ein neues BMS-Kommunikationssystem an, um Informationen von der Batterie-Kontrolleinheit (Battery Control Unit, BCU) zu den Zell-Sensor-Einheiten (Cell Sensor Units, CSU) zu übertragen. Findet dabei die Übertragung über frequenzselektive Kanäle statt, wie innerhalb einer Batterie, werden Multi-Carrier Modulation-Techniken eingesetzt. Eine dieser Techniken ist der orthogonale Frequenzmultiplex (Orthogonal Frequency Division Multiplexing , OFDM).

OFDM bietet einen hohen Datendurchsatz in Umgebungen mit unterschiedlichen Kanalbedingungen, wie bei Schmalbandstörern oder der Mehrweg-Interferenz, an. Hierbei wird intensiv Forschung an der Optimierung des OFDM-Systems betrieben. Das Institut für Industrielle Informationstechnik (IIIT) am Karlsruher Institut für Technologie (KIT) schlägt hierzu einen neuen Ansatz innerhalb des IntLIon-Projektes vor.Das Ziel dieses Projektes ist die individuelle Kontrolle und Überwachung jeder einzelnen Batteriezelle ohne zusätzliche Kabelverbindungen und mit einer höheren Bandbreite als es aktuelle Systeme mit dem Standard CAN-Bus erreichen.

Die Arbeit dieser Gruppe umfasst insbesondere die Untersuchung der kabellosen Kanäle innerhalb der Batterie und die Realisierbarkeit des Ansatzes als BMS-Alternative. Die vorliegende Thesis schlägt hierzu eine Emulation eines OFDM-Systems vor, bei dem ein vektorieller Netzwerkanalysator verwendet wird um die Übertragungsfunktion zwischen den einzelnen Antennen innerhalb der Batterie zu untersuchen. Die OFDM-Parameter werden dabei dem Kanalverhalten und verschiedenen Parametern wie der Modulation, Konstellation, dem Cyclic Prefix und anderen angepasst. Durch die Anwendung von Frequenzdiversitäts-Techniken in Verbindung mit Kanalkodierung wird insgesamt ein robusteres Ergebnis gegen Störeffekte erzielt.

Contents

List of Figures

List of Tables

Chapter 1

Introduction

The battery Management system (BMS) aims to transmit information related with the state-of-charge (SoC), state-of-health (SoH), the charge balance and the detection of failures of the individual cells within the lithium-ion batteries employed in electric and hybrid cars. The network communications is established between the Battery Control Unit (BCU) and the Cell Service Units (CSU). A wireless approach consists of installing an antenna in each CSU as well as in the BCU to establish a communication. In battery pack a set of lithium-ion cells are connected in series and grouped in modules, as shown in figure 1.1.

Since the communication is performed in the battery pack interior, wireless transmission deals with a complicated medium. Owing to the battery packs confined to a housing made of metal, there are many reflected waveforms causing a multipath propagation. This produces several resonant and notch frequencies, which results in a very strongly frequency-selective fading channel. It follows that the transfer function presents a high number of notches in the spectrum. The channel behavior depends not only on the dimensions of the battery form but also on the position of the antenna inside the battery pack [8]. Frequency-selective fading channel could be a big drawback for narrow band communication system with a fixed frequency carrier. Since it could happen that the selected transmission bandwidth is affected by notch and therefore the transmission would be highly attenuated.

The motivation is designing a model that can establish a communication between a pair of nodes, characterized by two pairs of equal PIF antennas. PIF antenna presents transfer functions above -20 dB in some portions of the evaluated frequency range (1.5 GHz-6.5 GHz). Making of these portions a potential frequency transmission bandwidth with the aim of arranging a better data rate than the standard CAN-Bus [8].

The purpose of my thesis is to develop a multi-carrier modulation that can carry out the communication in such media as the above explained. Orthogonal Frequency Division Multiplexing (OFDM) in conjunction with channel coding and frequency diversity technique are proposed as model to perform the communication network between BCU and CSU.

OFDM is a technique that allows a major spectral efficiency of the radio frequency channel. In this scheme, a large number of narrowband orthogonal sub-carriers overlapped are transmitted in parallel. Efficient use of the radio spectrum includes modulated sub-carriers as close as possible without causing Inter-Carrier Interference (ICI), theoretically the sub-carrier bandwidth would be adjacent to its neighbors avoiding wastage of spectrum, but in practice, a guard band must be placed between each sub-carrier. Thus, the adjacent sub-carrier signal can be attenuated but some portions of the used bandwidth are lost. In addition, OFDM gives a solution when the

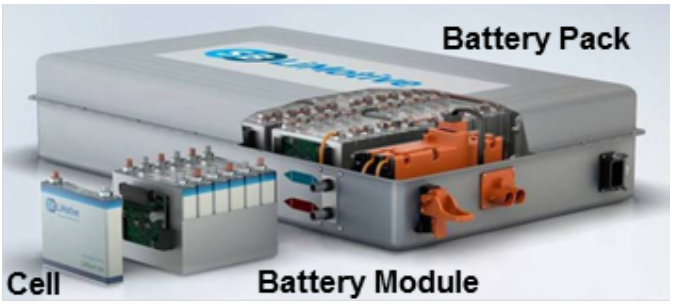

Figure 1.1: Representation of a battery pack (source: SB Limotive)

information is transmitted through fading channels. The Inter-Symbol Interference (ISI) caused by frequency selective channels can be controlled. Moreover, using narrowband sub-channels is obtained a very low symbol rate, which makes the symbol period larger than the channel impulse response, effecting that the delayed version of the previous symbol does not arrive during the processing period of the actual symbol. Applying codification to give robustness to error transmission that are produced by the frequency selective fading channels and inserting a special guard (cyclic prefix) can avoid the loss of orthogonality between the OFDM symbol.

There are two main drawbacks with OFDM, its sensitivity to frequency errors and the large dynamic range of the signal (also referred as peak-to average ratio [PAR]).

The purpose of the following sections are to provide information concerning OFDM.

- Theoretical background
- Analysis of the parameters selection
- Implementation of a model in Matlab/Simulink

Chapter 2

Basic principles of OFDM

2.1 Fundamentals

The sequence to transmit is a complex symbol $\alpha[n] = \alpha_{Re}[n]+\mathrm{j}\alpha_{Im}[n]$ taken from some conventional modulation scheme (such as quadrature amplitude modulation or phase-shift-keying). The sequence is split/sub-divided in N symbols and each one is transmitted in a frame at different sub-carriers frequencies [12].

The principal target of this processing before the transmission consists combating the effect that is produced by the frequency selective channels ($H_c(f)$ not ideal). On condition that the impulse response is not longer that the symbol period, thus it can be expected to be an ISI-free channel (typically 10 times as big τ_{RMS} would be good).

The figure 2.1 depicts the effect that produces the channel frequency response over a QAM and OFDM signal. Both of them with the same rate bit (R_b).

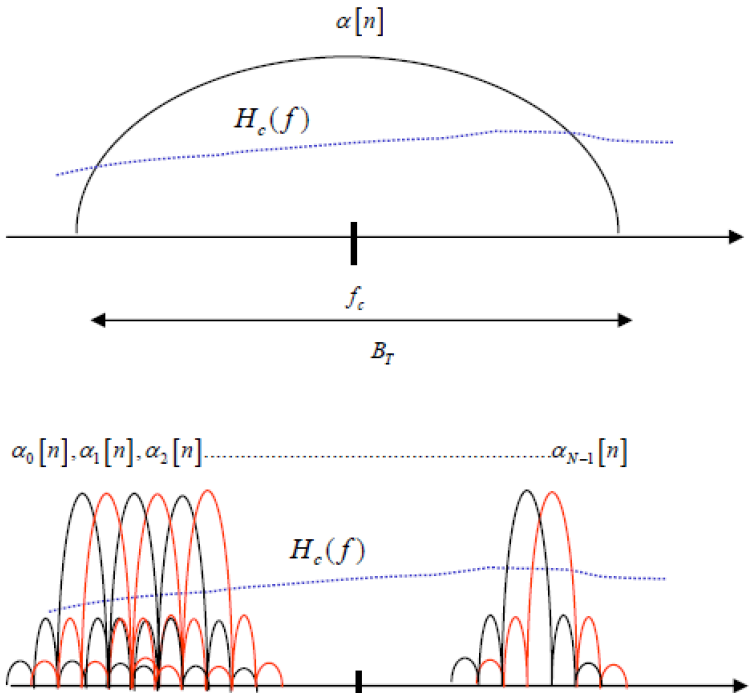

Figure 2.1: Spectrum QAM and OFDM with same (R_b) [12]

Given that each N symbols QAM/QPSK/BPSK..etc makes an OFDM symbol, the rate of an

OFDM symbol is N times lower than the QAM symbol. The relationship is expressed by

$$R_{OFDM} = \frac{R_{sc}}{N} = \Delta f = f_b \tag{2.1}$$

$$T_{OFDM} = T = T_{sc}N \tag{2.2}$$

Where R_{sc} is the symbol rate at the sub-carrier.

2.1.1 Baseband Equivalent

In the section (2.1), the OFDM symbol was described as a complex number. For this reason it is better to work directly with the baseband equivalent of the signal. The equivalent baseband of a temporal signal consists in N temporal functions, which come to N orthogonal frequencies [12].

$$\begin{aligned} b_s(t) &= i_s(t) + jq_s(t) \\ &= \sum_{n=-\infty}^{\infty} b_{s_m[n]}(t - nT) \\ &= \sum_{n=-\infty}^{\infty} \sum_{k=1}^{N} \alpha_k[n]\phi_k[n](t - nT) \\ &= \sum_{n=-\infty}^{\infty} \sum_{k=1}^{N} \alpha_k[n] e^{j(2\pi f_k(t-nT))} \frac{1}{\sqrt{T}} \Pi\left(\frac{t - \frac{T}{2} - nT}{T}\right) \end{aligned} \tag{2.3}$$

Where,

$$f_k = \left(k - 1 - \frac{N}{2}\right)\Delta f; \quad k = 1.....N \tag{2.4}$$

$$\alpha_k[n] = \alpha_{Re,k}[n] + \mathrm{j}\,\alpha_{Im,k}[n] \tag{2.5}$$

The baseband functions that generate an orthogonal space baseband of the transmitted signal are giving by [12]:

$$\phi_k(t) = \frac{1}{\sqrt{T}} e^{j(2\pi f_k(t-nT))} \Pi\left(\frac{t - \frac{T}{2} - nT}{T}\right) \text{ with } \frac{B_t}{N} = f_b = \frac{1}{T} \tag{2.6}$$

Since the sub-carriers are modulated by orthogonal waveforms, the sub-carriers can have overlapped spectrum, thus achieving higher spectrum efficiency.

These baseband functions are orthogonal each other, it means that the dot product over a fundamental period is equal to zero.

Continuous time:

$$\begin{aligned}\langle \phi_k(t), \phi_l(t) \rangle &= \int_{-\infty}^{\infty} \phi_k(t)^* \phi_l(t) dt = R_{\phi_l \phi_k}(0) \\ &= \int_0^T e^{j2\pi(f_k - f_l)t} dt = \delta[k-l]\end{aligned} \tag{2.7}$$

Discrete time:

$$\begin{aligned}\langle \phi_k[m], \phi_l[m] \rangle &= \sum_{-\infty}^{\infty} \phi_k[m]^* \phi_l[m] = R_{\phi_l \phi_k}(0) \\ &= \sum_{m=0}^{N} e^{j2\pi(f_k - f_l)m} = \delta[k-l]\end{aligned} \tag{2.8}$$

Where,

$$\delta[k-l] = \begin{cases} 1, & \text{if } k = l, \\ 0, & \text{if } k \neq l. \end{cases} \text{ is the Kronecker delta function.} \tag{2.9}$$

Due to relationship in (2.4), $f_k - f_l$ is integer multiple of $f_b = \frac{1}{T}$.

Furthermore, although the spectrum is overlapping, it does not cause interference at carrier locations due to orthogonal nature of the sub-carries.

2.1.2 Transmitted Signal

The pass-band transmission signal is obtained by its baseband equivalent signal as [12]:

$$\begin{aligned}s(t) &= \mathrm{Re}\left\{ A_c b_s(t) e^{j2\pi f_c t} \right\} \\ &= \mathrm{Re}\left\{ A_c \sum_{k=-\infty}^{\infty} \sum_{k=1}^{N} \alpha_k[n] \phi_k(t - nT) e^{j(2\pi f_c)t} \right\} \\ &= \mathrm{Re}\left\{ A_c \sum_{k=-\infty}^{\infty} \sum_{k=1}^{N} \alpha_k[n] p_k(t - nT) e^{j(2\pi (f_c + f_k)t} \right\}\end{aligned} \tag{2.10}$$

Finally, using the Euler's formula the time domain representation of the transmission signal takes the following expression:

$$s(t) = A_c \sum_{k=-\infty}^{\infty} \sum_{k=1}^{N} \alpha_{Re,k}[n] \cos(2\pi(f_c + f_k)) p(t - nT) - \alpha_{Im,k}[n] \sin(2\pi(f_c + f_k)) p(t - nT)$$

$$p(t) = \frac{1}{\sqrt{T}} \Pi \left(\frac{t - \frac{T}{2} - nT}{T} \right)$$

Hence, the appropriate basis real-valued functions for the signal space of (2.10), with dimension $L = 2N$. It is given by [12]:

$$\begin{aligned}\phi_{Re,k}(t) &= \sqrt{\frac{2}{T}}\cos(2\pi(f_c + f_k))\Pi\left(\frac{t - \frac{T}{2} - nT}{T}\right)\\ \phi_{Im,k}(t) &= -\sqrt{\frac{2}{T}}\sin(2\pi(f_c + f_k))\Pi\left(\frac{t - \frac{T}{2} - nT}{T}\right)\\ k &= 1, 2....., N\end{aligned} \tag{2.11}$$

Using these orthogonal basis (2.11), the referenced coordinates of the signal with respect to the function $\phi_{Re,k}$ is $\frac{A_c}{\sqrt{2}}\alpha_{Re,k}$ and respect to $\phi_{Im,k}$ is $\frac{A_c}{\sqrt{2}}\alpha_{Im,k}$.

The inphase and quadrature components of the pass-band signal with respect to the carrier frequency f_c are giving by [12]:

$$\begin{aligned}i_s(t) &= \sum_{n=-\infty}^{\infty}\sum_{k=1}^{N}\alpha_{Re,k}[n]\cos(2\pi f_c)p(t - nT) - \alpha_{Im,k}[n]\sin(2\pi f_c)p(t - nT)\\ q_s(t) &= \sum_{n=-\infty}^{\infty}\sum_{k=1}^{N}\alpha_{Re,k}[n]\sin(2\pi f_c)p(t - nT) - \alpha_{Im,k}[n]\cos(2\pi f_c)p(t - nT)\end{aligned}$$

The figure 2.2 shows, the inphase component as a sum of the different orthogonal cos functions, each one transports the real part of a complex symbol.

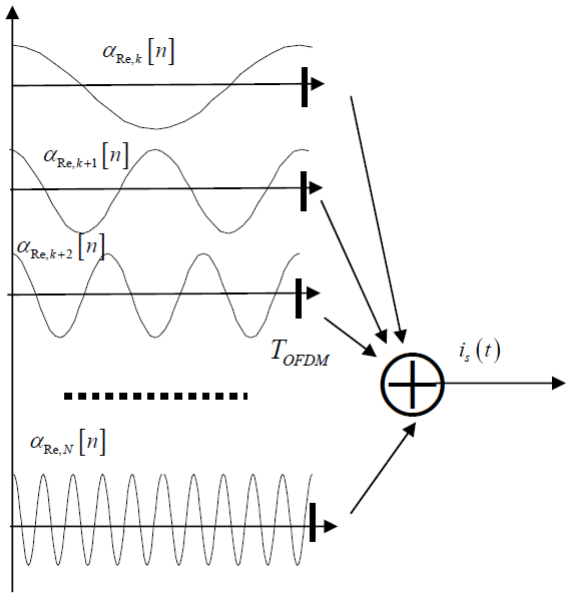

Figure 2.2: OFDM inphase component [12]

2.2 OFDM Modulator

If it is assumed that there are a set of complex symbols (2.5) at the output mapping block (see figure 2.3), which can be represented as a vector $\boldsymbol{\alpha}$. This vector collects a set of N complex symbol in different sub-carriers, where $k = \{0, 1, \ldots..N-1\}$ represents sub-carrier index, ignoring the temporal dependence *n*, it is obtained:

$$\boldsymbol{\alpha} = [\alpha_0 \;\; \alpha_1 \;\; \alpha_2 \;\; \cdots\cdots\cdots \;\; \alpha_{N-1}]^{\mathrm{T}} \tag{2.12}$$

The symbols $\alpha_k[n]$ are generated at rate $f_s = \frac{1}{T_{sc}}$, and modulate separately the N orthogonal sub-carriers (2.4) during the whole *n*-th time interval $I_n = [nT, nT + T]$ defined for one OFDM symbol with period $T_{OFDM} = T = NT_{sc} = \frac{N}{f_s}$ at the *k*-th sub-carrier frequency. In other words, the QAM symbol modulates the *k*-th sub-carrier during the whole *n*-th OFDM symbol interval. As a definition of stationarity for OFDM signals, $\alpha_k[n]$ are normally assumed to be mutually independent and identically distributed symbols from some kind of alphabet, e.g., from M-QAM, $M = \left[(2m-1-\sqrt{M}) + j(2n-1-\sqrt{M})\right]; (m,n) = \left\{1, 2, ...\sqrt{M}\right\}$. According to this, we will constrain our analysis (without loss of generality) to the first OFDM symbol, transmitted in the interval I_0. Then from (2.3) the corresponding OFDM symbol at the sampling rate f_s consists of the set of T_{sc}-spaced baseband signal samples.

$$\mathbf{b_s} = [b_s[0] \;\; b_s[1] \;\; b_s[2] \cdots\cdots\cdots \;\; b_s[N-1]]^{\mathrm{T}} \tag{2.13}$$

elements $b_s(t) = b_s(nT_{sc}) = b_s[n],$ with $n = \{0, 1, \ldots.N-1\}$ obtained by talking the IDFT of the first incoming data frame $\boldsymbol{\alpha}$ (elements $\alpha_k[0] = \alpha_k$), with $k = \{0, 1...., N-1\}$. The *n*-th element in the discrete-time baseband signal vector $\mathbf{b_s}$ is then given by

$$b_s[n] = b_s(nT_{sc}) = \frac{1}{\sqrt{N}} \sum_{k=0}^{N-1} \alpha[k] e^{j(\frac{2\pi}{N}nk)} W\left[\frac{n}{(N-1)}\right] \tag{2.14}$$

where $W[\cdot]$ is a discrete rectangular window that is defined by

$$W[r] = \begin{cases} 1; & 0 \leq r \leq 1 = 0 \\ 0; & \text{otherwise} \end{cases} \tag{2.15}$$

Moreover, it can be operated upon the same sequences within other interval I_n different to 0. Then, for one step generation of $\mathbf{b_s}$, the calculation of (2.12) for $(n,k) = \{0, ..., N-1\}$, can be equivalently defined as the following matrix operation:

$$\mathbf{b_s} = \mathbf{F}^H \boldsymbol{\alpha} \tag{2.16}$$

where $\mathbf{F}$ is the DFT matrix whose hermitian is associated to the inverse operation IDFT, then the DFT matrix is given by

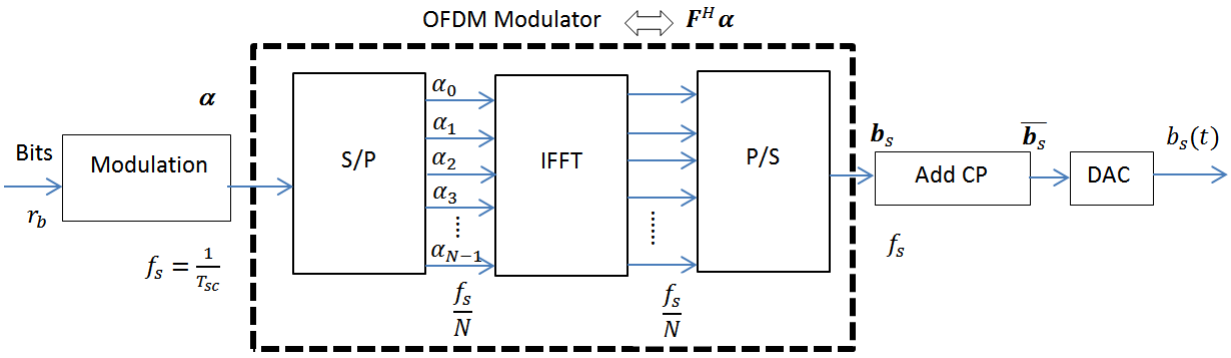

Figure 2.3: OFDM Baseband Modulator

$$\mathbf{F}_{(\mathbf{NxN})} = \frac{1}{\sqrt{N}} \begin{bmatrix} 1 & 1 & 1 & 1 & \cdots & 1 \\ 1 & e^{j\frac{2\pi}{N}} & e^{j\frac{4\pi}{N}} & e^{j\frac{6\pi}{N}} & \cdots & e^{j2\pi\frac{N-1}{N}} \\ 1 & e^{j\frac{4\pi}{N}} & e^{j\frac{8\pi}{N}} & e^{j\frac{12\pi}{N}} & \cdots & e^{j4\pi\frac{N-1}{N}} \\ 1 & e^{j\frac{6\pi}{N}} & e^{j\frac{12\pi}{N}} & e^{j\frac{18\pi}{N}} & \cdots & e^{j6\pi\frac{N-1}{N}} \\ \vdots & \vdots & \vdots & \vdots & \ddots & \vdots \\ 1 & e^{j2\pi\frac{N-1}{N}} & e^{j4\pi\frac{N-1}{N}} & e^{j6\pi\frac{N-1}{N}} & \cdots & e^{j2\pi\frac{(N-1)^2}{N}} \end{bmatrix} \tag{2.17}$$

Where it can be easily observed that it is a symmetric matrix and its inverse matrix is itself applying the hermetic operator.

$$\mathbf{F}^H\mathbf{F} = \mathbf{F}^{-1}\mathbf{F} = \mathbf{I}_{(N)} \tag{2.18}$$

Note that every column in (2.17) corresponds to a complex sub-carrier with a normalized frequency that depends on the size of the DFT. It recommends that DFT size must be power of 2 in order to perform the IFFT and FFT.

In the figure 2.3, the basic OFDM modulator is represented, where the input is a code binary data and the output the analog baseband signal (2.14), then this signal will be drive to the RF block, which modulates the baseband to the carrier frequency of interest.

2.3 OFDM Demodulator

In this section, it is shown how the OFDM demodulator works to recover the transmitted signal. It is assumed that the received signal is completely synchronized and it is sent through ideal channel with impulse response $h_c(t) = \delta(t)$. Hence, its baseband equivalent is $b_{h_c(t)} = 2\delta(t)$, obtaining the received baseband signal $b_r(t)$ as

$$b_r(t) = A_c b_s(t) * \frac{1}{2} b_{h_c}(t) + b_n(t) = b_s(t) + b_n(t) \tag{2.19}$$

where the signal $b_n(t) = i_n(t) + jq_n(t)$ is the equivalent baseband of the pass-band noise $n(t)$, whose power spectral density is [28]

$$S_n(f) = \frac{N_o}{2}\left(\Pi\left(\frac{f - f_c}{B_t}\right) + \Pi\left(\frac{f + f_c}{B_t}\right)\right) \tag{2.20}$$

and equivalently its baseband power spectral density.

$$\begin{aligned} S_{i_n}(f) &= S_{q_n}(f) = N_o\Pi(\frac{f}{B_t}) \\ S_{i_n q_n}(f) &= Sq_n i_n = 0 \end{aligned} \tag{2.21}$$

The equivalent baseband of the impulse response of the channel in (2.19) is such that [15]

$$\mathcal{F}\left\{\frac{1}{2}b_{h_c}(t)\right\} = H_c(f + f_c) \tag{2.22}$$

2.3.1 Noise Statistics Characterization

The pass-band noise is a white Gaussian process, it means the probability density function (pdf) f_{β_k} [15] is a Gaussian distribution defined by

$$\begin{aligned} \beta_k : N(0, \sigma^2); \qquad \sigma^2 &= \frac{N_o}{2} \\ f_{\beta_k}(\beta_k) = \frac{1}{\sqrt{2\pi\sigma}}e^{(-\frac{\beta_k^2}{2\sigma^2})} &= \frac{1}{\sqrt{\pi N_o}}e^{(\frac{\beta_k^2}{N_o})} \end{aligned} \tag{2.23}$$

Where β_k is the noise component at the *k*-th sub-carrier. Due to independence of the different noise component (noise in each sub-carrier), the cross-correlation among one of them with another is equal to zero, except with itself. If it is calculated the second moment with themselves, e.g., at *k*-th and *l*-th sub-carries of the *n*-th and *m*-th OFDM symbols respectively. See figure 2.4. It results

$$\begin{aligned} \mathrm{E}\{[\beta_k[m]\beta_l[n]^*]\} &= \frac{N_o}{2}R_{\phi_l\phi_k}((m-n)T) \\ &= \frac{N_o}{2}\delta[m-n]\delta[k-l] \end{aligned} \tag{2.24}$$

where, $R_{\phi_l\phi_k}$ is (2.8).

Thus, this can be understood that at the *k*-th branch, there is only noise power contribution provided for itself variances but not from others noise branches, it is giving by the orthonormal

basis (2.6) propriety of the pulses (2.9). All of this is assumed with a perfect time-frequency synchronization. Another explanation is due to natural behavior of the white noise. That is, if it is taken a sample noise in a *n*-th time, this sample noise does not have any relationship with other sample noise taken in a *m*-th time. All of this concept can be encompassed with the idea of independent variables, that can be explained with the following mathematical statements. Independence between two noise random variables b_k, b_l is defined as

$$f_{b_k b_l}(b_k b_l) = f_{b_k}(b_k) \cdot f_{b_l}(b_l) \Longrightarrow \mathrm{E}\{b_k b_l\} = \mathrm{E}\{b_k\} \cdot \mathrm{E}\{b_l\} \Longrightarrow R_{b_k b_l}(0) = 0 \; \forall k \neq l \quad (2.25)$$

So the joint p.d.f is modified in the following manner

$$\begin{aligned} f_{\mathbf{n}}(\mathbf{n}) &= f_{\beta_1,\beta_2....\beta_N}(\beta_1, \beta_2....\beta_N) = \prod_{k=1}^{N} f_{\beta k}(\beta_k) \\ &= \prod_{k=1}^{N} \frac{1}{\sqrt{\pi N_o}} e^{\left(-\frac{\beta_k^2}{N_0}\right)} = \frac{1}{(\sqrt{\pi N_o})^N} e^{\left(-\frac{\sum_{k=1}^{N} \beta_k^2}{N_0}\right)} \\ &= \frac{1}{(\pi N_o)^{\frac{N}{2}}} e^{-\frac{\|\mathbf{n}^2\|}{N_o}} = N(0, \frac{N_o}{2}\mathbf{I}) \end{aligned} \quad (2.26)$$

the noise auto-correlation matrix is $\mathbf{R_n} = \frac{N_o}{2}\mathbf{I}$ [15].

2.3.2 Noise Power Characterization

To perform this calculation, a graphic of the equivalent OFDM demodulator based on equivalent function diagram of the FFT is used. Each one of this function is interpreted as a matched filter of the FFT according to figure 2.4. Where each matched filter is represented by [25]:

$$\psi_k(t) = \begin{cases} \phi_k^*(T-t), & 0 \leq t \leq T \\ 0, & \text{otherwise.} \end{cases}$$

and, the received baseband signal in the OFDM demodulator is given by

$$b_r(t) = A_c b_s(t) * \frac{1}{2} b_{h_c}(t) + b_n(t) \quad \in \mathbb{C}$$

The matched filter output at k-th branch is analyzed and it is concluded that

$$\begin{aligned}\hat{\alpha}_k(t) &= b_r(t) * \psi_k(t) \\ &= A_c \sum_{m=-\infty}^{\infty} \sum_{l=1}^{N} \alpha_l[m]\phi_l(t-mT) * \phi_k^*(T-t) + \beta_k(t) \\ &= A_c \sum_{n=-\infty}^{\infty} \sum_{l=1}^{N} \alpha_l[m] R_{\phi_k\phi_l}(t-T-mT) + \beta_k(t)\end{aligned} \tag{2.27}$$

With aim of detecting the vector $\boldsymbol{\alpha}$, a sampling time $t_n = (n+1)T$ is set, so a sample at the moment n-th is obtained by

$$\begin{aligned}\hat{\alpha}_k(t_n) &= A_c \sum_{m=-\infty}^{\infty} \sum_{l=1}^{N} \alpha_l[m] R_{\phi_k\phi_l}(t_n-(m+1)T) + \beta_k(t_n) \\ &= A_c \sum_{m=-\infty}^{\infty} \sum_{l=1}^{N} \alpha_l[m] R_{\phi_k\phi_l}((m-n)T) + \beta_k(t_n)\end{aligned} \tag{2.28}$$

where $R_{\phi_k\phi_l}((m-n)T)$ was explained in (2.6) with the particularity that $R_{\phi_k\phi_l}((m-n)T) = \delta[m-n]$. Finally we lead to

$$\hat{\alpha_k}[n] = A_c\alpha_k[n] + \beta_k[n] \tag{2.29}$$

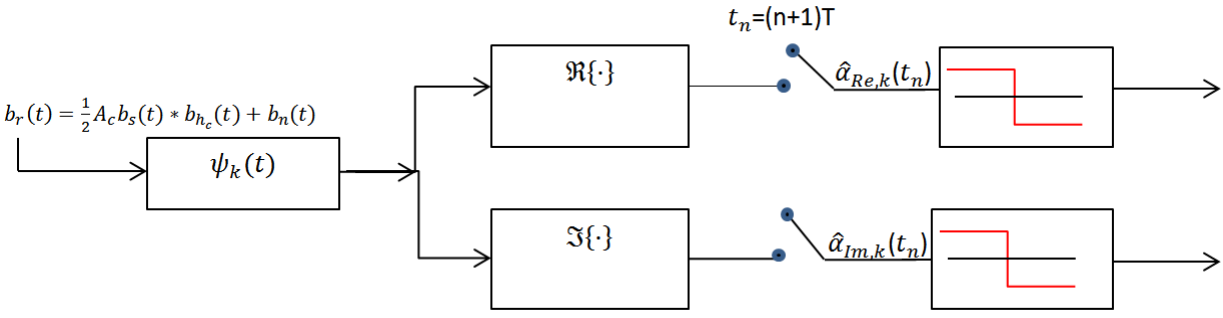

Figure 2.4: Equivalent OFDM Receiver

The output of system is the decided symbol, that is decided by the slicer i.e, ML or MAP detector. Apart of this, The k-th matched filter can be split in a real part and imaginary part in order to explain the noise power, the split matched filter is such that:

$$\psi_{Re,k}(t) = \frac{1}{\sqrt{T}}\cos(2\pi f_k t)\Pi\left(\frac{t-\frac{T}{2}}{T}\right)$$
$$\psi_{Im,k}(t) = -\frac{1}{\sqrt{T}}\sin(2\pi f_k t)\Pi\left(\frac{t-\frac{T}{2}}{T}\right) \tag{2.30}$$

The relationship between the outputs of the $\mathrm{Re}\{\cdot\}$ and $\mathrm{Im}\{\cdot\}$ blocks, and the $\psi_k(t)$ block is

$$\begin{aligned}\hat{\alpha}_k(t_n) &= \hat{\alpha}_{Re,k}(t_n) + \hat{\alpha}_{Im,k}(t_n) = A_c\alpha_k[n] + \beta_k(t_n) \\ &= A_c\alpha_{Re,k}[n] + \beta_{Re,k}(t_n) + j\left(A_c\alpha_{Im,k}[n] + \beta_{Im,k}(t_n)\right)\end{aligned} \tag{2.31}$$

The noise components have a Gaussian distribution (2.23):

$$\begin{aligned}\beta_k(t) &= b_n(t) * \psi_k(t) = (i_n(t) + jq_n(t)) * \left(\psi_{Re,k}(t) + j\psi_{Im,k}(t)\right) \\ &= \beta_{Re,k}(t) + j\beta_{Im,k}\end{aligned} \tag{2.32}$$

$\beta_{Re,k}(t), \beta_{Im,k}(t)$ are baseband process that have a Power Spectral Density (2.21)
Taking into account (2.21) it is demonstrated that:
$\beta_{Re,k}$: N $\left(0, \sigma^2_{Re}\right)$, then

$$\begin{aligned}\sigma_{Re,k} &= \mathrm{E}\{\beta^2_{Re,k}(t_n)\} = \int_{-\infty}^{\infty} S_{i_n}(f)\left|\Psi_{Re,k}(f)\right|^2 df + \int_{-\infty}^{\infty} S_{q_n}(f)\left|\Psi_{Im,k}(f)\right|^2 df \\ &= N_o E_{\Psi Re,k} + N_o E_{\Psi Im,k} = \\ &= N_o\end{aligned} \tag{2.33}$$

$\beta_{Im,k}$: N $\left(0, \sigma^2_{Im}\right)$, then

$$\begin{aligned}\sigma_{Im,k} &= \mathrm{E}\{\beta^2_{Im,k}(t_n)\} = \int_{-\infty}^{\infty} S_{i_n}(f)\left|\Psi_{Re,k}(f)\right|^2 df + \int_{-\infty}^{\infty} S_{q_n}(f)\left|\Psi_{Im,k}(f)\right|^2 df \\ &= N_o E_{\Psi Re,k} + N_o E_{\Psi Im,k} = \\ &= N_o\end{aligned} \tag{2.34}$$

In the case of the cross-correlation of in-phase and quadrature noise components.

$$\begin{aligned}&\mathrm{E}\{\beta_{Re,k}(t_n)\beta_{Im,k}(t_n)\} = \\ &\int_{-\infty}^{\infty} S_{i_n}(f)\left|\Psi_{Re,k}(f)\right|\left|\Psi_{Im,k}(f)\right|^* df + \int_{-\infty}^{\infty} S_{q_n}(f)\left|\Psi_{Re,k}(f)\right|^*\left|\Psi_{Im,k}(f)\right| df \\ &= 0\end{aligned} \tag{2.35}$$

This result is zero, since the matched filter (2.30) outputs are uncorrelated each other.

Finally, the noise distribution in the each matched filter is represented by

$$\begin{pmatrix} \beta_{Re,k}(t_n) \\ \beta_{Im,k}(t_n) \end{pmatrix} : \mathrm{N}\left(\begin{pmatrix} 0 \\ 0 \end{pmatrix}, N_o \begin{pmatrix} 1 & 0 \\ 0 & 1 \end{pmatrix} \right) \tag{2.36}$$

2.3.3 Received Signal

In reception the FFT is applied to the received base-band signal samples $b_r[n]$ coming from (2.19), going through to ADC and removing the cyclic prefix to recover the original modulated data. Hence, the *k*-th data symbol is given by

$$\hat{\alpha}[k] = \frac{1}{\sqrt{N}} \sum_{n=0}^{N-1} b_r[n] e^{-j(\frac{2\pi}{N} nk)} \tag{2.37}$$

Then, the vector $\hat{\boldsymbol{\alpha}} = [\hat{\alpha}[0] \cdots \hat{\alpha}[N-1]]^T$, with the demodulated symbols from the respective transmitted block, can also be obtained as the FFT of the received sequences $\mathbf{b_r}$

$$\hat{\boldsymbol{\alpha}} = \mathbf{F}\mathbf{b_r} \tag{2.38}$$

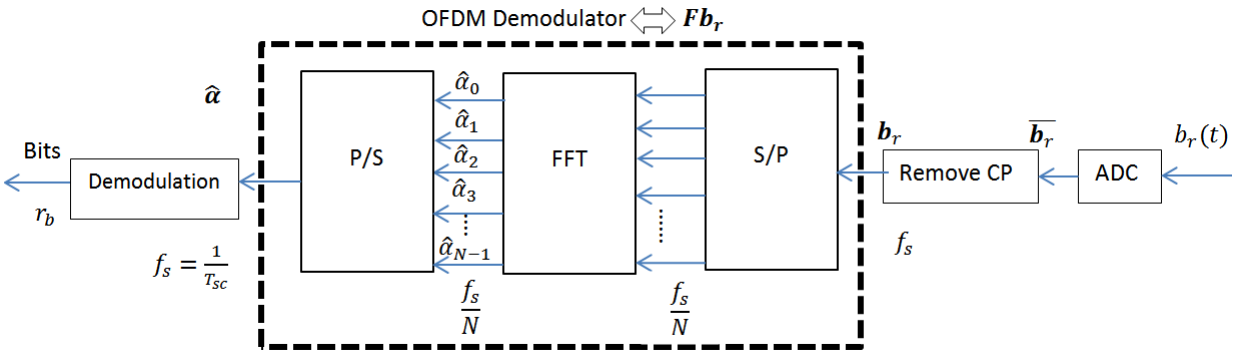

Figure 2.5: OFDM Base-Band Demodulator

The time-invariant constraints ensures that the channel is constant during one OFDM symbol period. Additionally, we assume that the transmitter and receiver are perfectly synchronized. Assuming that the cyclic prefix L_{CP} is longer than channel response i.e.,

$$h_c[n] = \begin{cases} 0, & \text{if } n \notin [0, L_{CP} - 1] \end{cases} \tag{2.39}$$

The channel between transmitter and receiver link is modeled as a multi-tap channel with the same statistics [24].The typical channel at time t is expressed as,

$$h_c(t,\tau) = \sum_{l=0}^{L-1} h_l(t)\delta(\tau - \tau_l), \tag{2.40}$$

Where L is the number of taps, h_l is the l-th complex path gain and τ_l is the corresponding path delay. The path gains are WSS complex Gaussian processes. The individual paths can be correlated, and the channel can be sparse. This type of channel will be explained in detail in the next chapter.

The Channel Frequency Response (CFR) and the Channel Impulse Response (CIR) is defined as,

$$H_c(t,f) = \int_{-\infty}^{\infty} h_c(t,\tau)e^{-2\pi f\tau}d\tau \tag{2.41}$$

With proper CP and timing, the CFR can be written as [24],

$$H_c[n,k] \equiv H_c(nT_{OFDM}, k\Delta f) = \sum_{l=0}^{L-1} h_c[n,l]e^{-\frac{2\pi}{N}kl} \tag{2.42}$$

where $h[n,l] = h(nT_{OFDM}, kT_{FFT})$. In matrix notation, for the n-th OFDM symbol, (2.42) can be rewritten as

$$\mathbf{H_c} = \mathbf{F}\mathbf{h_c} \tag{2.43}$$

At the receiver, after perfect synchronization, down sampling and taking into account the constraint (2.39), the simplified received base-band model of the samples $b_r[n]$ for the receiver antenna, can be formulated as

$$b_r[n] = \sum_{m=0}^{L_{CP}-1} b_s[m]h_c[n-m] + w[n] \tag{2.44}$$

$w[n]$ is the AWGN sample with zero mean and variance of σ_w^2 (2.23). Removing the CP from the incoming sequence $b_r[n]$, resulting in a vector $\mathbf{b_r} = [b_r[L_{CP}]\ b_r[L_{CP}+1]\cdots\ b_r[L_{CP}+L_{FFT}-1]]$, after taking FFT of the time domain samples (2.44), the received samples in frequency domain can be expressed as,

$$\hat{\alpha}[l] = \frac{1}{\sqrt{N}} \sum_{n=0}^{N-1} b_r[n+L_{CP}]e^{-j(\frac{2\pi}{N}nl)} \tag{2.45}$$

Substituting for $b_r[n]$ from (2.44), we get

$$\begin{aligned}\hat{\alpha}[l] &= \frac{1}{\sqrt{N}}\sum_{n=0}^{N-1}\left(\sum_{m=0}^{L_{CP}-1} h_c[m]b_s[n-m+L_{CP}] + w[n+L_{CP}]\right)e^{-j(\frac{2\pi}{N}nl)} \\ &= \frac{1}{\sqrt{N}}\sum_{n=0}^{N-1}\left(\sum_{m=0}^{L_{CP}-1} h_c[m]b_s[n-m+L_{CP}]\right)e^{-j(\frac{2\pi}{N}nl)} + \frac{1}{\sqrt{N}}\sum_{n=0}^{N-1} w[n]e^{-j(\frac{2\pi}{N}nl)}\end{aligned} \tag{2.46}$$

Substituting for $b_s[n]$ from the equation (2.14), we obtain

$$\hat{\alpha}[l] = \underbrace{\frac{1}{\sqrt{N}}\sum_{n=0}^{N-1}\left(\sum_{m=0}^{L_{CP}-1} h_c[m]\left(\frac{1}{\sqrt{N}}\sum_{k=0}^{N-1}\alpha[k]e^{j(\frac{2\pi}{N}(n-m)k)}W\left[\frac{(n-m)}{(L_{FFT}+L_{CP}-1)}\right]\right)\right)e^{-j(\frac{2\pi}{N}nl)}}_{Signal\ term} + \underbrace{\frac{1}{\sqrt{N}}\sum_{n=0}^{N-1} w[n]e^{-j(\frac{2\pi}{N}nl)}}_{Noise\ term} \tag{2.47}$$

Focusing on the signal term $\tilde{\alpha}[l]$,

$$\begin{aligned}&= \frac{1}{\sqrt{N}}\sum_{n=0}^{N-1}\left(\sum_{m=0}^{L_{CP}-1} h_c[m]\left(\frac{1}{\sqrt{N}}\sum_{k=0}^{N-1}\alpha[k]e^{j(\frac{2\pi}{N}(n-m)k)}W\left[\frac{(n-m)}{(L_{FFT}+L_{CP}-1)}\right]\right)\right)e^{-j(\frac{2\pi}{N}nl)} \\ &= \frac{1}{\sqrt{N}}\sum_{n=0}^{N-1}\left(\sum_{m=0}^{L_{CP}-1} h_c[m]\left(\frac{1}{\sqrt{N}}\sum_{k=0}^{N-1}\alpha[k]e^{j(\frac{2\pi}{N}nk)}e^{-j(\frac{2\pi}{N}mk)}W\left[\frac{(n-m)}{(L_{FFT}+L_{CP}-1)}\right]\right)\right)e^{-j(\frac{2\pi}{N}nl)} \\ &= \frac{1}{\sqrt{N}}\frac{1}{\sqrt{N}}\sum_{k=0}^{N-1}\alpha[k]\left(\sum_{m=0}^{L_{CP}-1} h_c[m]e^{-j(\frac{2\pi}{N}mk)}W\left[\frac{(n-m)}{(L_{FFT}+L_{CP}-1)}\right]\right)\sum_{n=0}^{N-1} e^{j(\frac{2\pi}{N}nk)}e^{-j(\frac{2\pi}{N}nl)} \\ &= \frac{1}{N}\sum_{k=0}^{N-1}\alpha[k]\left(\sum_{m=0}^{L_{CP}-1} h_c[m]e^{-j(\frac{2\pi}{N}mk)}W\left[\frac{(n-m)}{(L_{FFT}+L_{CP}-1)}\right]\right)\sum_{n=0}^{N-1}\left(e^{j(\frac{2\pi}{N}(k-l))}\right)^n\end{aligned} \tag{2.48}$$

for $k = l$

$$\tilde{\alpha}[l] = \frac{1}{N}\alpha[l]\left(\sum_{m=0}^{L_{CP}-1} h_c[m]e^{-j(\frac{2\pi}{N}mk)}W\left[\frac{(n-m)}{(L_{FFT}+L_{CP}-1)}\right]\right)\cdot N \tag{2.49}$$

for $k \neq l$ and knowing that $\left|e^{j\frac{2\pi}{N}(k-l)}\right| < 1$. As a result the summation converges as a geometric series, obtaining

$$\begin{aligned}\sum_{n=0}^{N-1}\left(e^{j(\frac{2\pi}{N}(k-l))}\right)^n &= \frac{1-\left(e^{j\frac{2\pi}{N}(k-l)}\right)^N}{1-e^{j\frac{2\pi}{N}(k-l)}} \\ &= \frac{1-e^{j2\pi(k-l)}}{1-e^{j\frac{2\pi}{N}(k-l)}}\end{aligned} \tag{2.50}$$

Owing to the orthonormal basis (2.9), as well as (2.4), it can be concluded that $e^{j2\pi(k-l)} = e^{j2\pi m} = 1$ for integers of m, it follows that

$$\sum_{n=0}^{N-1} \left(e^{j(\frac{2\pi}{N}(k-l))} \right)^n = 0 \tag{2.51}$$

which leads to

$$\tilde{\alpha}[l] = 0 \text{ for } k \neq l$$

Finally, the signal term can be written as

$$\tilde{\alpha}[l] = \alpha[l] \cdot H_c[l] \tag{2.52}$$

where $H[l]$, the windowing frequency response of the channel is given as

$$H_c[l] = \sum_{m=0}^{L_{CP}-1} h_c[m] e^{-j(\frac{2\pi}{N}ml)} W \left[\frac{(n-m)}{(L_{FFT} + L_{CP} - 1)} \right] \tag{2.53}$$

the noise term was analyzed in (2.3.2). In conclusion, the received data symbol $\hat{\alpha}[k]$ in equation (2.45) can be rewritten as

$$\hat{\alpha}[k] = \alpha[k] \cdot H_c[k] + w[k] \tag{2.54}$$

How was demonstrated the received data symbol $\hat{\alpha}[k]$ on each sub-carrier k is equivalent to the data symbol $\alpha[k]$, that was transmitted at the sub-carrier k, multiplied with the corresponding frequency-domain channel coefficient $H_c[k]$ plus the noise contribution at the k sub-carrier $w[k]$.

It is important to remember, the condition under which the above equation is valid. Perfect synchronization, the L_{CP} is longer than channel impulse response (2.5) and behavior of the channel can be characterized (2.39).

Therefore, the modulation and demodulation processes can be modeled as K parallel channels, each one associated at each sub-carrier, which transmits a symbol. This symbol is multiplied by the CFR at the corresponding sub-carrier, as it is shown in the figure 2.6

In other words, a sparse channel such as a frequency selective channel (wideband) can be transformed in N-set of parallel channels, where they do not have frequency selective channel (namely narrowband). Moreover, it allows to apply an independent treatment over transmission parameters at each channel. Allowing changes in the codification or modulation depending on the channel behavior.

As a consequence of the channel effects in the symbols, it is scaled in magnitude and phase rotation over transmitted symbol. In reception, it will be necessary to apply some mechanism to

compensate this variation. One common possibility is multiplier each one of detected symbols by a factor that can be made up for the CFR. This procedure corresponds to frequency-domain equalization [32]. This kind of equalization is easier to implement than the normal equalization in time, that is typical in communication system. The process consists of multiplying each received symbol for a coefficient, that depends on CFR. Using pilots tones or training sequences,which are known apriori by the receiver, and are transmitted in specific times and frequencies, it makes it possible to achieve the channel frequency estimation, and then the equalization. There are several basic techniques to estimate the radio channel in OFDM system. The estimation can be performed using time or frequency domain samples. These estimators depend on the behavior of the channel along with performances, their complexity and the apriori information they use in time [24], frequency [14] or spatial domain [29].

The matrix notation for a single OFDM symbol is denoted as

$$\hat{\boldsymbol{\alpha}} = \text{Diag}\left(\boldsymbol{\alpha}\right)\mathbf{H_c} + \mathbf{w} \tag{2.55}$$

where,

Diag $(\boldsymbol{\alpha})$ is a diagonal matrix with elements of $\boldsymbol{\alpha}$.

$\boldsymbol{\alpha}$ is the transmitted data symbol vector $\boldsymbol{\alpha} = [\alpha_0 \;\; \alpha_1 \;\; \cdots\cdots\cdots \;\; \alpha_{N-1}]^{\mathrm{T}}$.

$\mathbf{H_c}$ is the frequency domain coefficient vector $\mathbf{H_c} = [H_c[0] \;\; H_c[1] \cdots\cdots\cdots H_c[N-1]]^{\mathrm{T}}$.

$\hat{\boldsymbol{\alpha}}$ is the received data symbol vector $\hat{\boldsymbol{\alpha}} = [\hat{\alpha}_0 \;\; \hat{\alpha}_1 \cdots\cdots\cdots \;\; \hat{\alpha}_{N-1}]^{\mathrm{T}}$.

$\mathbf{w}$ is the frequency domain AWGN vector $\mathbf{w} = [w_0 \;\; w_1 \cdots\cdots\cdots \;\; w_{N-1}]^{\mathrm{T}}$.

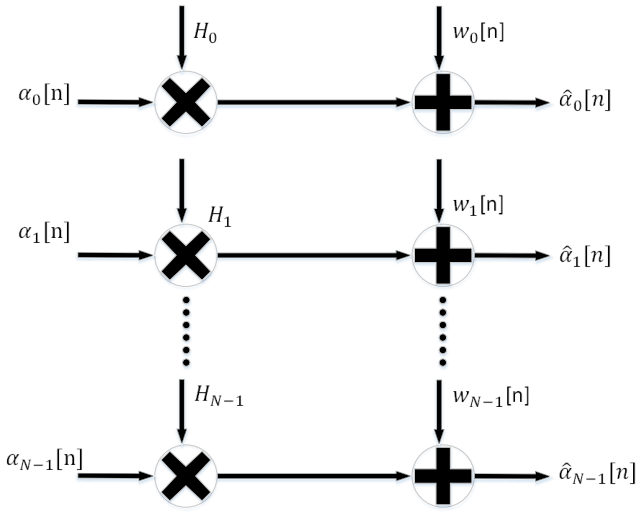

Figure 2.6: OFDM system interpreted as parallel channels

2.4 OFDM System Model

In the previous sections was explained how the OFDM modulator and demodulator works. In this section, it will be explained the whole structure system, where the thesis will be developed. Also, the baseband channel representation and its working.

So the basic OFDM model is represented in the figure 2.7

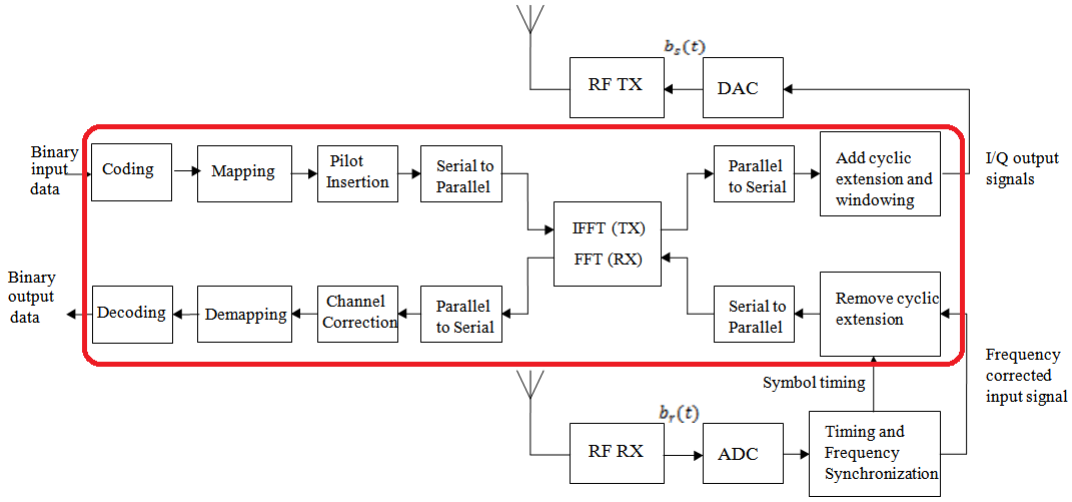

Figure 2.7: Block diagram of an OFDM transceiver

If the red remarked zone is analyzed, the complex base-band transmitted sample $b_s[n]$ is represented by its in-phase and quadrature components. In the OFDM transmitter this discrete signal is DA converted, quadrature modulated, up-converted to RF and sent to communication channel. Due to communication channel impairments and clock differences, the front-end of OFDM receiver is subject of various synchronization errors. Demodulation of the received signal usually involves down-conversion to intermediate frequency (IF), and if oscillator frequencies are not precise, this conversion causes carrier frequency offset. Moreover, demodulation introduces an additional phase noise. A signal in the OFDM receiver, after down-conversion to base-band and automatic gain control (AGC), must be sampled and A/D converted. After A/D conversion a signal in the OFDM receiver can be represented by stream of complex samples $b_r[n]$, The beginnings of OFDM symbols must be found, for doing down-conversion to separate data substreams by means of FFT [6]. It will be explained in the section (4).

Since we are working with complex signals, it will be better if the space signal basis is defined into complex space. Taking into account that $A_c e^{j(2\pi F_c t)} = A_c(\cos(2\pi F_c t) + j\sin(2\pi F_c t))$ and that the carrier frequency is larger than the bandwidth of the filters, the complex baseband channel can be represented as shown in the figure 2.8. The advantage of working with signals at lower frequency is that they are easier to simulate and analyze.

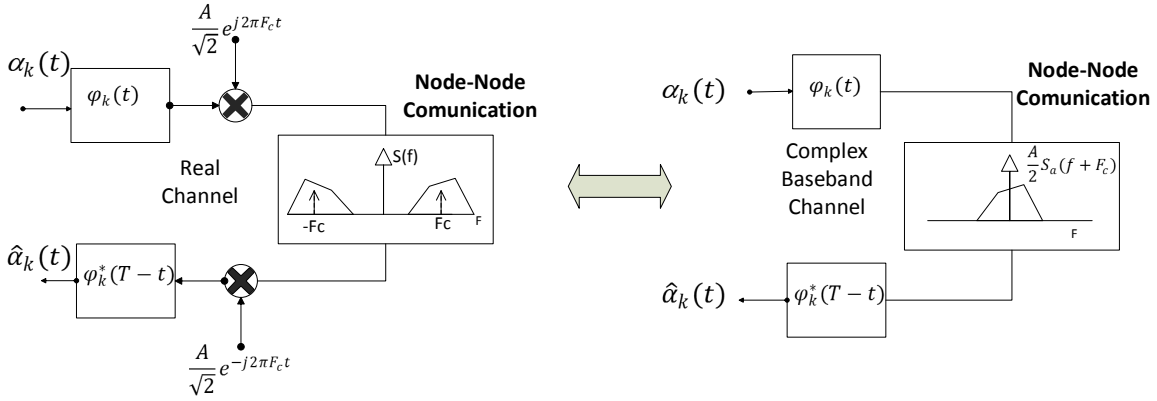

Figure 2.8: Baseband Channel Representation

2.5 Guard Interval and Cyclic Prefix

Up to this point we have considered that no ISI and ICI are introduced in the system. To avoid theses issues, it is necessary to use the guard band and the cyclic prefix.

In practice, the relation (2.1) (2.2) are not used. Since if they are used, the ISI can not completely avoided at least that the channel can be considered perfectly ideal.

If T_h is the maximum duration of the impulse response between OFDM symbols, the new OFDM period will extend T_g seconds more, this guard time is normally chosen larger that the expected delay spread, avoiding that multipath components from one symbol do not interfere with the next one. The guard itself will usually consist of a sub-set of null or zero-valued signals. However, in such cases, although ISI is already prevented by the inter-symbol distances, inter-carrier interference (ICI) may arise causing the sub-carriers to lose orthogonality. Hence, to overcome the ICI problem, normally a cyclically repetition of the last T_g seconds of the OFDM symbol along the guard time is placed $T_g = T_{CP}$. Owing to the orthogonality among the different sub-carriers, it can be ensured that any subcarrier coming from direct or delayed replicas of the signal will continue to have an integer number of cycles within an FFT window duration T_{FFT}. This ensures the orthogonality among the different sub-carriers as long as the delay remains smaller than the selected guard time.

Also, it is important to remark that the liner convolution with the channel impulse response is converted into a cyclic convolution. In this way, a circular convolution in time domain corresponds to a scalar frequency multiplication in frequency domain.

In section (3), the time-dispersive behavior of the wireless transmission channel has been characterized by the power delay profile (PDP) with maximum delay τ_{max}. Since the transmission is not stopped after one OFDM symbol, several ray multipath (wave reflexitions) could be falling into the sampling period, producing the ISI.

In other words, as well as considering multipath delay, the guard time must be chosen larger than the maximum duration of the impulse response among the N sub-carriers [4].

In terms of frequency spectrum, this means that in OFDM the ICI is avoided since the maximum of the any single sub-carrier should correspond to the zero crossing of all the other carriers as shown in the example of figure 2.9.

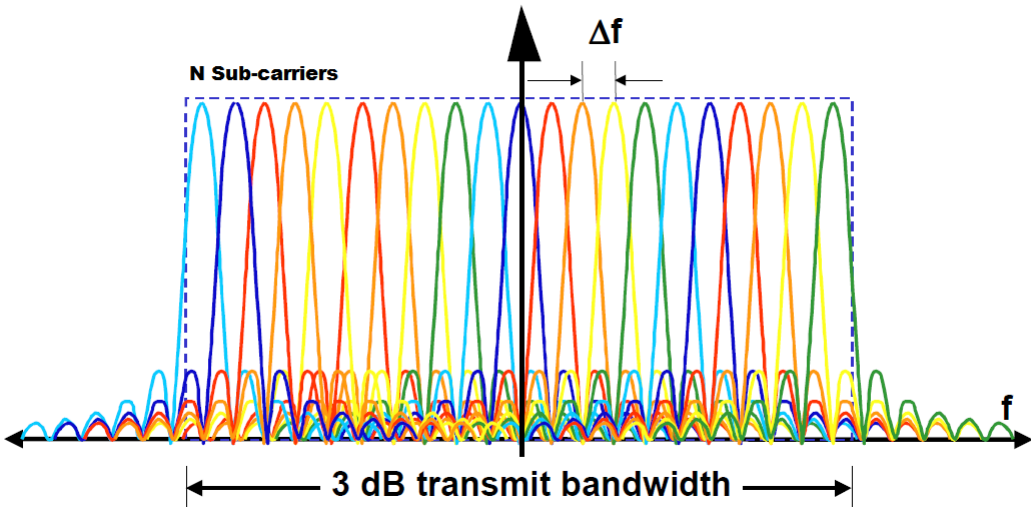

Figure 2.9: Orthogonal subcarrier spectrum

Taking into account the presence of the cyclic prefix, the relationship presented in (2.1) (2.2) takes the form:

$$T_{OFDM} = T_{FFT} + T_{CP} \tag{2.56}$$

$$\Delta f = f_b = \frac{B_T}{N} = \frac{1}{T_{FFT}} = \frac{1}{(T - T_{CP})} \tag{2.57}$$

where f_b represents the sub-carrier spacing. As well as the new reading period is defined as $((n+1)T_{CP} \leq t \leq (n+1)T)$

In many OFDM application design, a guard interval approximately between 10% to 25% of the original symbol duration is employed [16]. In a IEEE802.11a, for example, a cyclic prefix of duration 0.8 μs ($T_{CP} = \frac{T_{FFT}}{4}$) is copied from a 3.2 μs useful symbol part to obtain a 4.0 μs a symbol interval.

This behavior is represented by the figures 2.11.

Hereafter to refer the cyclically extended version of the signal b_s, the notation $\bar{b_s}$ will be used and it is defined as the length of the discrete CP (in number of samples) as an integer of L_{CP}, we obtain:

$$T_{CP} = L_{CP} \cdot T_{sample}$$

$$\bar{b_s}[n] = \frac{1}{\sqrt{N}} \sum_{k=0}^{N-1} \alpha[k] e^{j(\frac{2\pi}{N} nk)} W \left[\frac{n}{L_{FFT} + L_{CP} - 1} \right] \tag{2.58}$$

Alternatively, the CP operation over the input vector $\mathbf{b_s}$ is defined as

$$\bar{\mathbf{b_s}} = \mathbf{P}\mathbf{b_s}$$

$$\bar{\mathbf{b_s}} = \begin{bmatrix} 0 & \vdots & \mathbf{I_{L_{CP}}} \\ \cdots & \cdots & \cdots \\ & \mathbf{I_{L_{FFT}}} & \end{bmatrix} \mathbf{b_s} \tag{2.59}$$

Nevertheless, there is a drawback for the use of a guard interval. Since the guard interval is transmitted as well, it consumes additional transmitter energy and degrades the power ratio.

$$\mathbf{P}_{Data} = \frac{T_{FFT}}{T_{FFT}+T_{CP}}\mathbf{P}_{OFDM_{Sym}} = \frac{1}{1+\left(\frac{T_{CP}}{T_{FFT}}\right)}\mathbf{P}_{OFDM_{Sym}} \tag{2.60}$$

Consequently, there is a loss in the data rate of $\frac{L_{FFT}}{L_{FFT}+L_{CP}} \cdot 100\%$. To minimize overhead $T_{CP} << T_{FFT}$, i.e. the longer the data frame the better. To guarantee that the channel can assumed to be time-invariant during the transmission of the one OFDM symbol, T_{FFT} has to be smaller than the coherence time of the channel and therefore the duration of the T_{FFT}. How it will be explained in chapter (3), the analyzed system has not this restriction, since it does not show frequency Doppler effect (movement during the transmission).

2.6 Pilots Sub-carries and OFDM Structure Frame

Finally, we will discuss about OFDM structure frame, as well as of the pilots sub-carriers and its functions into OFDM system.

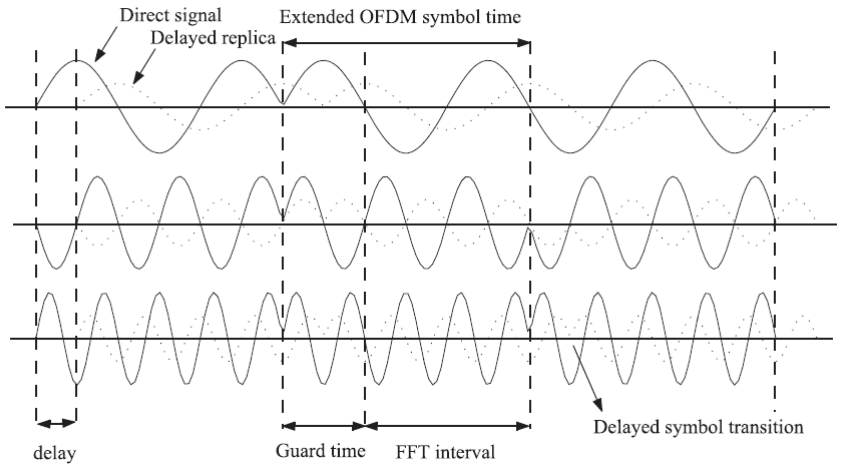

Figure 2.10: Tree consecutive OFDM sub-carriers modulated with BPSK during three symbol intervals.The cyclic extension of T/2 prevents the effect of the two-ray multipath at the receiver [4].

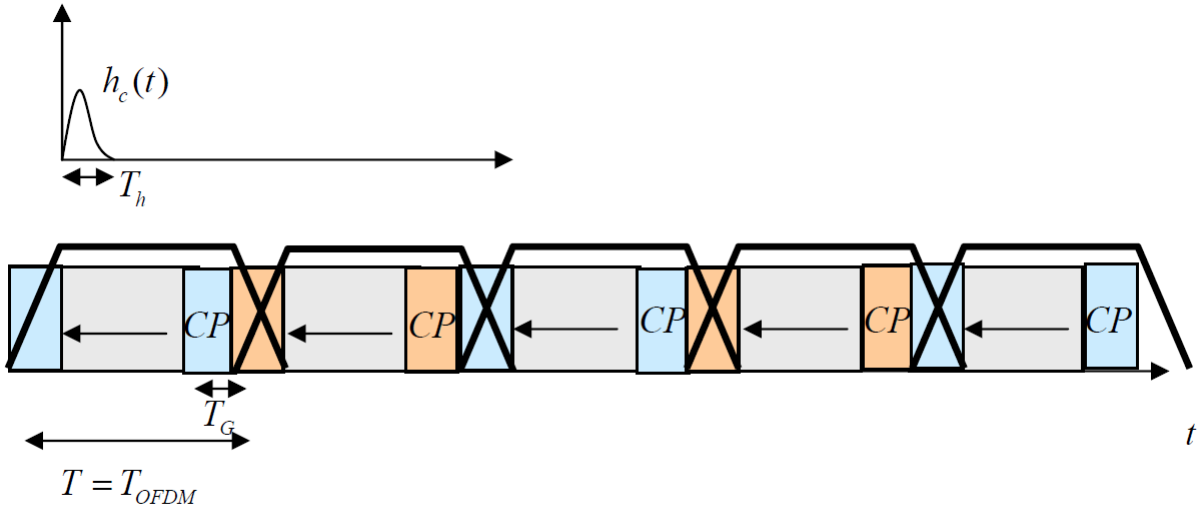

Figure 2.11: OFDM Symbol Temporal Activity [12]

The pilots sub-carriers are embedded in each OFDM symbol, and they are separated from information symbols in the frequency-domain. The function of the pilots can be Carrier Frequency Offset (CFO) estimation (effect of non-synchronization), Channel Estimation and Equalization [6].

The disposition of the pilots into the OFDM symbol depends on the channel behavior, this behavior is studied in detail in the chapter (3). Unlike other guided media, the radio channel is highly dynamic. The transmitted signal travels to the receiver after undergoing many detrimental effects that corrupt the signal and often place limitations on the performance of the system. Transmitted signals are typically reflected and scattered, arriving at receivers along multiple transmission paths. Also, due to the mobility of the transmitters, receivers (the system studied, does not have mobility as we will see soon) or reflecting object, the channel response can change rapidly over time. The multipath propagation, mobility and local scattering cause the signal to be spread in time, frequency and angle. All of this effects can be included in the statistical characterization of the channel , that depends on environment. The spreads, which are related to the selectivity of the channel, have significant implication on the received signal. Some algorithms exploits the statistical information to perform better channel estimation [18].

Taking into account the before explained, there are two methods to inserting the pilots sub-carries into OFDM symbol. *The Block-Type pilots* , pilots are inserting into all of the sub-carries of OFDM symbol with a specific period, or *The Comb-Type pilots* inserting pilot tones into each OFDM symbol. The first one has been developed under the assumption of slow fading channel [13], this assumes that the channel transfer function is not changing very rapidly. The later, the Comb-type pilot was introduced to satisfy the need when the channel changes even in OFDM frame. In the chapter (3) will discuss more about how and what kind of algorithms are implemented to develop the channel estimation.

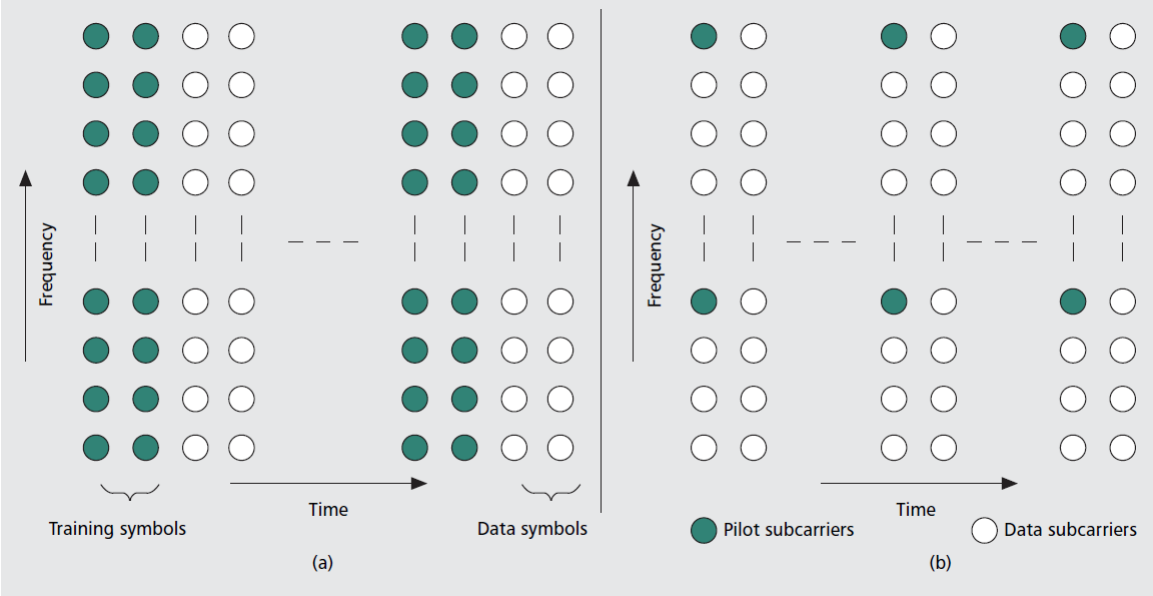

Figure 2.12: Typical training symbols and pilots subcarriers arrangement [9]

A number of steps that can be taken when designing a multi-carrier system to mitigate the effects of fading.

- In time domain, the data symbol duration can be made much longer than the maximum excess delay of the channel. $T >> \tau_{max}$
- In frequency domain, the bandwidth of the sub-carries can be made small compared to coherence bandwidth of the channel $B_{coh} >> B_T/N$. Therefore, the sub-carriers experiences flat-fading, which reduces the equalization to a single complex multiplication per carrier.

The structure frame implemented to achieve the practical work is detailed in this section. First, it will be explained how the structure of the OFDM symbol in the frequency-domain is, as well as the disposition of the pilots sub-carrier. Finally, the OFDM frame structure is presented as the concatenations of the OFDM training symbols and OFDM data symbols.

The OFDM symbol has the following parameters:

- 64 L_{FFT}
- 48 data sub-carries K_c
- 4 pilots sub-carries K_p
- 11 null sub-carrier (DC and guard frequency bands) K_{null}

  5 first left frequencies

  6 last right frequencies

- $T_{FFT} = 2.5\ \mu s$

- $T_{CP} = \left\lceil \frac{T_{FFT}}{4} \right\rceil = 0.7\ \mu s$
- $T_{OFDM} = T_{FFT} + T_{CP} = 3.2\ \mu s$

Others relevant parameters are:

- Frequency spacing $f_b = \frac{1}{T_{FFT}} = 400\ KHz$
- Transmission Bandwidth $BW = f_b \cdot (K_c + K_p) = 20.8\ MHz$
- Frequency Sampling $F_s = L_{FFT} \cdot f_b = 25.6\ MHz$
- Effective Symbol Rate $R_s = \frac{1}{T_{OFDM}} = \frac{BW}{L_{FFT}+L_{CP}} = 312.5\ KHz$

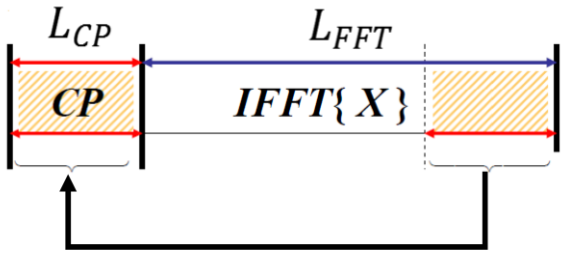

Figure 2.13: Time domain OFDM symbol with CP

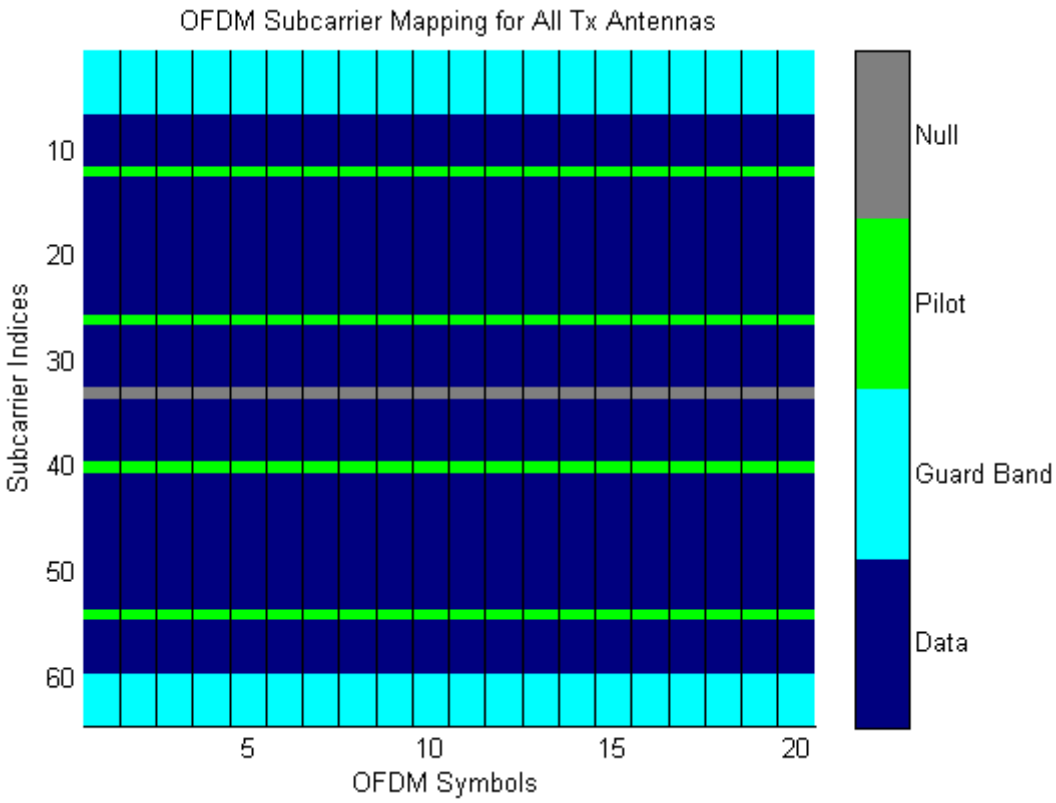

Figure 2.14: Frequency domain of 20 OFDM Symbol

The values of this parameter is explained in section (3.4.3).

A long training symbol which contains 52 modulated sub-carriers like a normal data symbol is multiplexed four time at the begging of the frame. The length of this training symbol is equivalent to four OFDM symbols, which is done for two reasons: first, it makes it possible to do a precise channel estimation and frame synchronization on the long training. Apart of the training symbols, there is a set of 20 data symbol, comprising a frame

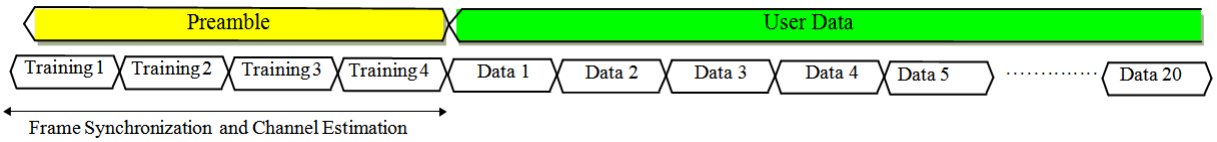

Figure 2.15: OFDM structure frame

Chapter 3

Channel Characteristics

Performing a wireless communication system is mainly constrained by the wireless channel, which consists of one transmitter, receiver antenna and the wave propagation between them. Depending on channel characteristics, that is to say topological environments (reflecting objects, buildings, hills, etc..), movements and the mobile speed making the radio-frequency channel a random process in magnitude, phase and frequency.

For being a random process, it has to be characterized by a probability density function that tries to say how the channel changes over time. In this way, the variability of the channel can be predicted. Thus, it is necessary to have an overall understanding about wireless communication channel.

3.1 Wireless Channel

The characterization of the wireless channel is fundamental to take a model, by means of the model we can realize which drawbacks or inconveniences has the channel and therefore to know its characteristics. Since the radio environment presents a multipath channel, this can be defined either NLOS (Non-line of sight) or LOS (Line of sight). The channel under study has a LOS behavior. It makes it possible take some considerations that with NLOS can not be applied.

For a typical wireless system, RF signal transmission between two antennas commonly suffers from power loss which affects its performance. This power loss between transmitter and receiver is a result of three different phenomena: 1) distances-dependent decrease of the power density called path loss or free space attenuation, 2) absorption due to the molecules in the atmosphere and 3) signal fading caused by terrain and weather conditions in the propagation path. Atmospheric absorption is due to the electrons and molecules that conform the air. Path loss is a theoretical attenuation which occurs under free-line-of-sight conditions and which increases with the distances between antennas [30]. Fading refers to the variation of the signal amplitude over time and frequency. In contrast with the additive noise as the most common source of signal degradation, fading is another source of signal degradation that is characterized as a non-additives signal disturbance in the wireless channel. Fading may be either due to multipath propagation, referred to as multipath fading (several or tens wavelength, Small-Scale-Fading) or to shadowing from obstacles that affect the propagation of a radio waves, referred to as shadow fading (hundreds of wavelength, Large-Scale-Fading). A consequence of movements among antennas, the instantaneous change of space is converted to the instantaneous change of signal when the antennas move through the multipath area. It presents the time-varying of wireless

channel, such as Doppler shift. This concept will not have repercussions in the evaluated channel 3.4.

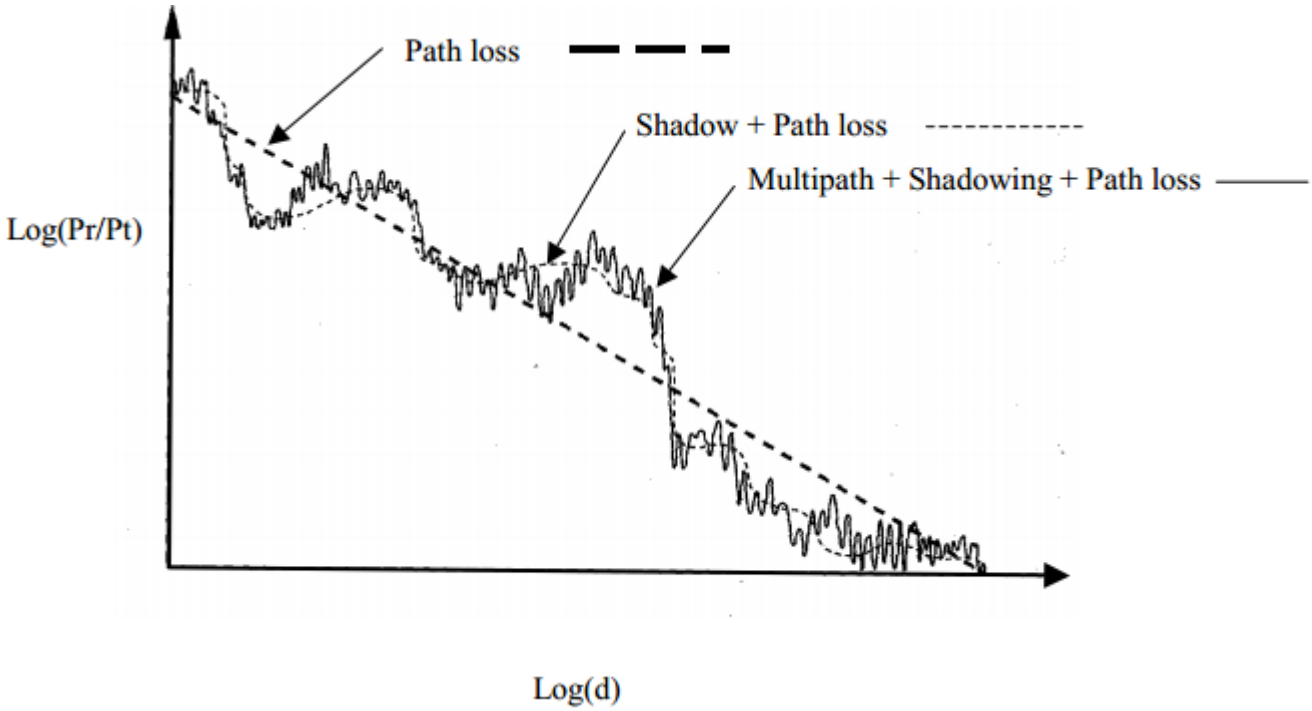

Figure 3.1: Path loss, shadowing and multipath [17]

Fading channel models are often used to model electromagnetic transmission of information over wireless media such as WLAN, Cellular and Broadcast communications.

In the following section, it will be dedicated only for multipath fading of small-scale fading wireless channel.

3.2 Multipath Propagation and Time Varying

Multipath propagation occurs typically in a wireless channel. The RF transmitted signal via radio channel from transmitter antenna to receiver antenna is not from a single path, but a number of different reflected waves. Consequently, many signals with different phase and amplitude are synthesized in receiver, which results in a signal that changes in time, frequency and spatial domain. From time domain, the multipath propagation is produced by different paths apart of the direct sight. In this way, the received signal not only contains the original transmitted signal but also arrived and delayed echos of transmitted signal.

These arrived and delayed echos can be explained by the Power Delay Profile (PDP), which can be used to extract certain channel parameters such as the delay spread τ_{max} (standard deviation of the PDP) [31].

Time-varying provides variations of the channel transfer function, because channel impulse response changes over time, giving transmitted signals, that differs with received signals. When the communication is established in motion, the frequency of the received signal will change. In

multipath conditions, each multipath wave has a frequency shift, called Doppler spread f_D and it is proportional to the speed of the mobile antenna.

$$f_D = f_c \frac{v}{c} \cos\theta_i = \frac{v}{\lambda} \cos\theta_i = f_m \cos\theta_i \tag{3.1}$$

where v is speed of antenna, λ is radio wavelength, f_c frequency carrier, c is speed of light, θ_i is angle between radio wavelength and antenna, f_m is the maximum Doppler frequency shift, respectively.

3.3 Fading Channel

This section is dedicated to introduce the mainly parameters of a small-scale fading channel, that is rapid variations in the signal level, due to the constructive or destructive interferences of the multipath propagation. Depending on the relative extent of the multipath, frequency selectivity of the channel is characterized (e.g., *by frequency-selective* or *frequency flat*) for small-scaling fading. Meanwhile, depending on the time variation in a channel due to mobile speed (characterized by the Doppler spread), short-term fading can be classified as either fast fading or slow fading. The figure 3.2 explains the classification of the fading channels, the red remarked blocks are focused in this section.

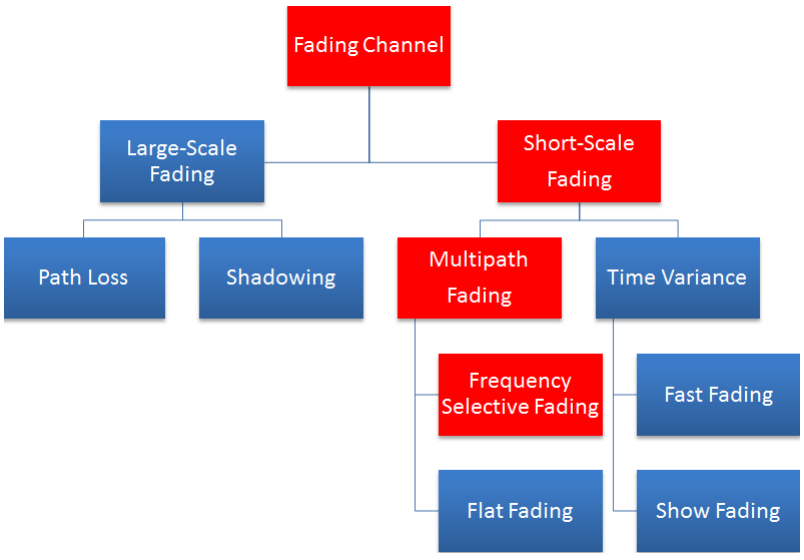

Figure 3.2: Classification of fading channels

First of all, the parameters of mobile multipath channel, which are delay spread (τ_{max}), coherence bandwidth (B_{coh}), Doppler spread (f_D) and coherence time (t_{coh}). The first two are used to describe multipath channel dispersion in time, and the latter two are used to describe multipath channel dispersion in frequency [34].

- *Parameters of time dispersion and frequency selectivity*.

The time-dispersive channel causes that the receiver picks up multiple copies of the signal transmitted giving by the presences of multiple scatterers objects (buldings,vehicles,hill,etc), because of temporally smeared-out version of transmitted signal. Therefore, time-dispersive channels are *frequency-selective* in the senses that different frequencies are attenuated differently. These differences in attenuation becomes more severe when the difference of the path delays is large and the difference between the path attenuation is small.

Although multipath propagation has traditionally been viewed as a transmission impairments, nowadays there is a tendency to consider it as beneficial since it provides additional information (realizations) to exploit techniques as *delay diversity* or *frequency diversity*. For instance the Rake receiver for Broadband CDMA[11].

In multipath propagation conditions, the received signal will produce delay spread. The Power Delay Profile characterizes the average power of multipath propagation [31]

$$P(\tau) = \mathrm{E}\{|h(\tau,t)|^2\} \tag{3.2}$$

The first moment of PDF is the average delay defined by,

$$\bar{\tau} = \frac{\int_{\infty}^{\infty} \tau P(\tau)}{\int_{\infty}^{\infty} P(\tau)} \tag{3.3}$$

RMS delay spread is the square root of second order of PDP

$$\tau_{RMS} = \frac{\sqrt{\int_{\infty}^{\infty} (\tau - \bar{\tau})^2 P(\tau)}}{\sqrt{\int_{\infty}^{\infty} P(\tau)}} \tag{3.4}$$

Coherence bandwidth B_{coh} is one of the parameters used to characterized the frequency selective fading. In other words, if the signal bandwidth is greater than the coherence bandwidth, the signal is not distorted by the channel that is named as *Flat Fading*.Otherwise, the signal is distorted in which case is named *Frequency Selective Fading*.

The coherence bandwidth is determined value from RMS delay spread and can be written as below

$$B_{coh} \approx \frac{1}{k\tau_{RMS}} \tag{3.5}$$

where k is a constant of proportionality. The two concepts above are *Flat Fading* and *Frequency Selective Fading* which can be summarized with the following statements.

Flat Fading is the reason of

$$B_t << B_{coh}$$

$$T_s >> \tau_{max} \tag{3.6}$$

Where B_t is the transmission bandwidth and T_s is the period of symbol, τ_{max} is the maximum delay spread. *Frequency Selective Fading* occurs when above statements are not satisfied. From the frequency domain, components with different frequency have different fading. From the time domain received signal passes many several path fading, so serious ISI occurs.

In this thesis the channel is characterized by frequency selective fading although at the subcarriers could be shown as flat fading (3.6), in a narrowband approach. Because of the communication is performed with fixed antennas, the channel does not have problems with frequency dispersion.

According to [31], the channel response h_c can be represented by

$$h_c[n] = \sum_{i=0}^{p-1} h_i e^{j(\frac{2\pi}{N}) f_{D_i} T_s n} \delta(\lambda - \tau_i) \quad 0 \leq n \leq N-1 \tag{3.7}$$

where p is the total number of propagation paths, f_{D_i} is the i-th Doppler frequency shift, λ is delay spread index, T_s is the symbol period and τ_i is the i-th path delay normalized by the sampling time and h_i is the complex impulse response of the i-th giving by [19]

$$\begin{aligned} h_i &= N(0, \frac{1}{2}\sigma_i^2) + jN(0, \frac{1}{2}\sigma_i^2) \\ \sigma_i^2 &= \sigma_0^2 e^{-i\frac{Ts}{T_{RMS}}} \text{ and } \sigma_0^2 = 1 - e^{\frac{Ts}{T_{RMS}}} \end{aligned} \tag{3.8}$$

where the power delay profile is assumed to be exponentially decaying.

3.4 OFDM Channel Model Description

As it has been explained in this chapter, a wireless communication channel can be manifested in different ways depending on its frequency-time variability. The channel under investigation manifests specific aspects which are detailed as the following properties:

- LOS communication.
- Frequency selective fading channel.

To achieve this behavior, Simulink RF toolbox [1] and a script developed from my advisor were used. The VNA (Vector Network Analyzer) is employed to measure the channel, obtaining the S-Matrix (scattering matrix). The S-Matrix of a biport network is defined as

$$\begin{pmatrix} S_{11} & S_{12} \\ S_{21} & S_{22} \end{pmatrix}$$

Each S-parameters of biport network has the following generic descriptions:

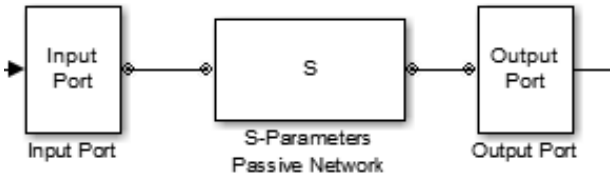

Figure 3.3: Baseband-Equivallent Modelling

- S_{11} is the input reflection coefficient with the output of the network terminated by a matched load.
- S_{12} is the reverse transmission with the input of the network terminated by a matched source.
- S_{21} is the direct transmission with the output of the network terminated by a matched load.
- S_{22} is the output reflection coefficient with the input of the network terminated by a matched source.

Those coefficients were calculated with the characteristic impedance of a line of $Z_o = 50\ \Omega$. As far as the studies of this thesis are concerned, the S_{21} or S_{12} are extremely important, since they represent in magnitude and phase the transfer function of the channel $H_c(f)$. Due to the fact that $S_{21} = S_{12}$, we can work with either of two. Channel parameters like the time delay spread will be decisive to select the OFDM parameters which consider the restrictions of the channel to avoid the distortion derived from multipath fading. For doing the channel simulation according with the constraint to guarantee a sample rate of $25\ Msps$ (Streaming Bandwidth per channel (16 bits) of the USRP2) at input port of the RF_block, the transmitted signal must be sampled with a time of $T_s = 0.4\ ns$.

The baseband equivalent modeling [1] simulates the physical system in the time domain using a complex baseband equivalent model that it creates from the passband frequency-domain parameters. Those come from the Vector Network Analyzer (VNA) taking values in the frequency range from 1.5 to 6.5 GHz with a fixed step of 1 MHz which are characterized by the S-Matrix. To calculate the baseband equivalent transfer function and then the impulse response of the system, the figure 3.3 was used. The first block of it is the Input Port, settings appropriately the parameter needed to calculate the model of the baseband equivalent transfer function and the impulse response for the physical system. The input port parameters that were set are :

- Source impedance (Z_o) 50 Ω
- Finite impulse filter length 1024 taps
- Fractional bandwidth of the baseband equivalent windows 0.01
- Modeling delay 511 samples
- Center Frequency $2.42\ GHz$

- Sample time 0.4 ns

The finite impulse filter length represents the number of point of the baseband impulse response, this parameter was chosen bigger than 512 since otherwise the τ_{rms} value was not coherent, with a resolutions of 1024 this value starts to be logic if it is compared with a theoretical value. Fractional bandwidth of the basedand equivalent window defines the ratio of the bandwidth of sections that are tapered using a Turkey window and the modeling delay is the number of time samples which impulse response of the baseband-equivalent is delayed. The fractional bandwidth as well as modeling delay are used to ensure that the baseband impulse response has a causal response which leads to a most accurate time-domain simulation of the specified band of frequency data.

The middle block is the S-Parameter Passive Network described by a S-Matrix, the frecuency range and the reference impedance. First at all, modifying appropriately the script of my advisor the data that comes from VNA, is imported to a matlab file and saved in $S\_PARAMS\_MATRIX(s_{row}, s_{column}, f, node)$. After that, the matrix is set as S-Parameters in the passive network.

The last block, the Output Port connects blocks from RF physical blocks to Simulink blocks. After running the simulation, various parameters of the RF system that is delimited by and Input Port block and this Output Port block can be visualized such as the magnitude or phase.

3.4.1 Cell Structure Prototype

The channel simulation arranges for set of a 33 PIFA antennas, 32 of them are denominated Cell Sensor Units (CSU) slave cells and the remaining the Battery Control Unit (BCU) master cell that emulate the viability of the Battery Management System (BSM) inside a battery emulator. Within the cell structure prototype a communication network is established between one slave cell and the master cell. The arrangement of the slave cells is vertically increasing in columns of 8 antennas, starting of the right side. The disposition of the master cell is centered in the right side of the flat, (see figure 3.5). The method of medium access of the CSU are not studied in this thesis, which can be OFDMA, Frequency Hopping, CDMA among others, that is because of in the measurements there are only two pair equal antennas.

Given that the channel is completely isolated, many reflections produced by the surfaces could falling into the reading time of the symbol, producing ISI. The target of this simulation is to characterize the constraint given by the delay spread of the channel that the system can tolerate and in this way providing a symbol time big enough to transmit without symbol interference. To perform this objective, a battery pack similar to the one in figure 1.1 which is completely contained in a single compartment made of metal, together with the cell cans and all the modules in only one level. This results in a rectangular prism, which has the same length and width as the battery housing, but its height is the distance between the cells upper side and the top of the housing. The prototype used in this thesis was "small" emulator with the following dimensions.

- length 80 cm

- width 50 cm
- height 5 cm

The "small" emulator is made of steel with a 1.5 mm of thick [8]. The scheme of the measurement is depicted in the figure 3.4.

The channel prototype will be evaluated 32 time, corresponding with the 32 node to node communications. It important remarks that the measure of each node to node communication was carried out changing the positions of the CSU (slave cell) among the different position within the cell structure prototype.

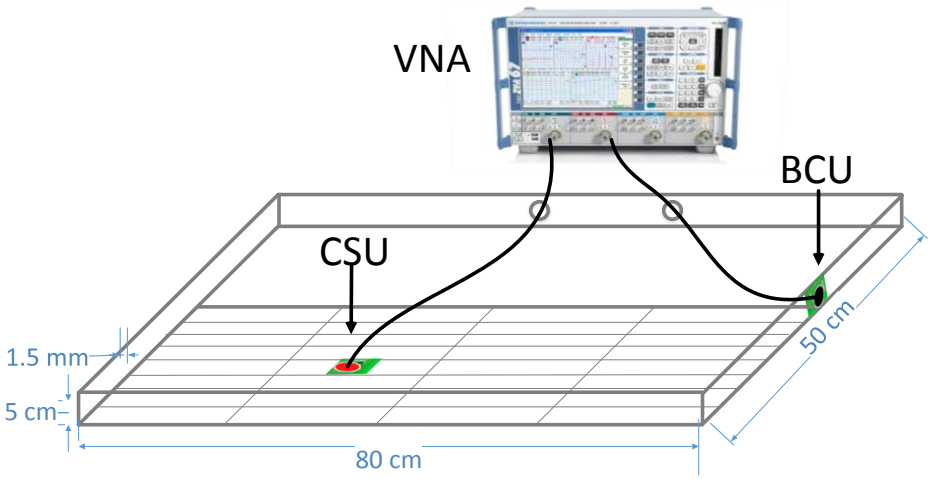

Figure 3.4: Measuraments setup inside the "small" emulator

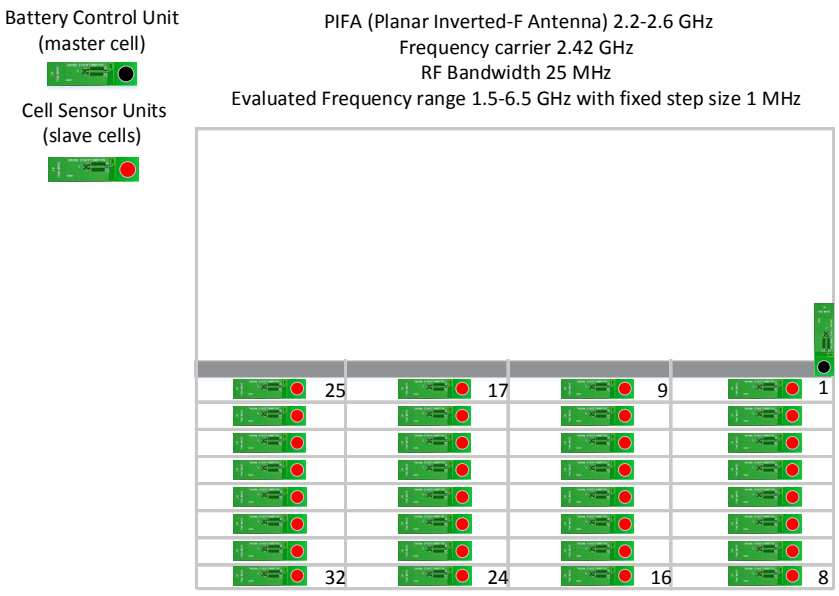

Figure 3.5: Cell Structure Prototype plan view

3.4.2 Node to Node Communication

The node to node communication is the communication between the master and any of the 32 slave cells inside the cell-structure prototype. The figure 3.5 shows the communication system model and each pair of node to node communication is depicted in figure 3.6

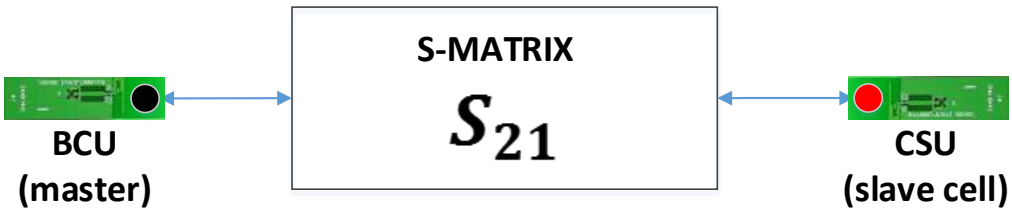

Figure 3.6: Node to node communication

Choosing one node of communication, the behavior of channel is reflected by the S_{21} parameter. Moreover, making used of the MatLab RF-toolbox other parameters can be calculated as the phase, e.g., $\angle S_{21}$. Some examples of the magnitude of the S_{21} parameters at different positions inside the battery emulator are depicted in the figures 3.7, which are visualized using the Output Port block of Simulink RF toolbox. The values of $|S_{21}|$ are used for comparing with the estimation of channel transfer function given by the channel estimator at the receiver.

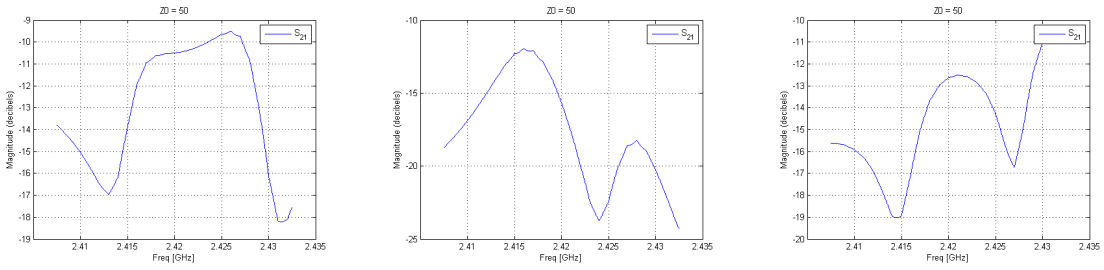

(a) Channel in 32-th position **(b)** Channel in 25-th position **(c)** Channel in 6-th position

Figure 3.7: Node to Node communication examples

After the simulation a vector $\boldsymbol{\tau}_{\mathbf{rms}}$ is obtained, plotting it we can see the values of the τ_{rms} (3.4) over the cell positions inside the box. Analyzing the results it is shown that some part of prototype have longer delay spread than others.

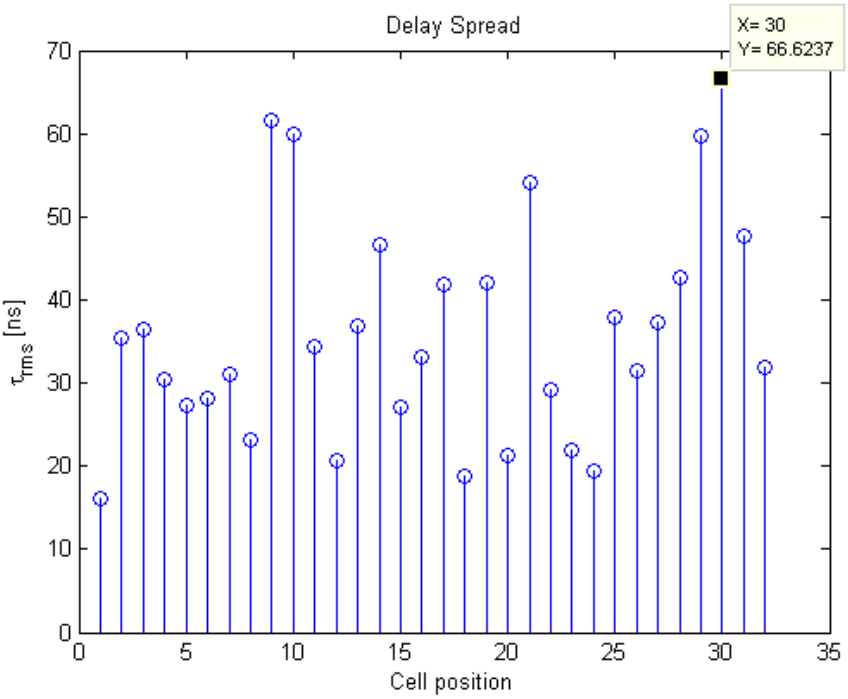

Figure 3.8: Delay spread inside the battery emulator

3.4.3 OFDM Parameter Selection Criteria

If the results are analyzed, it could be concluded that the maximal restriction is given by the position 30, since the maximum delay spread belongs from this position. Such value is $66,7\ ns$, on condition that no ISI at the receiver, the value of maximum delay must be contained along the cyclic prefix length. It imposes that the extension of the cyclic prefix must be longer that the maximum delay spread of the channel impulse response (CIR)

$$T_{CP} > \tau_{rms,max} \tag{3.9}$$

Since the channel under investigation presents time-disperse that is to say different frequencies are attenuated differently. Furthermore, when the antennas are fixed the channels do not have frequency dispersion and time selectivity. It means that the duration of T_{FFT} (FFT processing time) do not have any restriction to guarantee that the channel can assume time-invariant during the transmission of one OFDM symbol. However, T_{FFT} have to be lower than the polling time between slave (10 ms or in a similar way with a polling rate of 100 Hz). In addition, the T_{FFT} must be the time necessary to modulate 64 symbols taken from some signal constellation (e.g., PSK, QAM) on N subcarriers by an inverse discrete Fourier transform as well.

$$T_{FFT} = 2.5\ \mu s$$

The number of the FFT point are 64, the reason for this number is to accomplish with a symbol rate at each subcarriers equal to

$$f_b = \frac{1}{T_{FFT}} = \frac{F_s}{N} = 400\ KHz$$

where $F_s = 25.6\ MHz$ since streaming bandwidth per channel (16 bits) of the USRP2 is $25\ MHz$. As a result a minimum data rate of $2\ Mbps$ must accomplished, which is twice the rate of the high speed CAN-Bus.

The value of the cyclic prefix in the OFDM system is taken an integer multiple of the T_{FFT} and apart of that it has to be longer that the maximum delay as well.

The 32 measurements are obtained at each position of the antennas inside the prototype and saved in a vector of $\boldsymbol{\tau}_{rms}$ (see figure 3.8).

$$T_{CP} = \frac{T_{FFT}}{4} = 0,7\ \mu s >> \tau_{rms,Max} = 66,7\ ns \tag{3.10}$$

Besides, to track the channel during the transmission, pilots aided are multiplexed into the data stream. In multicarrier transmission system as OFDM, it is possible to not only insert pilots in the direction of the time t, but also in direction of the frequency f.

For channel estimation and equalization, pilots symbols with distance D_f in frequency direction and distance D_t in time direction in the OFDM frame have to embedded.

Those distances are limited by the following condition [9]:

$$D_f \leq \frac{1}{\tau_{max}\Delta f} \tag{3.11}$$

$$D_t \leq \frac{1}{2f_D T_{OFDM}} \tag{3.12}$$

Where, Δf is the sub-carrier spacing, f_D is the Doppler spread. The arrangement of the pilots is not constrained in time since the antennas are fixed. The pilots disposition at subcarriers $[-21, 7, 7, 21]$ was chosen by the standard IEEE 802.11a the pilots subcarriers for the n-th OFDM symbol is produced by Fourier transform of the sequence P [5], given by :

$$\begin{aligned} P_{-26,26} = {} & 0,0,0,0,0,1,0,0,0,0,0,0,0,0,0,0,0,0,0,1,0,0,0,0,0,0,0,0,0 \\ & 0,0,0,0,0,0,1,0,0,0,0,0,0,0,0,0,0,0,0,0,-1,0,0,0,0,0 \end{aligned} \tag{3.13}$$

The polarity of the pilots subcarriers is controlled by a pseudoradom noise (PN) sequence using a linear feedback shift register (LSFR) in Simulink model which is a cyclic extension of the 127 elements. The pn sequences is generated by the following Generator polynomial and Initial states

$$p(z) = z^7 + z^3 + 1 \ \text{ with a } seed = [1111111] \tag{3.14}$$

the seed has 7 elements since its length must equal to the degree of the generator polynomial.

The frequency carrier f_c at $2.42\ GHz$ was selected since the small emulator with PIF antenna presents transfers functions above -20 dB in considerably wide frequency ranges [8], revealing some potential portions of the bandwidth to transmit with considerable data rate.

Moreover, since the channel under study is time invariant, the aim of pilots will stay for a future extension of the system since in this thesis the phase estimation is not performed. The arrangement of the pilots was decided to exploit in a future the use of pilots in tasks such as phase estimation and as a hybrid synchronizer structure with timing-frequency estimation.

Chapter 4

Synchronization, Channel Estimation, Frequency Diversity and Equalization

In this section, the applied techniques in the OFDM system will be evaluated, such a synchronization, equalization and channel estimation. Considering that the channel where these techniques are applied were explained in section (3.3), that means a short-scale, multipath and frequency selective fading. The frame, transmitting through the channel, has four training symbols at the beginning, these symbols will help the receiver to synchronize the received signal and estimate the channel in order to apply an equalization to retrieve the information sent. The training sequence is based on standard IEEE802.11a, the time synchronization is based on ([35],[27]), the channel estimation and equalization are performed by an LS estimator [13] and zero forcing equalizer [33]. However, the structure of the transmitted OFDM symbol itself offers the opportunity for the simultaneous symbol timing and carrier-frequency offset estimation due to the inherent redundancy introduced by the cyclic prefix in the OFDM symbol.

4.1 Training Sequence

The training sequence based on the standard IEEE802.11.a consists of 53 subcarriers (including the zero value at DC), which are modulated by the elements of the sequences L [5], given by

$$\begin{aligned} L_{-26,26} = {} & 1,1,-1,-1,1,1,-1,1,-1,1,1,1,1,1,1,-1,-1,1,1,-1,1,-1,1,1,1,1,1,1,0 \\ & 1,-1,-1,1,1,-1,1,-1,1,-1,-1,-1,-1,-1,1,1,-1,-1,1,-1,1,-1,1,1,1,1 \end{aligned} \tag{4.1}$$

They are then periodically extended. In this manner the implemented model constructs four long training OFDM symbols, each of duration 3,2 μs with a cyclic prefix of duration 0,7 μs

These training symbols have the following properties:

- High correlation peak when the training sequences is alienated.
- Low correlation peak when the training sequences are not alienated with themselves.

These high correlation peaks are used to estimate the beginning of the new OFDM frames (a set of OFDM symbol), in this study the OFDM frame consists of a set of 24 with a symbol

period $3.2\ \mu s$ obtaining a duration of one OFDM frame equal to (4.2). The Frame synchronization block in the Simulink simulation will use these training sequences to perform the frame synchronization.

$$T_{OFDM_{block}} = 24 \cdot T_{OFDM} = 76.84\ \mu s \tag{4.2}$$

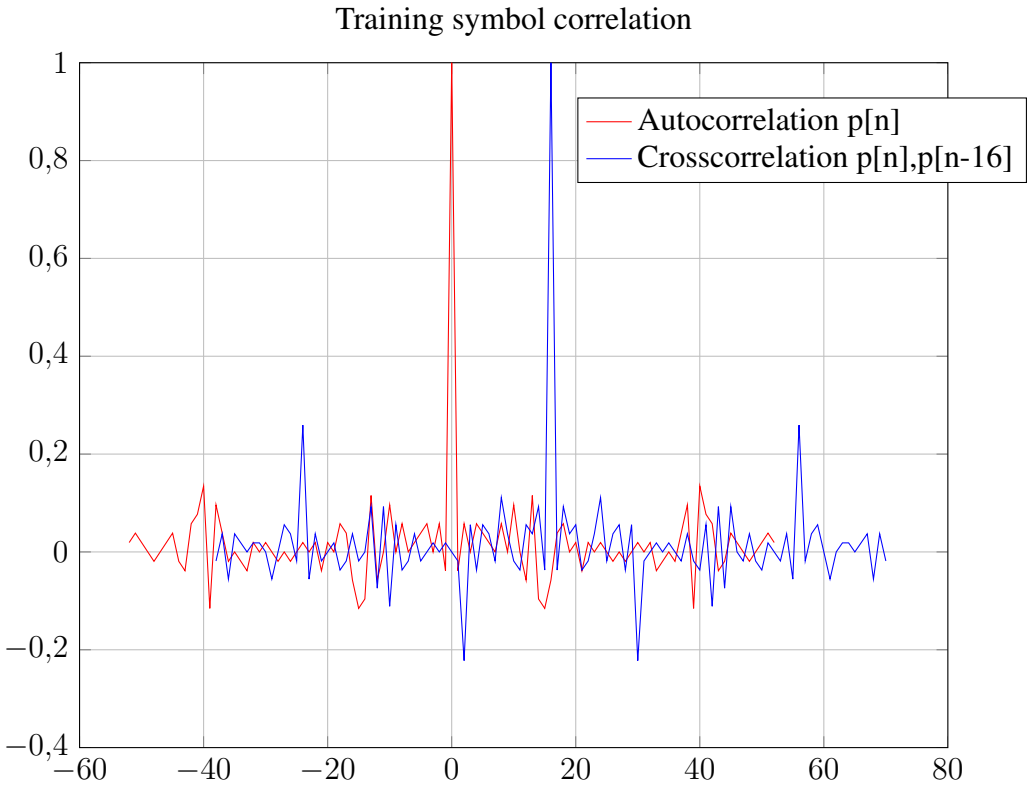

Figure 4.1: Training symbols correlation

Furthermore, the channel estimation is performed by training symbols. The training symbols are the above training sequences. These training sequences are known to the transmitter as well as to the receiver with the aim of estimating the channel. The process to achieve the channel estimation and frequency equalizer are explained in section (4.3).

4.2 Synchronization

As it was explained before, the training symbol are appended to perform different important tasks such as frame synchronization, channel estimation and equalization.

- **Timing and Frequency Estimation**

In [35] simultaneous Maximum Likelihood (ML) symbol timing and carrier-frequency offset estimation in Orthogonal frequency-division multiplexing (OFDM) system is presented. The

inherent redundancy introduced by the cyclic prefix of the OFDM symbols allows the estimation to be performed without additional training or pilots symbols. Two problems in the design of OFDM receivers are the symbol time offset (STO) and the carrier frequency offset (CFO). The former can be defined as the difference between the estimated timing instant and the correct timing instant. If the timing offset θ is with the CP it can be seen as if each complex OFDM symbol is multiplied by $e^{j\frac{2\pi k\theta\Delta f}{N}}$, where k is the subcarrier and Δf the frequency spacing. The multiplication causes a subcarrier dependent rotation in the complex plane with largest rotation on the edges of the frequency band [27]. As long as the timing offset is small enough this rotation can be estimated and corrected in the channel estimator. Besides, if the timing offset is larger than the CP minus the delay spread the subcarriers will lose their orthogonality. The latter can be represented as the mismatch of the oscillators in the transmitter and receiver, Doppler shift, etc., each path at the receiver signal is affected by CFO ϵ. It can be seen that each symbol sample n is multiplied by $e^{j2\pi n\epsilon\Delta f}$, causing a time varying rotation in the complex plane that causes the loss of orthogonality between subcarriers then resulting in ICI. The effect of the STO and CFO on the received signal can be observed and analyzed through the following expression of the time domain received signal.

$$b_r[n] = \frac{1}{\sqrt{N}} \sum_{k=0}^{N-1} H_c[k]\alpha[k]e^{j\frac{2\pi}{N}(k+\epsilon)(n+\theta)} + w[n] \tag{4.3}$$

This process, however, is not white, since the appearance of the cyclic prefix yields a correlations between some pairs of samples, spaced N samples apart. Hence, the $b_r[n]$ is not a white process either, but contains the information about the symbol time offset θ and the carrier frequency offset ϵ by its probabilistic structure. The *maximum likelihood* (ML) estimation of θ and ϵ, is the argument maximizing the log-likelihood function for θ and ϵ, it means the logarithm of the probability density function of observing the $2N + L_{CP}$ samples in $\mathbf{b_r}$ given the symbol time offset θ and the carrier frequency carrier ϵ, i.e. (4.4). The vector $\mathbf{b_r}$ contains $2N + L_{CP}$ samples of the received data $b_r[n]$, these samples contain one complete OFDM symbol $(N + L_{CP})$

$$\Lambda(\theta, \epsilon) = log f_{\theta,\epsilon}(\mathbf{b_r}|\theta, \epsilon) \tag{4.4}$$

for more information see [35].

The correlation of the received samples and delayed copy of them

$$\gamma(m) = \sum_{k=m}^{m+L_{CP}-1} b_r[n]b_r^*[n+N], \quad m \in \{0, 1.....N + L_{CP} - 1\} \tag{4.5}$$

and its sum

$$\xi(m) = \sum_{k=m}^{m+L_{CP}-1} |b_r[n]|^2 + |b_r[n+N]|^2 \quad m \in \{0, 1.....N + L_{CP} - 1\} \tag{4.6}$$

The simultaneous ML-estimation of θ and ϵ becomes

$$\hat{\theta}_{ML} = arg \overset{\theta}{Max} \{2\,|\gamma(\theta)| - \rho\xi(\theta)\} \tag{4.7}$$

$$\hat{\epsilon}_{ML} = -\frac{1}{2\pi}\angle\gamma(\hat{\theta}_{ML}) \tag{4.8}$$

where $\rho = \frac{\sigma_\alpha^2}{\sigma_\alpha^2+\sigma_w^2}$ is the correlation coefficient between $b_r[n]$ and $b_r[n+N]$. Since the CFO estimator depends on the angle of (4.5) it will be periodic and therefore the upper limit on the CFO that can be estimated is

$$|\epsilon| \leq \frac{\Delta f}{N} = \epsilon_{max} \tag{4.9}$$

If the CFO is greater than ϵ_{max} it will be impossible to determine the part of the CFO that consists of an integer number time of the distance between the subcarriers [27].

With the presented algorithms, the estimation of the STO and CFO will be carried out, but the tracking and correction of the STO and CFO were not implemented this thesis.

To evaluate the timing-frequency estimator by Simulink, two block were used viz., the variable fractional delay and the Phase/Frequency offset.

The following pictures depicts the signals that generate the ML-estimates

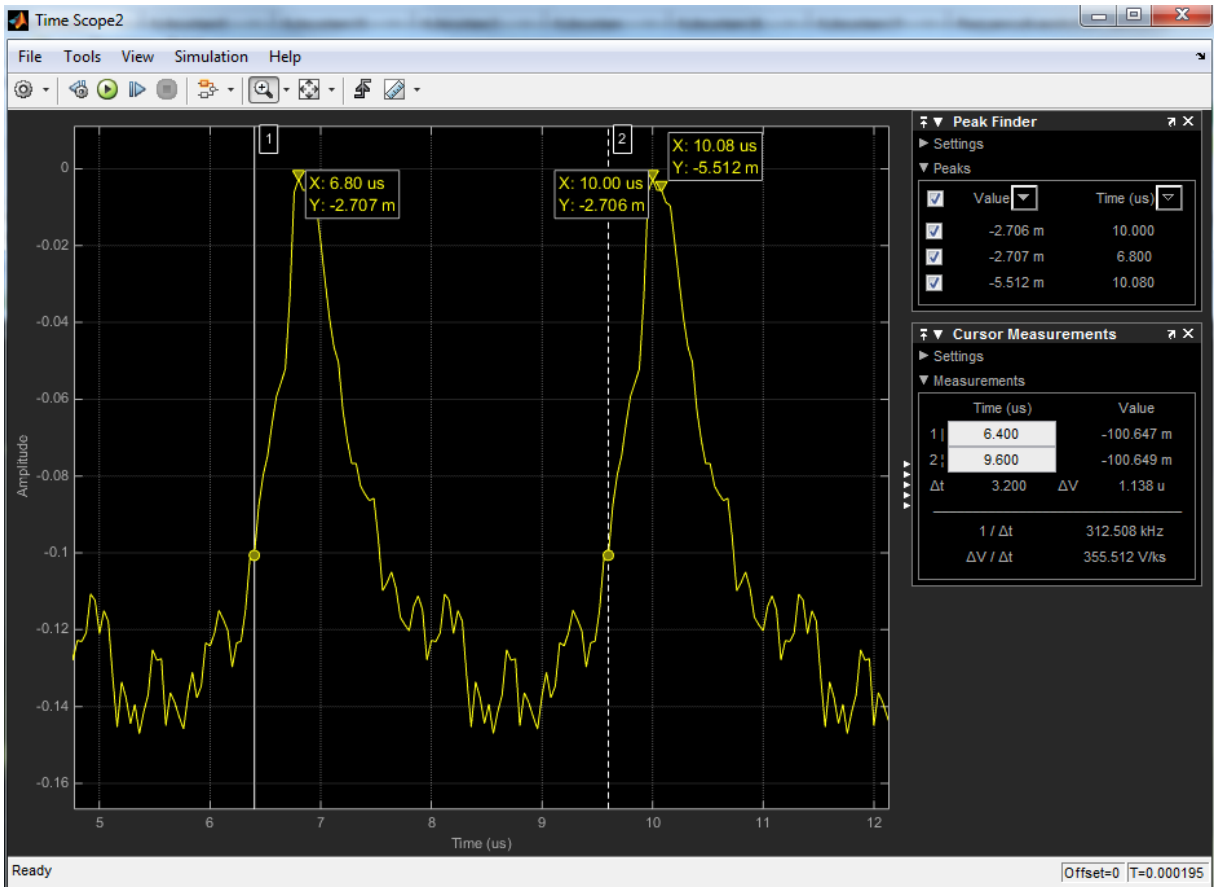

Figure 4.2: Symbol Time Offset estimation ($N = 64,\ L_{CP} = 16,\ \theta = 0.4\ \mu s$)

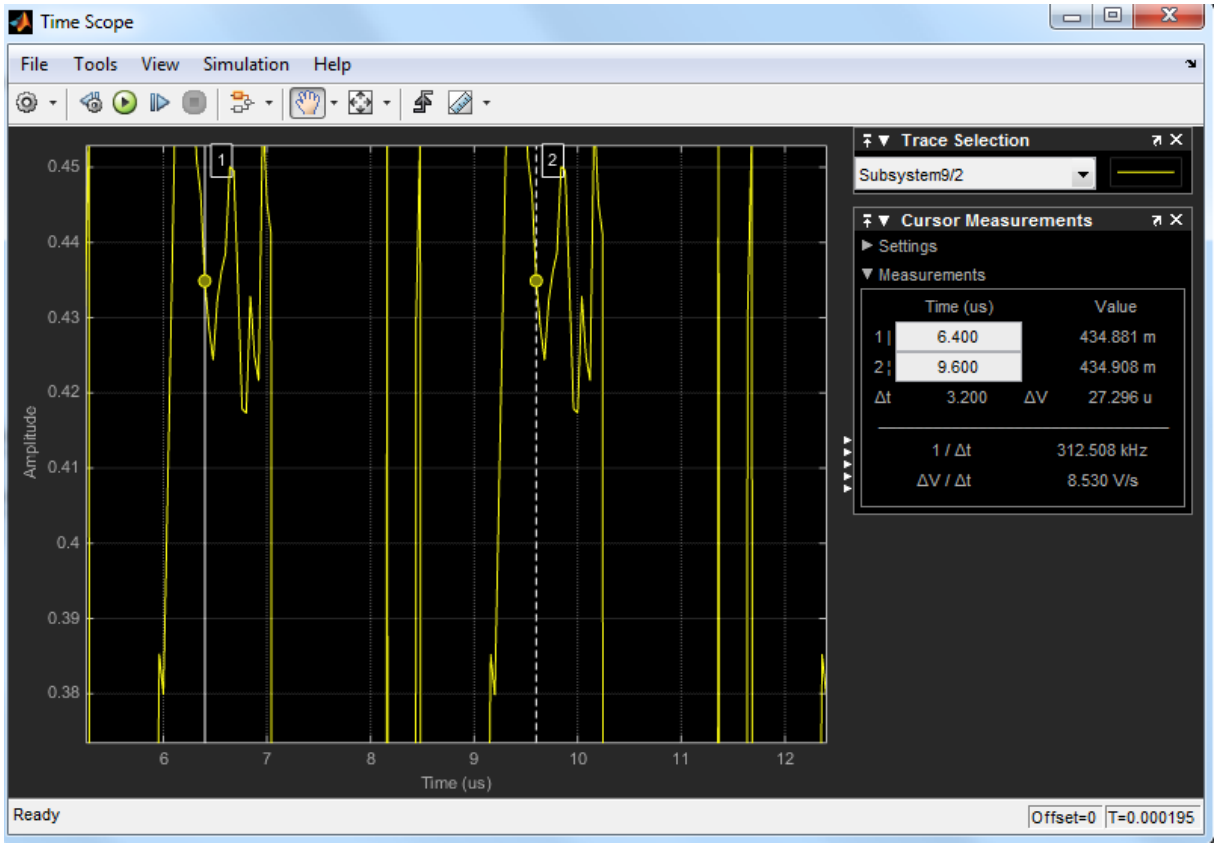

Figure 4.3: Carrier Frequency Offset estimation ($N = 64,\ L_{CP} = 16,\ \epsilon = 0.4$)

- **Frame Synchronization**

There are several methods to provide frame synchronization in an OFDM based communication system. The most obvious way is to introduce some kind of well known sequence (training symbols), which are used to mark the beginning of the frames. In time domain, the training symbols have remarkable correlation characteristics (4.1).

The OFDM receiver exploits these characteristics for searching the beginning of the frames. By performing appropriate correlations between the incoming sample stream and the training sequences, high peaks can be generated at the correlator output. This pattern of high peaks are used as flags for signaling the beginning of OFDM frame.

Frame synchronization is performed since the system at the transmitter sends symbols samples through the channel which is characterized by the parallel to serial block, as we will see later. At receiver symbol samples arrives one by one. However, the system OFDM works with a frame processing, it leads to the receiver having to wait a set of OFDM symbols to accomplish tasks such as demodulation, channel estimation and equalization. The preamble of the OFDM structure frame detailed in (2.15) is used.

After the timing-frequency synchronization, a buffer length of 24 OFDM symbols. This block applies the auto-correlation of the set of the OFDM symbols, high correlation peaks are generated showing the beginning of the OFDM frame.

Alternatively, the correlation of the training symbols with the received block can be also ensure the frame synchronization. Both manners can be defined as

$$R[m] = \mathrm{E}\Big\{\mathbf{B_r}\mathbf{B_r}^{H}\Big\} = \sum_{m=0}^{N+L_{CP}-1} \mathbf{B_r}[n]\mathbf{B_r}[n+m]^{H} \tag{4.10}$$

where $\mathbf{B_r} = \left[b_r^1[n], b_r^2[n].....,b_r^{N_{block}}\right]^{\mathrm{T}}$ and $[\cdot]^H$ is the hermitian operator. If the known training sequences are used to find the high peaks, we obtain

$$r[m] = \sum_{m=0}^{N+L_{CP}-1} \mathbf{B_r}[n]t[n+m] \tag{4.11}$$

where t is the training sequences (4.1) As result, the receiver has to estimate the frame start position, which determines the alignment of the FFT-window in the receiver with the useful portion of the OFDM symbol.

Figures 4.4, 4.5 shows high correlation peaks are generated when arrive a frame. The duration of OFDM symbol is given by (4.2)

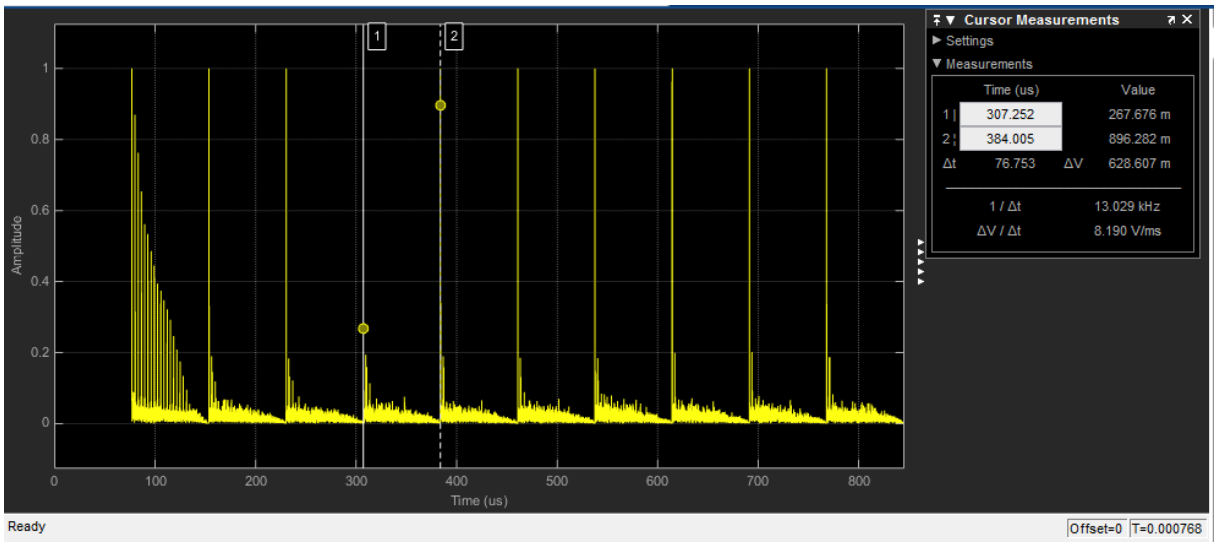

Figure 4.4: Frame timing estimation by means of the autocorrelation

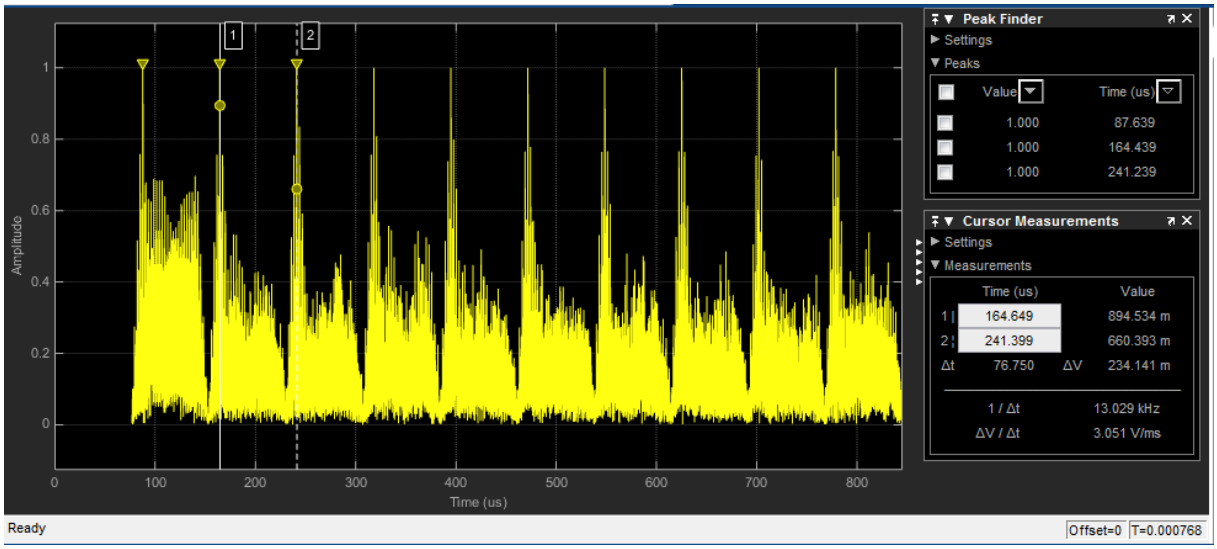

Figure 4.5: Frame timing estimation by means of cross-correlation

4.3 Channel Estimation

The channel of the system under investigation presents a time-invariant response, hence the channel estimation can be performed by means of *The Block-Type pilots*, training symbols are inserting into all of the sub-carries of OFDM symbol with a specific period techniques (see figure 2.12 part a). The preamble of the OFDM structure frame (figure 2.15) is used to perform this task.

- **Channel Estimation**

In section (2.54), the received signal at each sub-carrier can be expressed as the product between transmitted signal and the frequency response plus the noise component at each sub-carrier. Two channel estimation techniques usually implemented are with training symbols and pilots aided, both based on data aided information, that is to say, known information is inserted in OFDM symbol into the receiver so that the current channel can be estimated. In channel estimation with training symbols known information is sent over one or more OFDM symbols, but in pilot aided channel estimation known information is sent together with data [9].

The typical arrangement of the sub-carrier is represented in the figure 2.12. Channel estimation employing training symbols periodically sends training symbols that are used in the receiver in order to estimate the channel [36]. In some cases training symbols can be sent once and the channel estimation can then be followed by decision direct type channel estimation. For time domain estimation, the CIR is estimated first, the estimate of the CIR are then passed through a FFT operation to get the channel at each sub-carrier for the equalization in frequency domain. For frequency domain estimation, the channel at each pilot is estimated, and then these estimates are interpolated via different methods.

For the pilots aided channel estimation, the pilot spacing needs to be determined carefully. The spacing of pilot tones in frequency domain depends on the coherence frequency (channel

frequency variations) of the radio channel, which is related to the delay spread. According to the Nyquist sampling theorem, the number of sub-carriers spacing between the pilots in frequency domain, D_f must be small enough so that the variations of the channel in frequency can be all captured, that is

$$D_f \leq \frac{1}{\tau_{max}\Delta f} \tag{4.12}$$

When the above is not satisfied, the channel available at the pilot tones does not sample the actual channel accurately. Apart of it, when the channel is varying across OFDM symbols, in order to be able to track the variations of channel in time domain, the pilot tones need to be inserted at some ratio that is a function of coherence time (channel timing variations), which is related to Doppler spread, in this manner the maximum spacing of pilots tones across time is given by

$$D_t \leq \frac{1}{2f_D T_{OFDM}} \tag{4.13}$$

Hence, the rate of insertion of pilots in frequency domain and from one OFDM symbol to another cannot be arbitrary. The spacing of pilots should be according to (4.12) and (4.13).In general, within an OFDM symbol the number of pilots in frequency domain should be greater than the CIR length (maximum excess delay), which is related to the channel delay spread. Over the time, the Doppler spread is the main criteria for the pilots placement [9].

In [26], the effectiveness of preamble and pilot symbols designs in the IEEE 802.11a [5] and IEEE 802.16e (WiMax) [7] standards was demonstrated. For IEEE 802.11.a, an OFDM transmission frame with $N = 64$ sub-carriers is considered. Out of 64 sub-carriers, 52 sub-carriers are used for pilot and data transmission while the remaining 12 sub-carries are null sub-carriers. Similar to the preamble design, the study of the pilots arrangement for a multipath fading confirms that the pilot allocation at the sub-carries $K = \pm 7, \pm 21$, taking into account that (4.12) and (4.13) are appropriate to environments characterized by slow fading.

In my work, the channel behavior presents minimum slow fading. For this reason, the standard disposition of IEEE 802.11a was adopted. The figure (4.6) recreates the OFDM transmission frame.

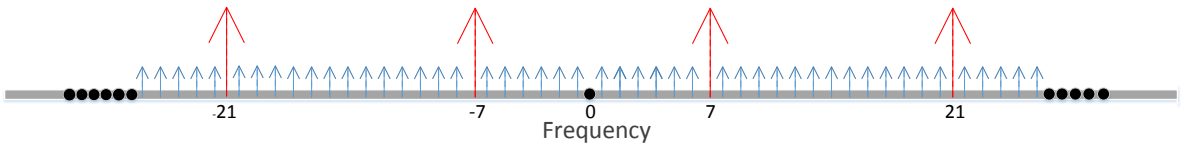

Figure 4.6: Pilots alignment

Due to the periodic behavior of the Fourier Transform, the sub-carriers at the beginning and the end of the OFDM symbol are correlated, this can be used to improve the channel estimation at

the edge sub-carriers. Simulations exploiting this property are reported to enhance the estimation accuracy of the edge sub-carriers [22].

Owing to channel conditions, the channel estimation was developed employing training sequences. As mentioned before, in the training mode, all the sub-carriers of an OFDM symbol are dedicated to the known training sequences. In the system over study, four OFDM symbols were reserved for the training sequence to perform channel estimation. Furthermore, due to the channel characteristics the same can be assumed over OFDM symbol for very slow variation channel. Once the channel is estimated over the training OFDM symbols, it can be exploited for the estimation of the channels of the OFDM symbols sent in between the training symbols. Depending on the variation of the channel along time, different techniques can be utilized. A very common method is to assume the channel being unchanged between OFDM training symbols [23]. In this method, the channel estimation is performed by training symbols used for the following symbols until new training sequence is received. Then, the channel is updated by using the new training sequences, and the process starts again.

Taking into account that one of the advantage to work with multicarrier modulation is the fact of subdivided the bandwidth in smaller parts (narrowband), where it could be a flat fading behavior. As a result, the frequency-selective channel (wideband) is converted to a number of parallel flat channels. Thus, N complex-valued channel coefficients gains on the parallel narrow-band sub-carriers channel can be estimated.

Assuming that the cyclic prefix is greater than channel response and the orthogonality among sub-carriers is maintained. In other words, the ICI and ISI are equal to zero or negligible. Under these assumptions the OFDM system can be expressed as a set of parallel Gaussian channels, shown in Figure (4.7).

Hence, the received signal at the k-th subcarrier at time n is given by [10]

$$\hat{\alpha}_k[n] = \alpha_k[n] \cdot H_k[n] + w_k[n] \tag{4.14}$$

The Least Squares (LS) estimate of the channel coefficient at the k-th subcarrier $\hat{H}_k[n]$, given by the received sample $\hat{\alpha}_k[n]$ and the known transmitted sample $\alpha_k[n]$ can be estimated with/as

$$\hat{H}_k[n] = \frac{\hat{\alpha}_k[n]}{\alpha_k[n]} = H_k[n] + \frac{w_k[n]}{\alpha_k[n]} \tag{4.15}$$

in matrix notations,

$$\hat{\mathbf{H}}_{LS} = \text{Diag}(\boldsymbol{\alpha})^{-1}\hat{\boldsymbol{\alpha}} + \text{Diag}(\boldsymbol{\alpha})^{-1}\mathbf{w} \tag{4.16}$$

where $H_k[n]$ denotes the true channel coefficients and $\frac{w_k[n]}{\alpha_[n]}$ is the residual noise. Despite the fact that the LS estimates are calculated by simple division without using any knowledge of the statistics of the channel, the main drawback of this approach is high mean-square error.

The MSE of LS estimation (4.16) is given by [10],

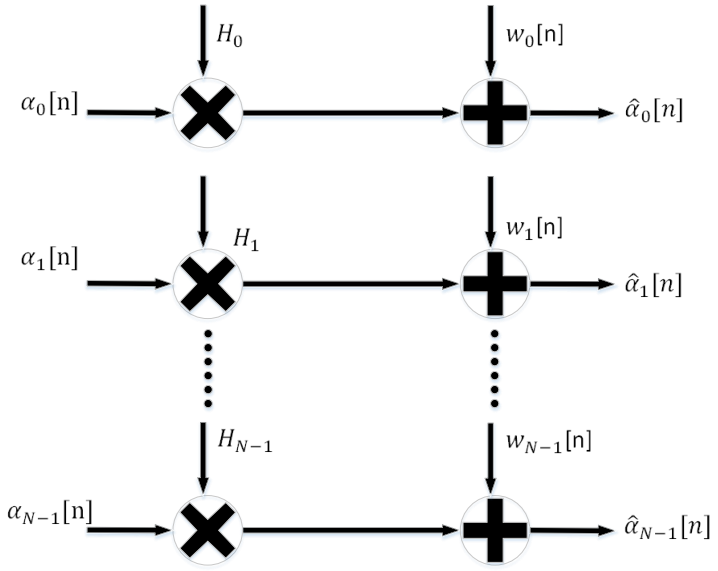

Figure 4.7: OFDM system interpreted as parallel channels

$$MSE_{LS} = \frac{N}{\mathrm{E}\{H_k[n]\} \cdot SNR} \tag{4.17}$$

where N denotes the number of subcarriers, LS method in general, is used to get a initial channel estimation at the pilot subcarriers [21] which are then further improved via different methods.

We first recall, it are defined by four training symbols. Taking advantage of this preamble structure non-zero values and good auto-correlation, it is calculated LS estimates for the first four OFDM symbols, which correspond with the known training sequences in accordance with equation (4.15). Then, the final channel estimate for k-th subcarrier of OFDM data symbols is the average of these four estimates:

$$\hat{H_k} = \frac{\hat{H}_k[1] + \hat{H}_k[2] + \hat{H}_k[3] + \hat{H}_k[4]}{4} \tag{4.18}$$

This technique is the so-called *averaged LS estimation* [20] and is only suitable for slow fading channels, the fast fading channel causes complete loss of estimated channel parameters. By averaging over four OFDM symbols, the effects of noise on the channel estimation process can be reduced. The results of the LS estimation is represented by the figure 4.8. Moreover, if the figure 3.7 is compared with the results of the LS estimation. The transfer frequency function are significantly equals.

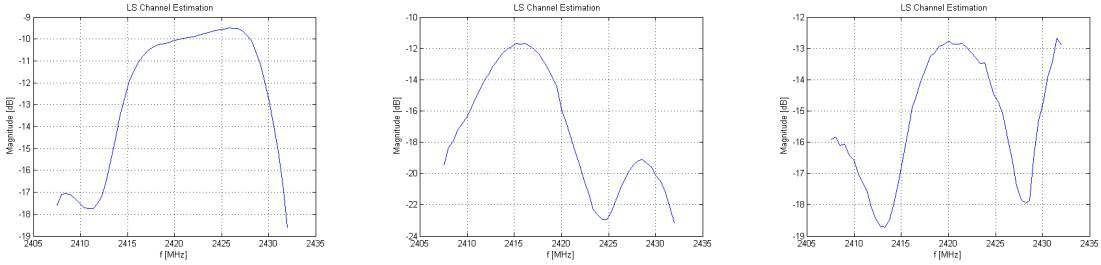

(a) LS estimation channel in 32-th position

(b) LS estimation channel in 25-th position

(c) LS estimation channel in 6-th position

Figure 4.8: LS estimation examples

4.4 Frequency Diversity

Frequency diversity consists of a system which transmits a unique signal on several carriers and selects the subcarrier or combines subcarriers at the receiver. With the aim of preventing that the transmitted symbol suffers the same degradation at different subcarriers, which is caused by frequency selective fading, the spacing frequency between carriers (center of subcarriers set) has to be a spacing that generates the subcarriers are uncorrelated among them. By means of the coherence bandwidth we can know which is the required bandwidth. This value can correspond to an important fraction of the transmission bandwidth, and therefore as a drawback requires a bandwidth significantly greater to a lower data rate. Moreover, there is the possibility that frequency selective fading may attenuate all of the subcarrier, so that reception becomes impossible even if diversity is applied. On the other hand, there is an advantage to the use of frequency diversity in multicarrier system such as OFDM systems, namely, that there is little probability that all carriers become impossible to receive simultaneously as a result of frequency selective fading, since there is a very larger number of carriers. The selection carriers is determined by the number of subcarrier available in OFDM symbol. Moreover, it could be possible to feed back the channel transfer function from the receiver to the transmitter, doing that the system can select the subcarriers set adaptively depending on the variability of the channel. Figures 4.9, 4.10 show the block diagram of the OFDM system using frequency diversity. In this new block diagram, a set of subcarriers is selected and parallel transmitted. In the receiver, N data symbols α are prepared and copied into M sets. In this way the NM data are mapped into the subcarriers and then the RF signal is transmitted as in an ordinary OFDM system. In this technique a unique symbol is transmitted at M subcarriers. Therefore, the transmission rate is degraded to 1/M compared to the conventional OFDM system. For carrier mapping, the transmission bandwidth was spit in integer parts. It means that the 48 data subcarriers are divided by the diversity order M, i.e. for M=2, 24 data subcarriers are used while in the reaming 24 subcarriers the same symbols are mapped. In the receiver data symbols as a frequency sequence are obtained by the same process as in an ordinary OFDM system. After that, the frequency sequence is divided into M sets by carrier demapping. However, these sets have common data symbols but the channel transfer functions $H(k, m)$ are different from each other. Hence, the

received frequency symbols are described as

$$\hat{\alpha}[k,m] = H_c[k,m]\alpha[k,m] + w[k,m] \tag{4.19}$$

where k is the symbol at the k-th subcarrier, m is the set number, $H_c[k,m]$ and $w[k,m]$ is the channel transfer function and additive Gaussian noise at the k-th subcarrier and in the m-th set mapped. Applying Frequency Diversity is guaranteed that the information data arrives at the receiver without need to retransmit the information data. This advantage gives robustness to the system since the probability of not receiving any symbol is much lower than it does not transmit applying frequency diversity.

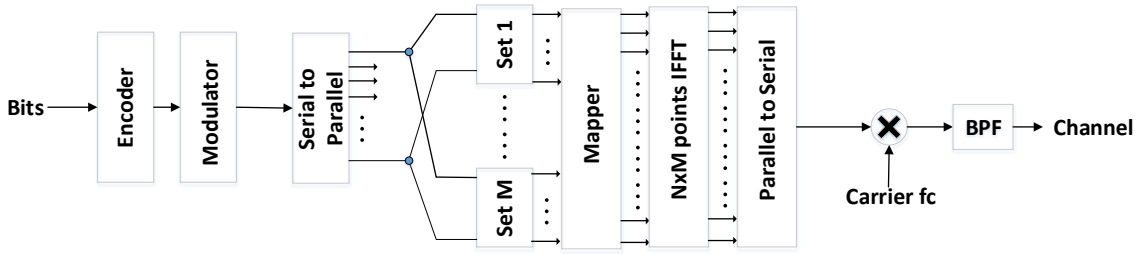

Figure 4.9: OFDM Transmitter with Frequency Diversity

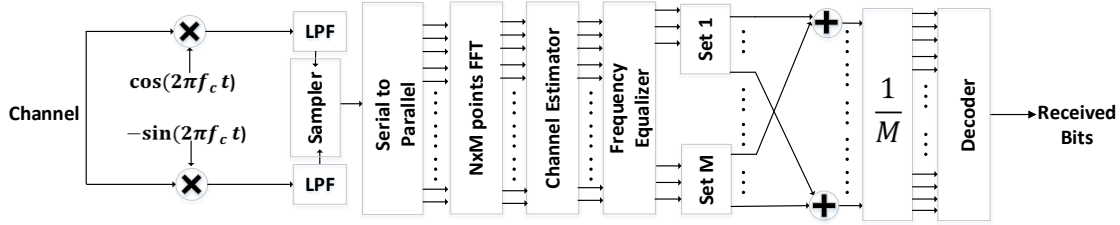

Figure 4.10: OFDM Receiver with Frequency Diversity

4.5 Equalization

The transmitted data symbol $\boldsymbol{\alpha}$ can be estimated by applying a single tap equalizer on the received data symbol $\hat{\boldsymbol{\alpha}}$. In the equalizer, the receiver divides each received symbol $\hat{\alpha}_k[n]$ by the inverse of channel coefficient estimate $\hat{H}_k$. The slicer output can then be rounded towards the nearest symbol in the modulation alphabet, thus providing a hard estimate of the transmitted

data symbols. Assuming that Channel State Information (CSI) is perfectly known, all channel coefficient can be calculated at each subcarrier independently. Moreover, the equalization in the complex domain can be corrected in both magnitude and phase.

The proposed system gets profit to send information at different subcarriers. Using Frequency Diversity one symbol can be multiplexed in several subcarriers. In this way, the robustness of the system is increased since the probability that in a certain moment two subcarriers are enabled in the same time is very low.

The equalizer coefficients $q[k,m]$ are calculated according to maximizing the $SNR(k)$, where the index refers to SNR of the symbol at k-th subcarrier.

Then, $q[k,m]$ is multiplied by $\hat{\alpha}[k]$ and their summation $y[k]$ is given by [33]

$$\begin{aligned} y[k,m] &= \sum_{m=1}^{M} q[k,m]\hat{\alpha}[k] \\ &= \sum_{m=1}^{M} q[k,m]\alpha[k]H_c[k,m] + \sum_{m=1}^{M} w[k,m]q[k,m] \end{aligned} \tag{4.20}$$

Hence, the SNR of the k-th symbol is described as

$$\begin{aligned} SNR(k) &= \frac{\mathrm{E}\left\{\left|\sum_{m=1}^{M} q[k,m]\alpha[k]H_c[k,m]\right|^2\right\}}{\mathrm{E}\left\{\sum_{m=1}^{M} w[k,m]q[k,m]\right\}} \\ &= \frac{\sigma_\alpha^2\left|\sum_{m=1}^{M} q[k,m]H_c[k,m]\right|^2}{2\sigma_w^2\left|\sum_{m=1}^{M} q[k,m]\right|^2} \end{aligned} \tag{4.21}$$

where $\mathrm{E}\{\alpha[k]\} = \sigma_\alpha^2$ on all k,m values, and $\mathrm{E}\{\cdot\}$ denotes the expectation value. In this case , the ***BER*** is minimized by maximizing ***SNR[k]*** with the constrain

$$\sum_{m=1}^{M} q[k,m]H_c[k,m] = 1 \tag{4.22}$$

which restricts the coefficient to $\alpha[k]$ to 1 , this leads that the optimum equalizer coefficients are

$$q_{opt}[k,m] = \frac{H[k,m]^*}{\sum_{m=1}^{M}|H[k,m]|^2} \tag{4.23}$$

As result the output $y[k]$ is obtained from (4.20) and (4.23) as

$$y[k] = \alpha[k] + \frac{\sum_{m=1}^{M} H[k,m]^* w[k,m]}{\sum_{m=1}^{M} |H[k,m]|^2} \tag{4.24}$$

and the SNR_{opt} is

$$SNR_{opt}[k] = \frac{\sigma_\alpha^2}{2\sigma_w^2} \sum_{m=1}^{M} |H[k,m]|^2 \tag{4.25}$$

In the above formula it is assumed that the receiver knows the channel transfer function. However, the great disadvantage of the ZF equalizer is its effect on the noise. The equalizer has a strong amplification if the values of $H[k,m]$ are small enough and the noise component increases. Due to the channel behavior being invariant in time, *The Block-Type pilots* techniques based on training symbols can be applied in the developed model to make a precise estimation. Summarizing, the equalization process can be express graphically as figure 4.11:

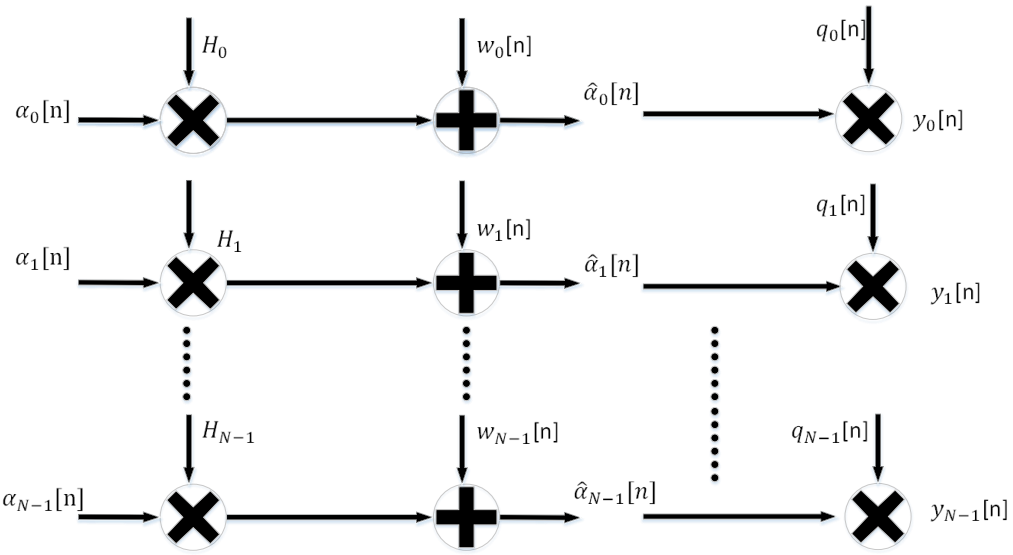

Figure 4.11: Frequency Equalization diagram

The channel equalization by the the Zero Forcing equalizer is depicted by the figure 4.12

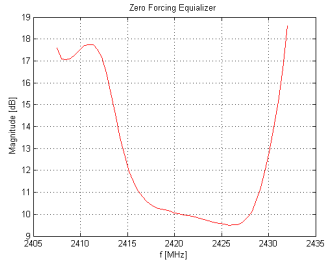

(a) Zero Forcing Equalization in 32-th position

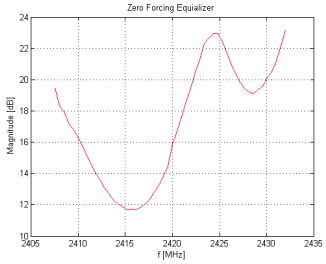

(b) Zero Forcing Equalization in 25-th position

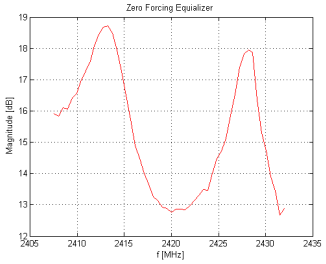

(c) Zero Forcing Equalization in 6-th position

Figure 4.12: LS estimation examples

Chapter 5

Simulation of the OFDM System (Simulink and MatLab)

This section is dedicated to showing how the OFDM system simulation was implemented. A explanation about the Matlab scripts, which should be run before the execution of the Simulink model. This script initializes the majority of the variables in the Simulink blocks. The CommOFDM.mat scripts finds in (B). Moreover the Comm OFDM library was created due to some blocks (e.g., Mapping, Demapping and Variable data source) are used quite often so in this way it will be better to create these common blocks and parametrized them according to their functions.

The system implemented is formed by three big different blocks such as OFDM transmitter, OFDM receiver and the Channel. The first one emulated an OFDM transmitter which consists of a binary data source, mapping, frequency diversity multiplexing and the OFDM modulator. In OFDM receiver all the complemented OFDM transmitter functions are developed, as well as frame synchronization, timing-frequency synchronization, channel estimation an equalization. The channel node-node prototype was explained in section (3.4) with the difference that now a AWGN block is inserted as a subsystem inside the channel prototype block .

After that, in the last section BER results are commented and discussed employing different parameters such as modulations, node to node channels, diversity order and SNR.

In outline, the scheme in which the thesis is performed can be seen in the section of the appendix (A.3)

5.1 Key Parameters

The script CommOFDM.mat contains the variables of the simunlink model and the S-matrix contains the channel coefficients for each one of the node communication. Therefore, always these scripts have to be built before the simulink model is executed. The CommOFDM library is composed by three blocks (Indexing , Modulator, Demodulator Diversity).

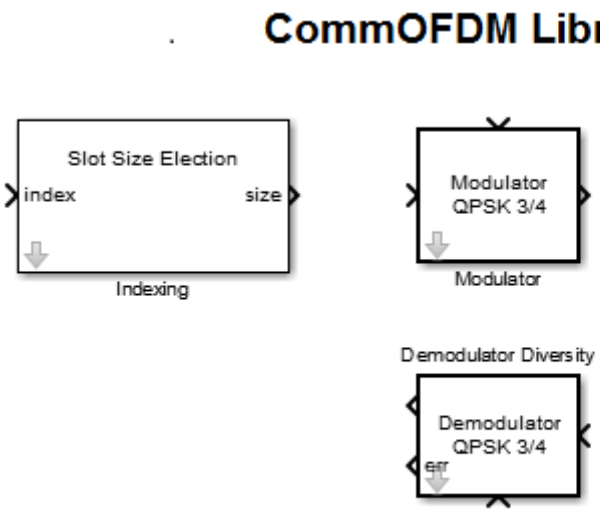

Figure 5.1: CommOFDM Library

- **Indexing**

The Indexing block chooses an element inside a vector. This block is used inside the Variable Binary Data Source block to generate as many pulses as slots according to the modulation block. Another task of the Indexing block is to choose the number of bit per block with aim of comparing the received bits with the transmitted bits. Its user interface has as a parameter the slot size that depends on the modes on the system works, see figure 5.2

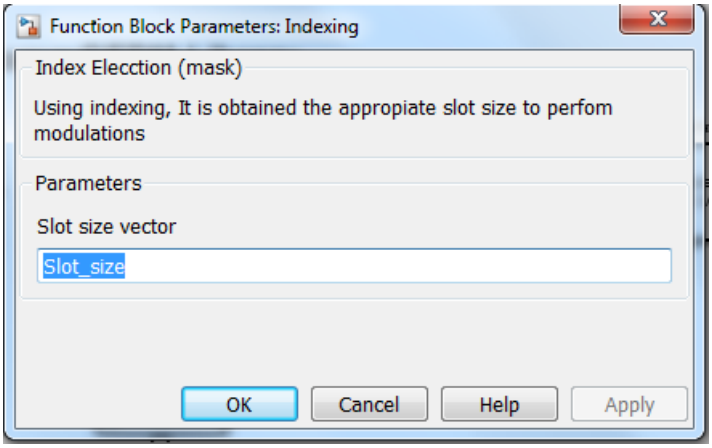

Figure 5.2: Indexing Block Interface

- **Modulator**

The Modulator block develops the task of modulation and coding of the bits. This block accepts four different types of modulation and codification which are named modes. The system is evaluated under these four modes. The modulation mode is described at the table 5.1. Setting

Table 5.1: System Mode

Mode	Modulation	Code rate
1	BPSK	$\frac{1}{2}$
2	BPSK	$\frac{3}{4}$
3	QPSK	$\frac{1}{2}$
4	QPSK	$\frac{3}{4}$

the parameter depending on the chosen mode is task of the interface modulator. The interface modulator has as parameter six items which are Number of symbols per block, Modulation, Code rate, Trellis structure and the Puncture vector.

The coding performed by a convolution encoder, using poly2trellis (Constraint Length, Code Generator) Matlab function performs the conversion for a rate k/n feedforward encoder and the puncture vector to generate different codes from 1/2 code rate, which is the code rate of the convolutional encoder. Further information in [3]. The parameters of the modulator block are contained in the CommOFDM_settings script (B) and are set in the block as it is shown in the figure (5.3)

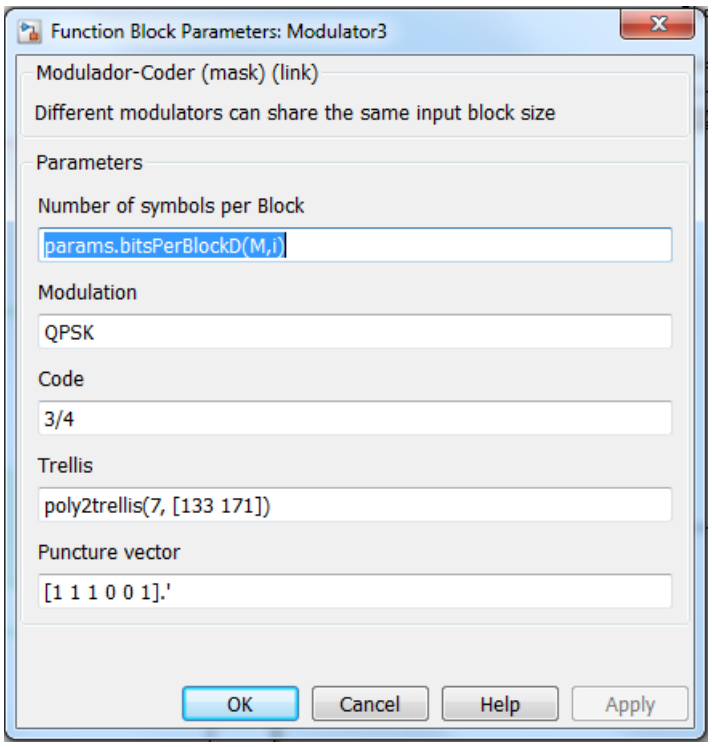

Figure 5.3: Modulator Block interface

- **Demodulator diversity**

The Demodulator block executes the complemented task as its equivalent (Modulator block). Depending on the mode the demodulator block responds in a different manner, that is to say if the mode 2 is chosen the demodulator block performs the mode 2 as well. Demodulating

the complex frequency symbol streams into a bits, then Viterbi decoder [2] decodes the coded bits into data bits employing the maximum likelihood decoding. It refers to finding the most likely transmitted data symbol stream from the received code word. To decode appropriately the coded stream, the same trellis structure that the corresponding convolutional encoder block as well as the same puncture vector is used. Viterbi traceback depth refers to the number of trellis branches to construct each traceback path. Thus, after decoding the bit error rate can be obtained. Furthermore, using frequency diversity the block respond according to the number of the transmitted symbols. The interface of the Demodulator block is represented by figure 5.4

The OFDM parameters have been defined as it is detailed in the script in the appendix (B).

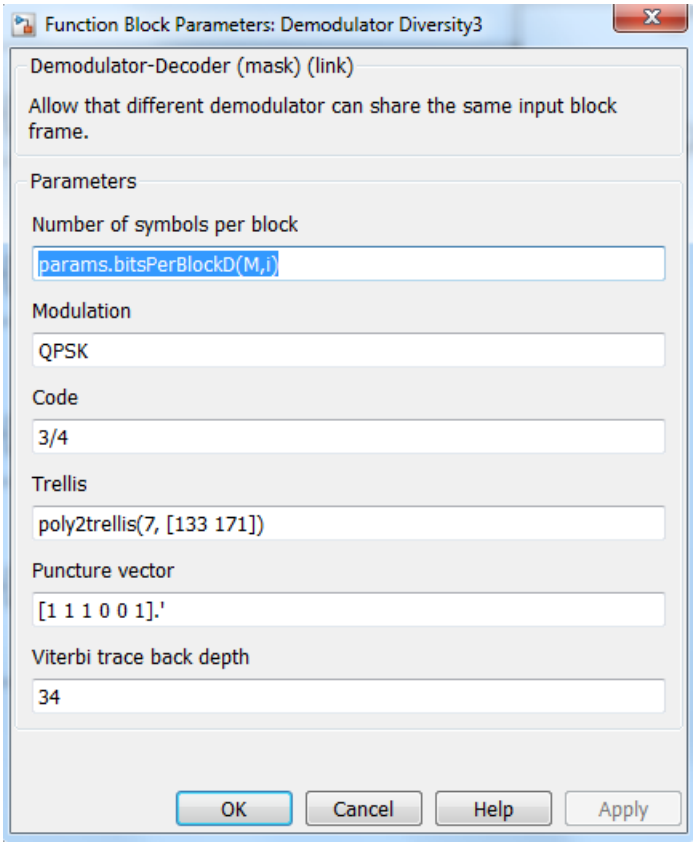

Figure 5.4: Demodulator Diversity block interface

5.2 System Blocks

This section is dedicated to explain the used block in the simulation, starting to OFDM transmitter blocks, Channel blocks and finally the OFDM receiver blocks.

OFDM Transmitter blocks

The blocks which are included in OFDM Transmitter block are Mapping, Frequency Diversity Multiplexing and OFDM modulator. Apart from them, the Variable Binary Data Source is explained in this section as well. In summary, the blocks of the OFDM Transmitter are shown

(5.5)

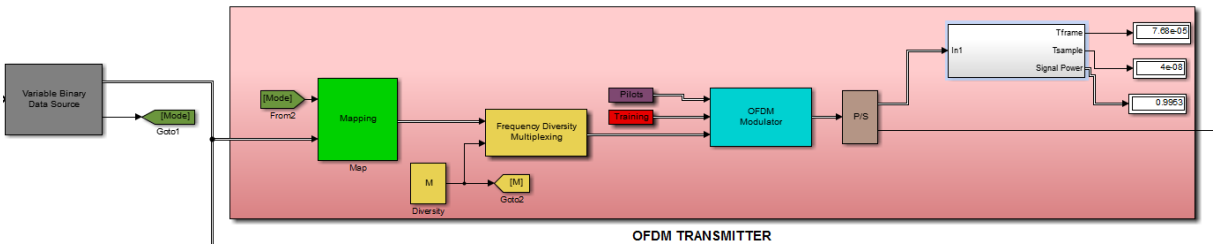

Figure 5.5: OFDM Transmitter

A random variable binary data is created by the block Variable Binary Data Source, depending on the chosen mode and the frequency order. There are four orders of frequency diversity (M) that are related to the number of a symbol is multiplexed at different subcarriers. M value belongs to integer number included in $[1, 4]$, being 4 the time that more a symbol is multiplexed at different subcarriers. The bit stream data is lead to the input mapping block which encodes and modulates it, giving as result a complex symbol stream. The complex symbol stream is multiplexed according to the order of the frequency diversity. OFDM modulator has the task to assemble the complex data symbols, the training symbols and the pilots in the same manner as (2.15), (2.12). Afterwards, the serial to parallel conversion is applied for the OFDM symbols which are D/A converted, quadrature modulated, upconverted to RF and sent through the communication channel.

- **Variable Binary Data Source block**

The binary data has the constraint that the output of the channel always have to be a constant sample rate equal to 25 Msps given by the system specifications. In order to accomplish this specification (sampling frequency of the USRP2), the bit time has to change constantly each time that the mode (modulation and coding) is changed. The binary data source is given by Bernoulli Binary Generator block that generate equiproblable bits. The number of generated bits and the bit time are given by the following variables.

$$N_{bitsPerBlock} = N_{BitsperOFDMsym} \cdot N_{OFDMsymFrame} \tag{5.1}$$

where $N_{BitsperOFDMsym}$ is the number of coded bits per OFDM symbol, in other words,

$$N_{BitsperOFDMsym} = N_{SD} \cdot N_{txBitsSymbol} \cdot r \tag{5.2}$$

where r is the code rate. On the other hand, the tramission period of this block corresponds with,

$$T_{Block} = N_{bitsPerBlock} \cdot T_b \tag{5.3}$$

Apart of this, the OFDM transmission time (2.56) is taken as

$$T_{OFDM} = (L_{FFT} + L_{CP})T_s \tag{5.4}$$

where, $T_s = \frac{1}{F_s}$.

Therefore, the bit rate is defined as the number of transmitted coded bits over OFDM transmission time .

$$\begin{aligned} R_b &= \frac{N_{BitsperOFDMsym}}{T_{OFDM}} \\ &= \frac{N_{SD} \cdot N_{txBitsSymbol} \cdot r}{(L_{FFT} + L_{CP}) \cdot T_s} \text{ if } T_b = \frac{1}{R_b} \\ T_b &= \frac{(L_{FFT} + L_{CP}) \cdot T_s}{N_{SD} \cdot N_{txBitsSymbol} \cdot r} \end{aligned} \tag{5.5}$$

If a frequency diversity of M order is applied the transmission bit rate is degraded by the factor M compared to the conventional OFDM system.

$$R_b^M = \frac{R_b}{M} \tag{5.6}$$

Given by the system characteristics, $T_s = \frac{1}{F_s} = 0,4\ ns$ must to be a constant but all the other parameters can be changed depending on the Channel State Information (CSI). By the equation (5.5), the variable data source can be generated obtaining with any mode the same frequency sample $F_s = 25\ Msps$ at input DAC.

- **Mapping block**

This block performs the codification and the modulation of the bit stream by using four Modulator blocks from the CommOFDM library. Each one of them develops the corresponded task depending on the mode on that the system works. To create appropriately the mapping block, it is necessary to fill the modulator block parameters such as number of symbol per block with diversity M, modulation, code rate, trellis structure and puncture vector. To encode data with a convolutional encoder Trellis structure parameters is used with constraint length and code generator equal to 7 and [133 177] respectively. The puncture pattern is specified by the punctured vector parameter. The puncture vector is a binary column vector. A "1" indicates that the bit in the corresponding position of the input vector is sent to the output vector and with "0" the bit is removed. Puncturing is a technique that allows the encoding and decoding of higher rate codes using standard rate 1/2 encoders and decoders defined by the punctured vector [1]. In the figure 5.3 the punctured vector is [1 1 1 0 0 1], it means that the bit in positions 4 and 5 are removed. As a result, for every 3 bits of input, the punctured vector generates 4 bits of output. This makes the rate $\frac{3}{4} = \frac{3}{2} \cdot \frac{1}{2}$.

Modulation part is defined by the QAM modulator baseband so if BPSK is desired the M-ary number parameters must be 2 and for a QPSK 4. Obtaining constellations with gray ordering as A.1 and A.2.

System blocks of the Modulator block is shown in the figure (5.6)

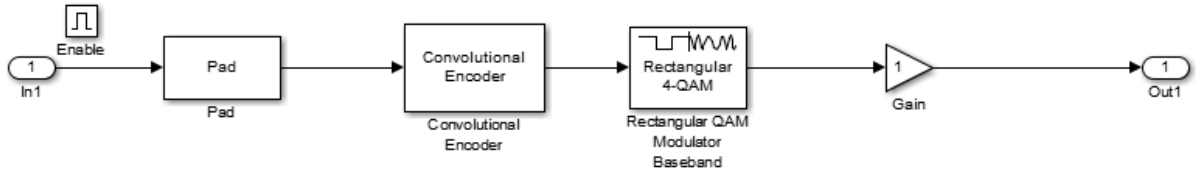

Figure 5.6: System block Modulator block

- **Frequency Diversity block**

Considering the easy possibility of sending the same symbols at different subcarriers, Frequency Diversity block performs this task depending on the diversity order, the block responds sending many times the symbol as order has been chosen, e.g., for $M = 2$ the symbols are sent twice, one at the negative subcarriers and the other at the positive subcarrier: For $M = 3$ the symbol is sent thrice and for $M = 4$ four times, splitting the transmission bandwidth as many times as the diversity order. This technique was explained in (4.4) which increases the possibility to receive a symbol since the probability that the frequency selective fading may attenuate all of the subcarriers is smaller than when a symbol is sent at only one subcarrier.

The system blocks of the Frequency Diversity block is detailed by the following figure 5.7

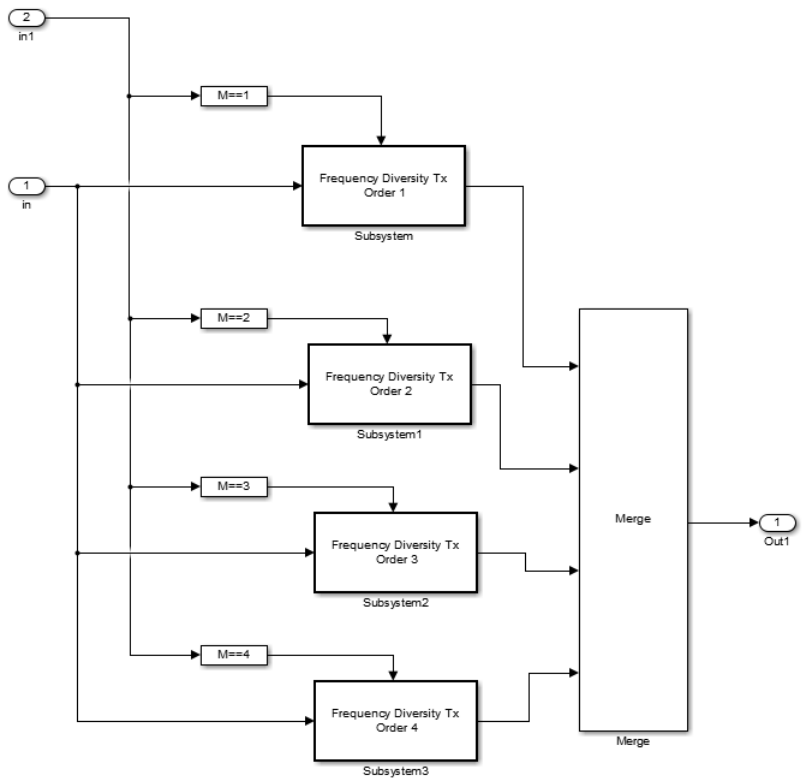

Figure 5.7: Frequency Diversity Multiplexation block

- **OFDM Modulator block**

The construction of the frame (figure 2.15) is characterized by the OFDM Modulator block, the pilots arrangement, the training sequences and zero padding are assembled here, then the stream is reordered with the aim of applying the IFFT. The bit stream is mapped with PSK scheme (Mapping block), and then those data are modulated by means of an IFFT on N-parallel subcarriers (2.5). Resulting in a complex time domain OFDM symbol that is cyclically extended to avoid the ISI and parallel-to-serial converted to transmit through the communication channel.

To perform all this, PSK-symbols and pilots are vertically concatenated in column vector and placed in the same way as the figure 4.6, then the training symbol is horizontally concatenated at the left side of the column vector to get a frame as figure 2.15. Then, Zero Padding is applied and shifting the index vector for IFFT. Its means to place all the negative subacarries in the right side of the interval $[1, NFFT]$ starting from $NFFT/2 + 1$. At this point, the IFFT can be applied over the steam, obtaining the complex time OFDM symbol that is then normalized.

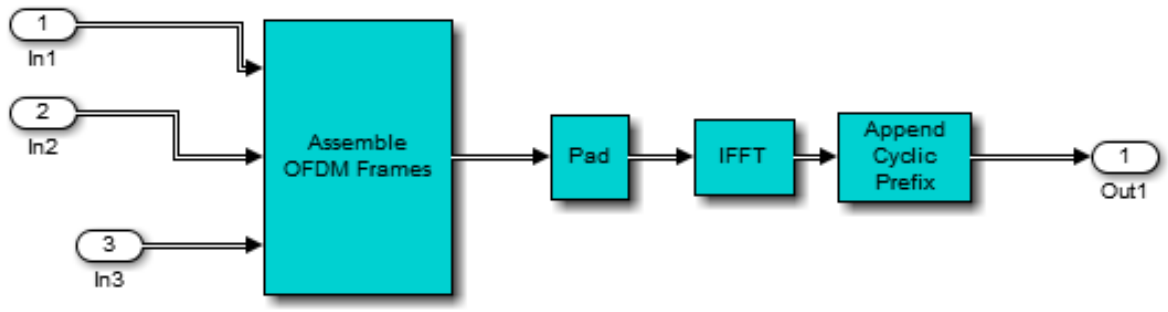

Figure 5.8: OFDM modulator block

OFDM Receiver blocks

By means of the OFDM receiver blocks, the simulation of an OFDM receiver is implemented. The complex timing symbol stream provided by the OFDM transmitter must be properly demodulated in the OFDM receiver. The stream in the OFDM receiver must be sampled and A/D converted. Sample clock of the A/D converter in the receiver must be with the same frequency as in the transmitter. A difference in sample clocks generates ISI creating rotation of PSK constellation. Therefore, before demodulating the received OFDM signal, the receiver has to make the symbol and frequency synchronization (Timing-Frequency synchronization block). Additionally, if burst transmission scheme is used a frame timing synchronization is needed (Frame synchronization block). The synchronization should be done to remove appropriately the cyclic prefix. The reason for using the CP is that the symbol boundary can be estimated, however a small error in symbol boundary estimation can occur but it can be corrected by the frequency domain equalizer. Now to separate data streams the FFT is used obtaining N orthogonal subcarriers (OFDM demodulator block), after that the channel estimation in frequency domain can be estimated with the aim of doing a frequency equalization (Channel estimation and Frequency equalization block). Once the equalized symbols are achieved, the frequency

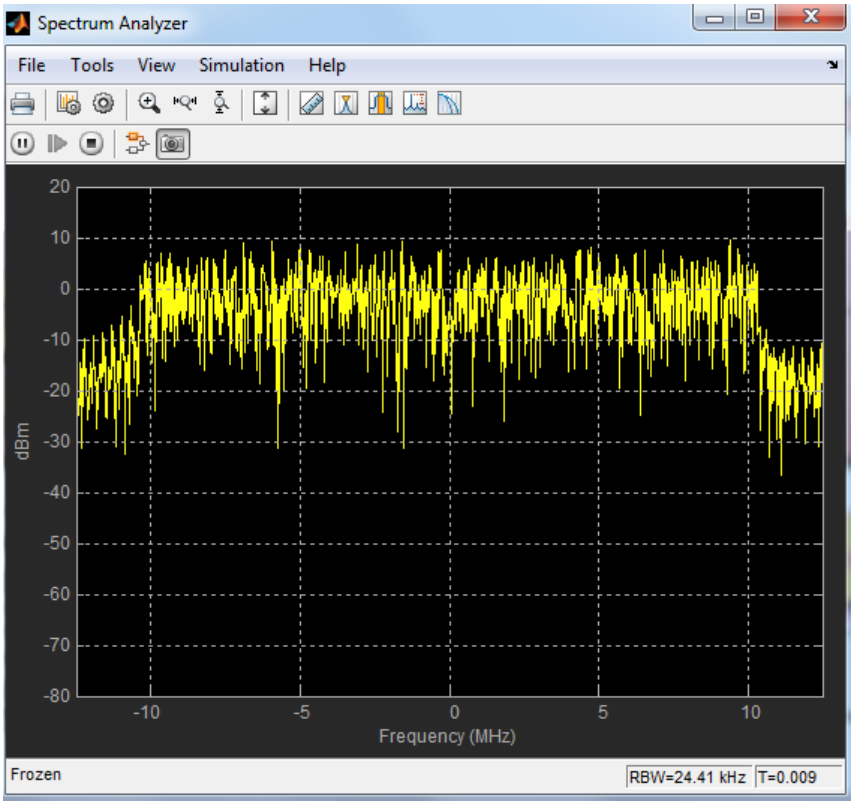

Figure 5.9: OFDM Transmitted Baseband Signal

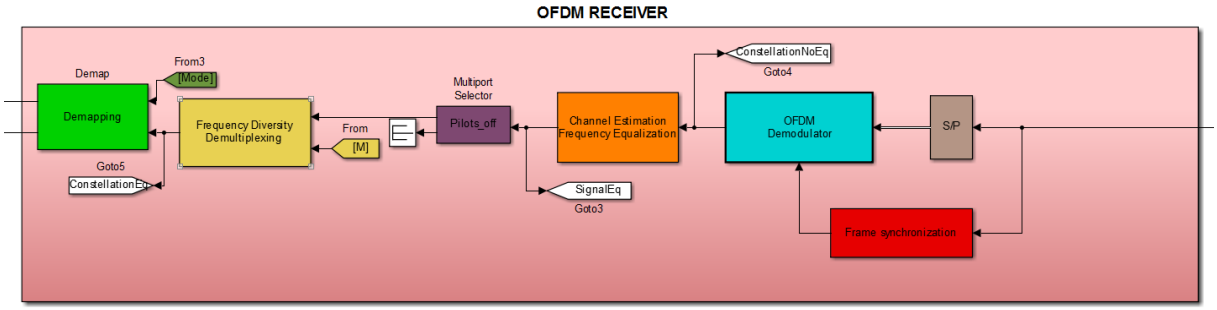

Figure 5.10: OFDM Receiver blocks

diversity demultiplexing can be applied, the new symbol is obtained by means of the average of the equalized symbols. Afterwards, the complex symbol is processed by the Demapping block that demodulates and decodes the symbols converting them in bit streams that subsequently are compared with the same bit streams but have not been transmitted. Hence, a BER can be obtained.

Four main synchronization tasks to be handled in OFDM communication systems which are :

- **Frame synchronization block**

Since the channel only allows OFDM symbols, a frame synchronization is needed at the receiver because the data at the receiver is processed as frames, and not symbols. This is

necessary because our system works with block of OFDM symbol exactly with a block of 24 OFDM symbols. The algorithm proposed in (4.2) is developed by the Frame synchronization block. Basically, the frame waits until 24 OFDM symbols to activate the OFDM modulator block since it processes the data in frames, that is defined in Simulink as a frame-based processing. By means of the auto-correlation the received data can obtain high correlation peaks when the training symbols are alignment. The Frame synchronization block can be performed the synchronization in two different manners. One of them, is performed by the auto-correlation of the received data and the another is the cross-correlation of the training sequences and the received data. I chose the first one, since the estimation is finer. In the figure 5.11, the system blocks of the Frame synchronization block is detailed and the result of the Frame synchronization output by auto-correlation and by cross-correlation can be shown in figure 4.4 and figure 4.5 respectively. The OFDM symbol period is $3.2\ \mu s$ so the OFDM block period is equal to $T_{OFDM_{block}} = 24 \cdot T_{OFDM} = 76.8\mu s$ this can be showed at the cursor measurements of the time scope viewer.

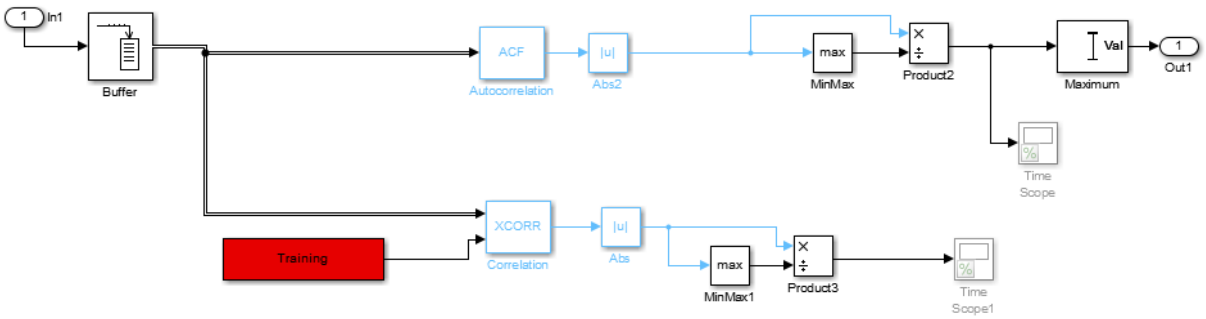

Figure 5.11: Frame Synchronization block

- **OFDM demodulator block**

This block is performed by the OFDM demodulator Simulink block, to use this block it is very important that its parameters are well chosen. Its parameters are the FFT length, number of guard bands, cyclic prefix length, number of receive antennas as well as enable the pilots signal output to separate it from the data signal after demodulation. The settings of the OFDM demodulator parameters is obtained in the same way that the figure 5.12 shows.

- **Channel Estimation and Frequency Equalization block**

The stream of complex symbols at the output of the OFDM demodulator block is driven to the Channel Estimation and Frequency Equalization block. Hereby, the channel estimation (4.3) and equalization (4.5) can be performed.

In (4.3) the channel estimation using the LS estimator given a training sequence was explained. The channel coefficients are obtained dividing the received data symbol by the training symbol. The equalizer coefficients are obtained by the equation (4.23) and the equalization is performed by a Zero Forcing. The figures 5.13 and 5.14 simulate this behavior.

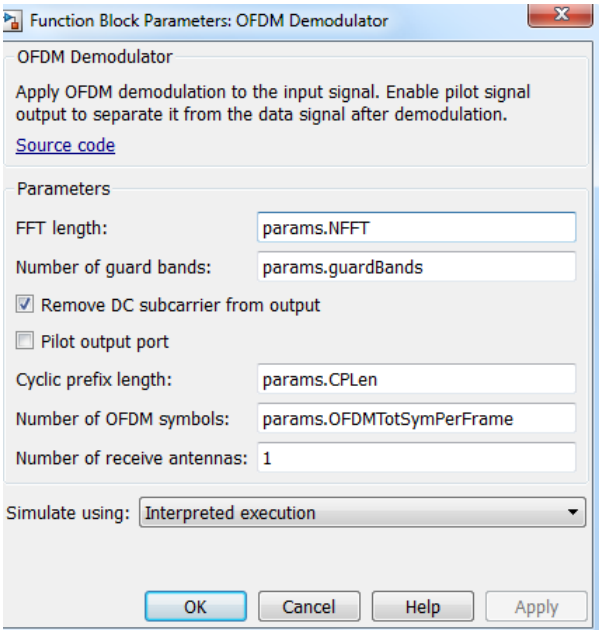

Figure 5.12: OFDM demodutor setting

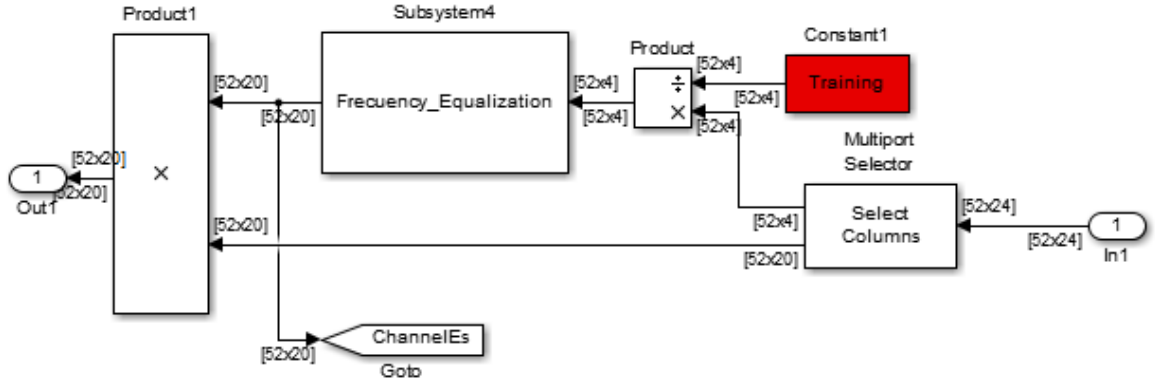

Figure 5.13: Channel Estimation Frequency Equalizer block

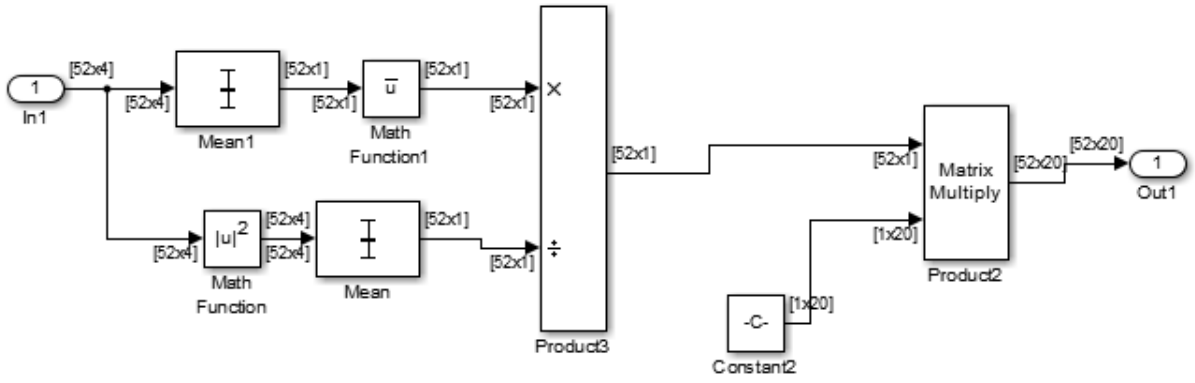

Figure 5.14: Frequency Equalization

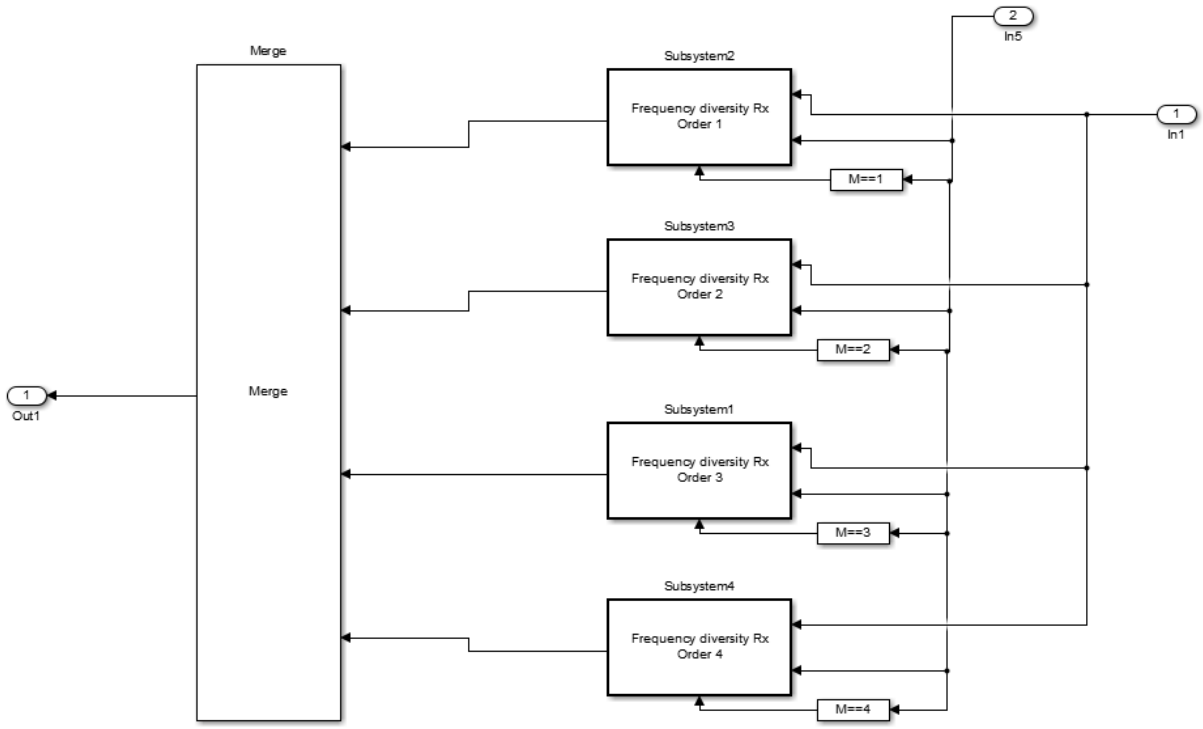

Figure 5.15: Frequency Diversity Demultiplexing block

- **Frequency Diversity Demultiplexing block**

As it has been said before, Frequency Diversity Demultiplexing block has the task to obtain the transmitted symbol from the different transmitted branches. As the received symbols in this block are already equalized. With a simple average of symbol in the different breaches, the transmitted symbol is obtained as following

$$y[k] = \frac{1}{M} \sum_{m=1}^{M} \hat{\alpha}[k,m] q[k,m] \tag{5.7}$$

The figure (5.15) represents the effect of the frequency diversity in the receiver.

- **Demapping block**

At this point, the demapping over the symbols $y[k]$ can be accomplished. The Demapping block performs the decoding and demodulation tasks using the block Demodulator Diversity from the CommOFDM library those tasks and setting its parameters as in figure 5.4. The aspect of the Demaping block is displayed in figure 5.17 and the demodulator diversity block in figure 5.16.

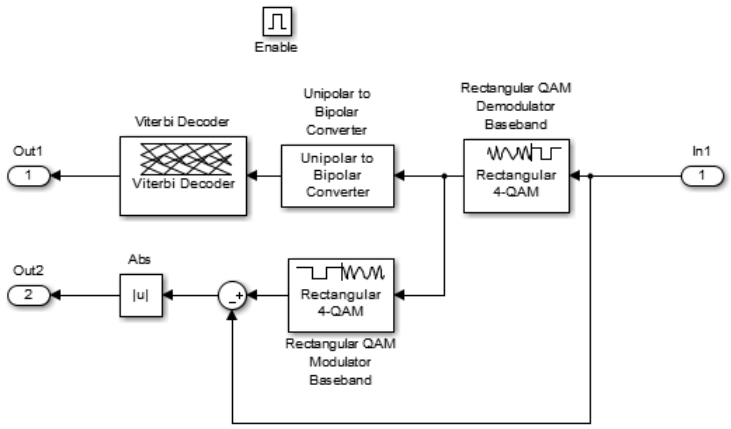

Figure 5.16: Demodulor Diversity block

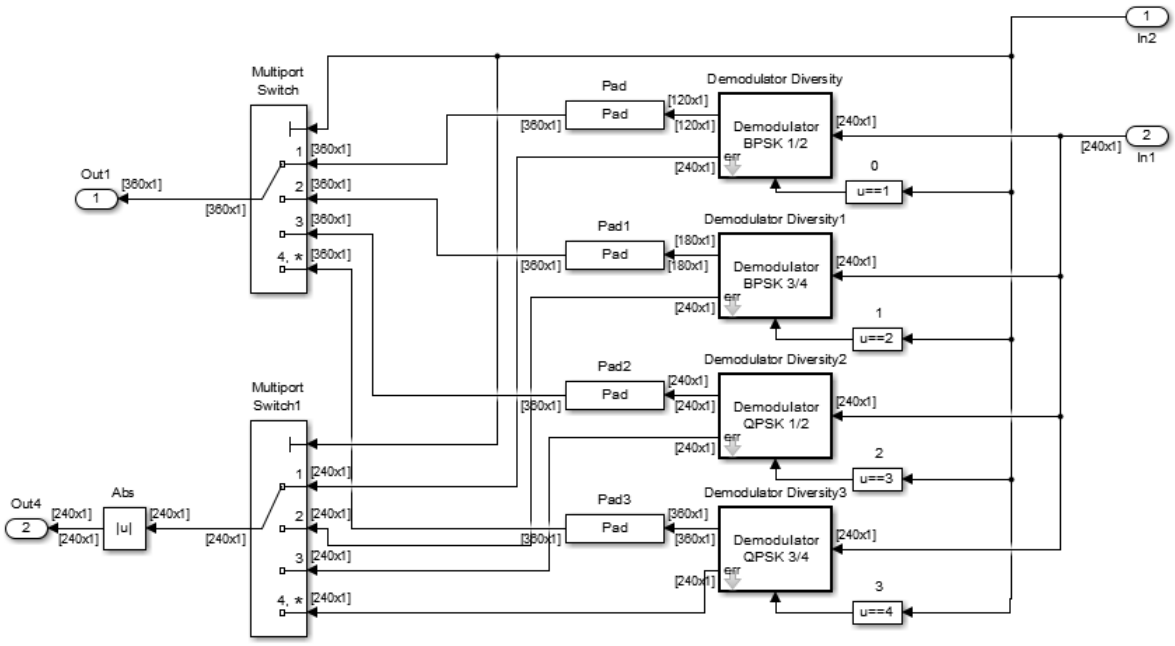

Figure 5.17: Demapping block

As it is shown in the figure 5.16, there is a subtraction which is applied to estimated the error variances of the samples and then the SNR can be estimated.

- **Timinig-Frequency Estimation block**

In this block, The Timing-Frequency Estimation is performed, the ML estimation is applied over the received samples. The block works according with the equations in section 4.2. To evaluated the timing-frequency estimation by Simulink, two block were used the variable fractional delay and the Phase/Frequency offset. The figure 5.18 shows the variable fractional delay blocks to force a symbol time offset (STO) and the Phase/Frequency offset block to

produce a carrier frequency offset (CFO). In this example, the output of the channel node to node prototype block is delayed 30 samples. As result of it , the block estimate in samples this STO as it can seen in the display.

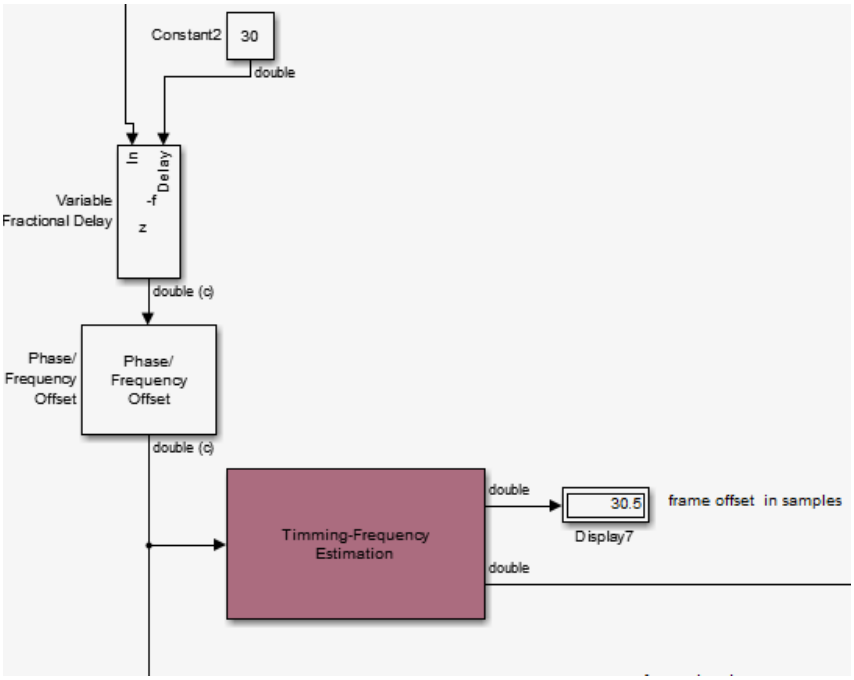

Figure 5.18: Timing offset estimation in samples

The equations (4.6) and (4.5) are simulated by the estimator block. The estimator has the following architecture in Simulink.

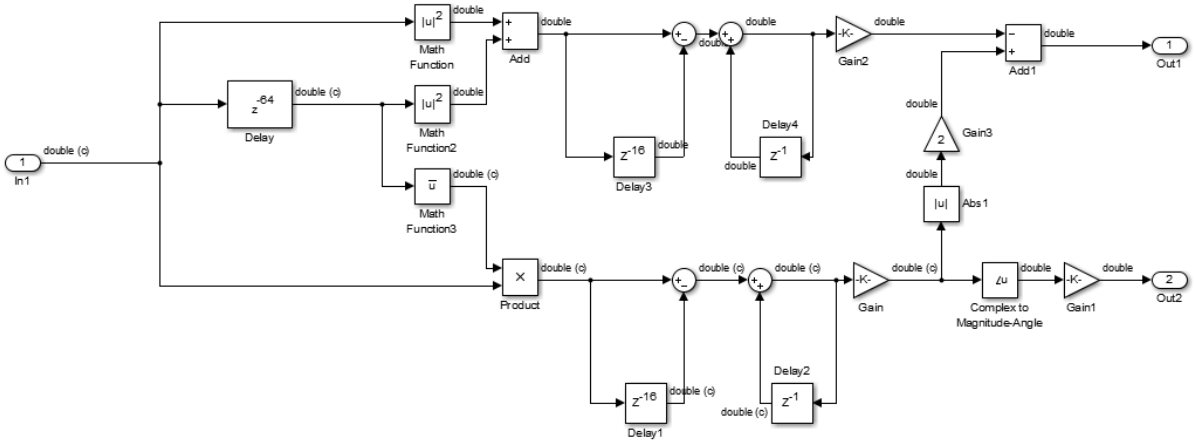

Figure 5.19: Overview of the ML estmiates in Simulink

The signal that generate the ML-estimates for 60 OFDM symbol and without forcing neither STO nor CFO can be seen in figures A.5, A.4.

5.3 Bit Error Rate (BER)

The BER was calculated with the Monte Carlo method provided by the BERTool environment to evaluate the performance of the Simulink model. The performance for an AWGN channel joint with the Node to Node channel is simulated. BERTool in conjunction with the Simulink model can be generated BER data. The Simulink model (A.3) simulates the communications system between one Battery Control unit (BCU) and one Cell Service Units(CSU) whose I want to study. BERTool manages the Simulink model and collects the data with the aim of doing a graphic representations. Moreover, the simulation is evaluated in frame-based since it often runs faster than Sample Based. I used the following criteria to obtain the BER data with Frequency Diversity.

- Eb/No range 0:6 dB
- Number of errors 100
- Maximum number of bits processed 10^6
- Channel 6

The result of these simulations are represented in the figures 5.21, 5.22, 5.23, 5.24.

Analyzing the BER results, it can be concluded that applying Frequency Diversity all the modulation in all the evaluated channels their BER decreases. By looking the BER at Eb/No 3 dB and 6 dB in Figure 5.21, it is observed that increasing the relation Eb/No the BER decreases a factor 10^3 for $Eb/No = 3\ dB$ comparing with the maximum Frequency Diversity $M = 4$ and without $M = 0$, for $Eb/No\ = 6$ decrease a factor 10^5. In addition if the figure 5.21 is compared with figure 5.22 it can be observed that the more robustness mode $BPSK\ \frac{1}{2}$ and $M = 4$ with $BER \approx 7 \cdot 10^{-4}$ at $Eb/No = 3\ dB$ dB gains 3 dB compared with $BPSK\ \frac{3}{4}$ and $M = 4$ with $BER \approx 6 \cdot 10^{-4}$ at $Eb/No = 6\ dB$. Thus, to guarantee a $BER = 10^{-3}$ the most robust mode ($BPSK\ \frac{1}{2}$) needs 3 dB less than $BPSK\ \frac{3}{4}$ and $M = 4$ so it can be maintained a $BER = 10^{-3}$ with 3 dB less of Eb/No but the price to obtain this results is paid decreasing the data rate. Obtaining a compromise between Eb/No and bit rate R_b. Analyzing the figures 5.23, 5.24. It is important to restate that all the modes (modulation and coding) imply a decrement of BER value when the Eb/No is incremented. Apart from it, all the modes without diversity manifest almost the same behavior, it is due to the range of Eb/No not being enough to see how it decreases the BER of the modes without Frequency Diversity. If the figure 5.20 is analyzed, it can observed that the best performance is provided by BPSK 1/2 since it is the most robust mode (1 code bit for 1 data bit) although with lowest data rate. $QPSK\ \frac{3}{4}$ (highest data rate) presents a $BER = 10^{-3}$ at $Eb/No = 13dB$ while with a $BSPK\ \frac{1}{2}$ at the same Eb/No the $BER = 10^{-6}$. The criteria used to evaluate the BER without Frequency Diversity was.

- Eb/No range 0:13 dB
- Number of errors 100

- Maximum number of bits processed $4 \cdot 10^6$

- Channel 25

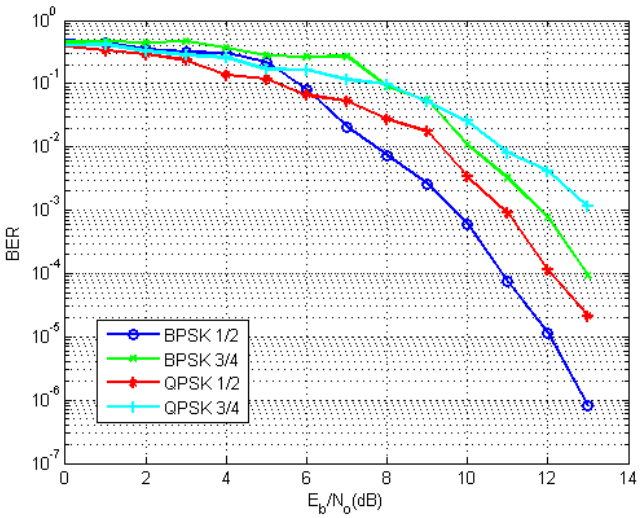

Figure 5.20: BER without Frequency Diversity

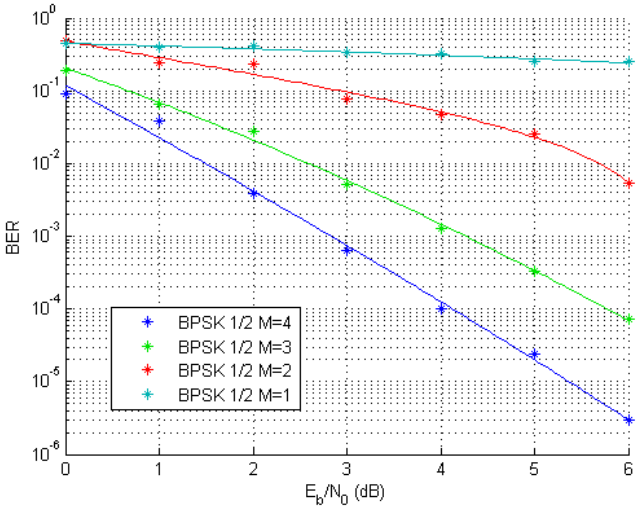

Figure 5.21: BPSK $\frac{1}{2}$ with Frequency Diveristy

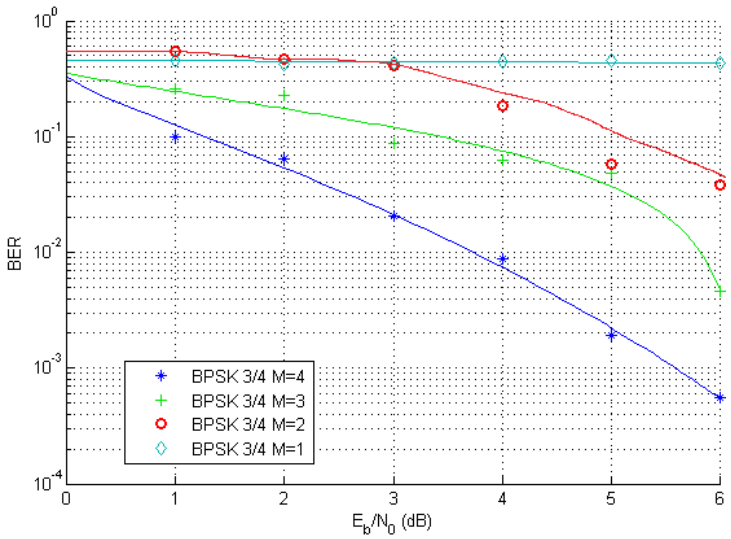

Figure 5.22: BPSK $\frac{3}{4}$ with Frequency Diveristy

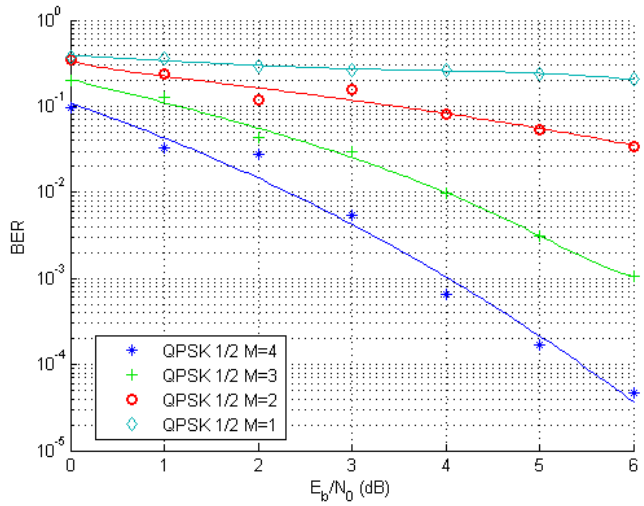

Figure 5.23: QPSK $\frac{1}{2}$ with Frequency Diversity

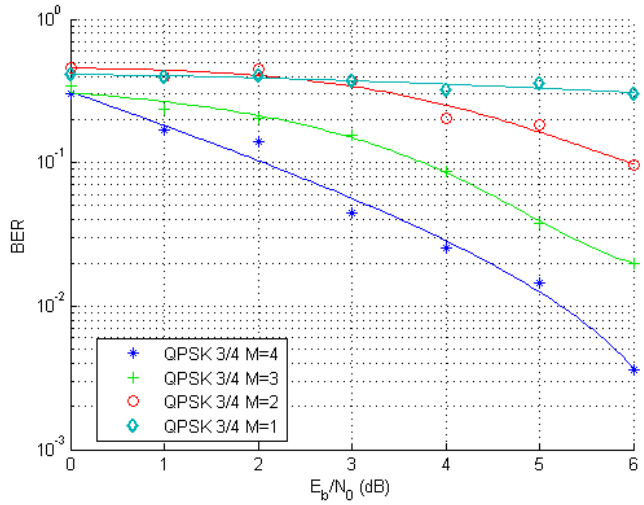

Figure 5.24: QPSK $\frac{3}{4}$ with Frequency Diversity

Chapter 6

Conclusion and Future Work

- **Conclusion**

In this thesis, the simulation of the performance of an OFDM system with frequency diversity inside the battery emulator was proposed. The cyclic prefix plays an important role avoiding the ISI as long as its duration is longer than the maximum delay spread of the channel, as well as eliminating the ICI when it is cyclically extended with the last L samples of symbol. The frame synchronization allows the data as frame, in this manner the channel estimation and frequency equalization can be performed in a frame-based mode. The timing-frequency estimation estimates the values of the symbol time offset and the carry frequency offset by using the Maximum Likelihood. The distorting events produced by the multipath propagation due to the presence of reflective objects (mainly metallic battery cell cans and housing) can be overcome with a correctly coding/decoding, channel estimation and frequency equalization. The use of coding guarantees more robustness at the system, transmitting redundancy over the data bit errors correction can be performed at the receiver. The price of transmitting this redundancy is reflected in the effective data rate. Moreover, to bring more robustness to the system, frequency diversity is applied to split the transmission bandwidth. Giving the option to transmit the same symbol at different subcarriers. The probability to not receive a symbol from two uncorrelated subcarriers is lower than when a symbol is transmitted only for a one subcarrier. However, the effective data rate is conditioned by the frequency diversity order as well. The BER shows how the system responds when different modes are applied (coding and modulation). In the case without frequency diversity, the more robustness coding is the BPSK 1/2, the best BER results but it is the encoder that applies the most redundancy, obtaining the lowest data rate. QSPK 3/4 requires more EbNo to achieve the same BER of the BPSK 1/2 but provides the highest data rate. In the case that frequency diversity is applied, the BER decreases significantly, the reason for this behavior is that the probability to receive the transmitted symbol correctly is greater than without the frequency diversity. Moreover, the frequency diversity demultiplexing is performed after the channel equalization so the symbols combined to obtain the transmitted symbol are therefore the equalized transmitted symbol assuming that the carrier frequency offset was compensated before.

Therefore, if it is fixed a data rate to the system, it has to adjust choosing the best mode to accomplish the requirement of data rate.

Finally, the mode should be selected choosing the best mode for the signal to noise ratio so there is a compromise between data rate and the signal to noise ratio.

- **Future work**

Based on this thesis some areas for further research are as follows:

1. The values of the timing and frequency estimation can be used to perform the timing-frequency synchronization.

2. In order to avoid the degradation of the transmission rate when it is used frequency diversity a more efficient modulation methods should be used (16-QAM or 64Q-AM). Apart from it, the implementation of a method of selecting the subcarrier adaptively depending on the channel transfer function requires that the receiver feeds back the transfer function to the transmitter. Then, extra traffic is produced on the channel but with the possibility to assign the best frequencies to transmit as long as transmitter-receiver share constantly the channel state information.

3. A hybrid synchronizer structure using both pilots and cyclic prefix could generate better timing-frequency estimation.

Appendix A

Simulink System Blocks

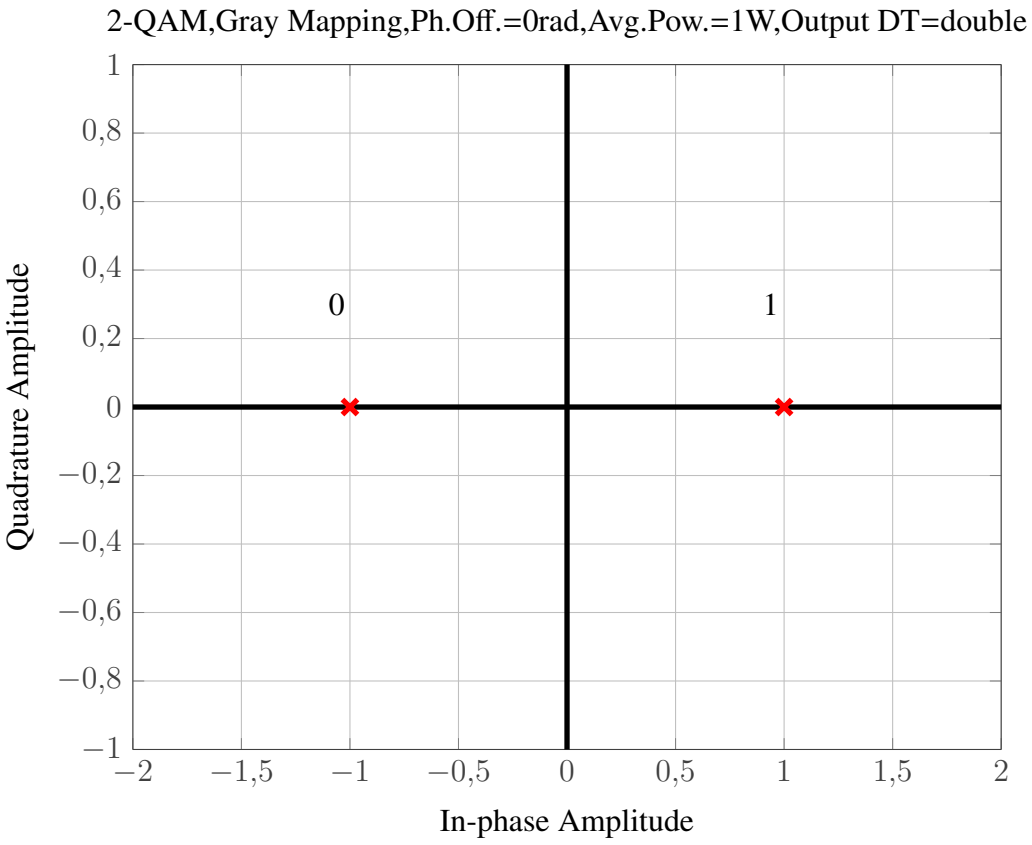

Figure A.1: QPSK modulation with Gray ordering

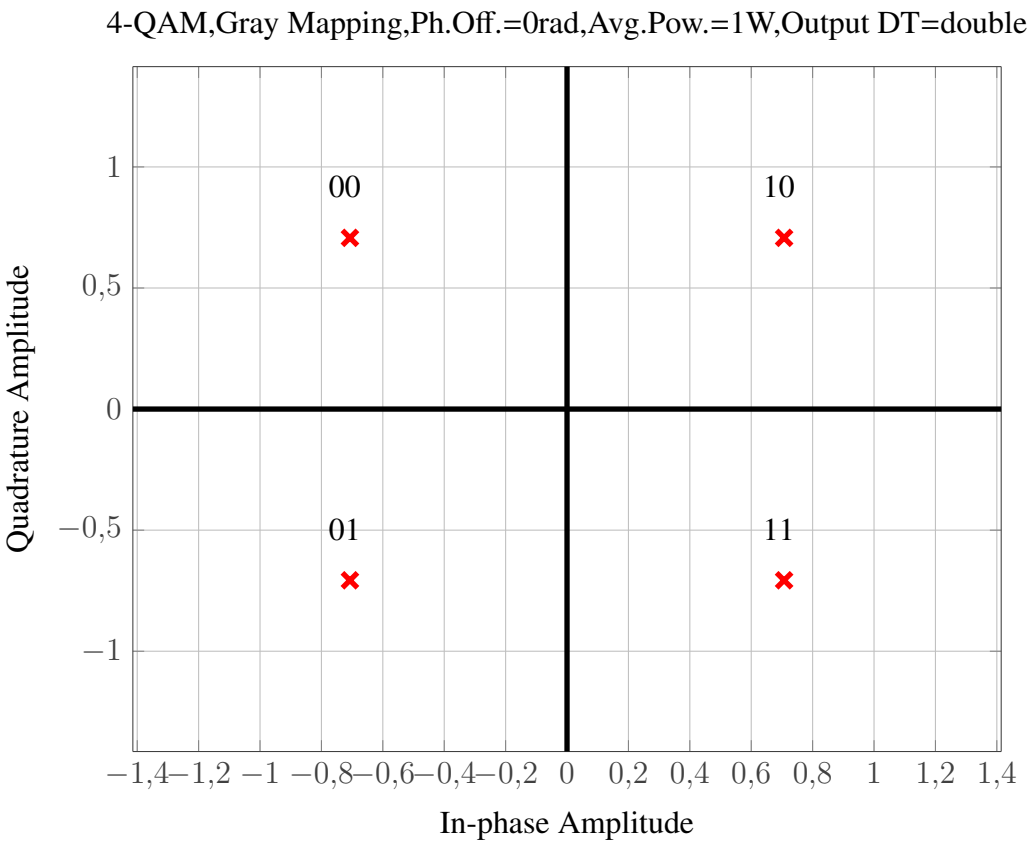

Figure A.2: QPSK modulation with Gray ordering

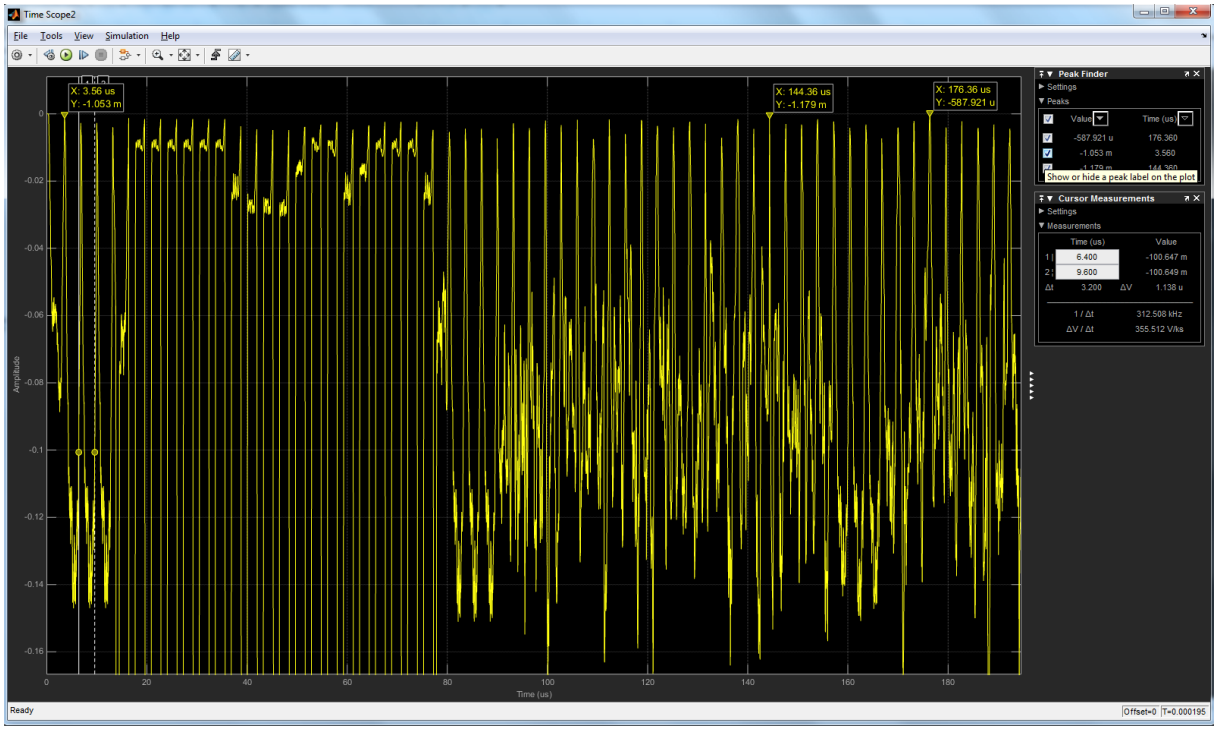

Figure A.4: ML Timing Estimation Signal ($N = 64,\ L_{CP} = 16$)

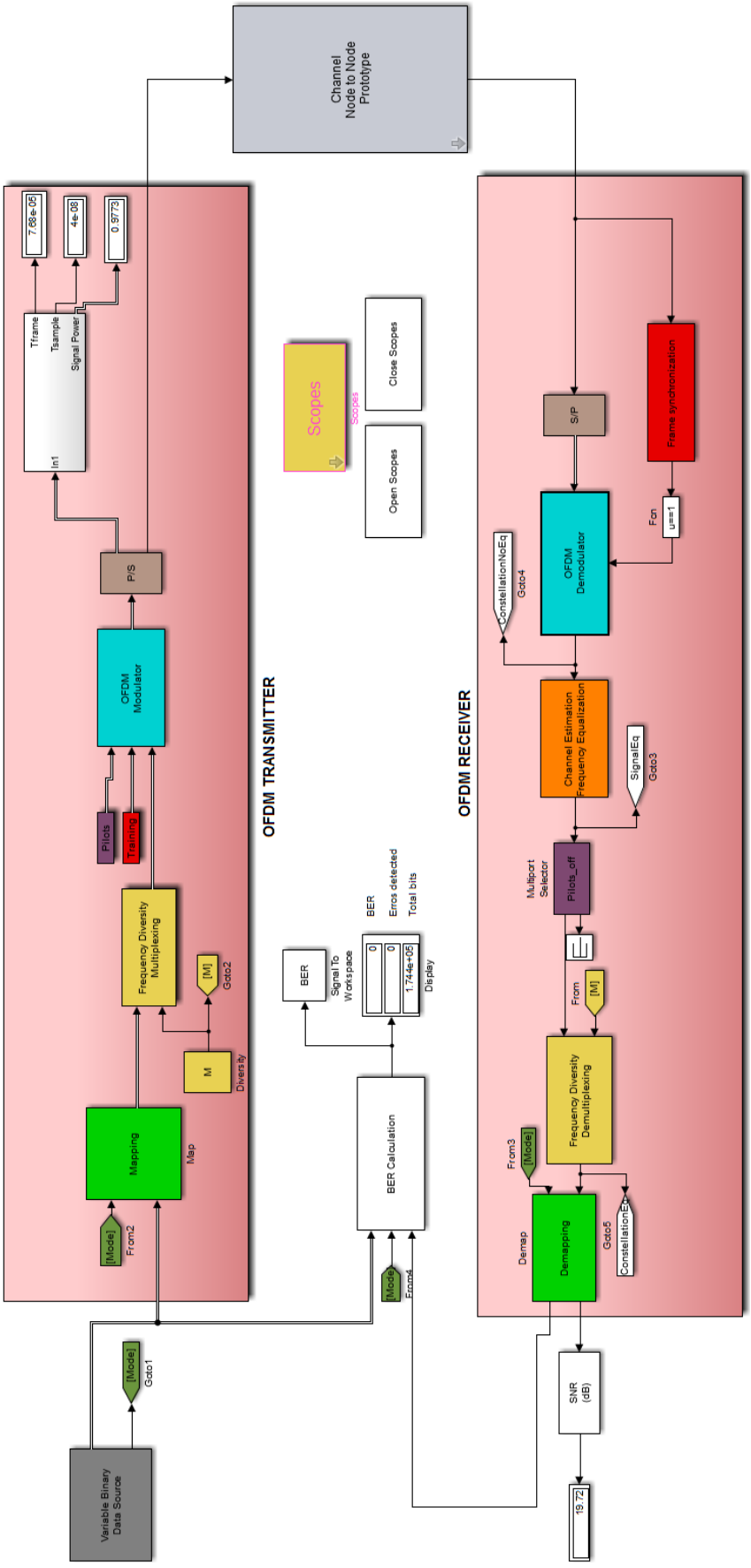

Figure A.3: Simulink OFDM with frequency diversity system model

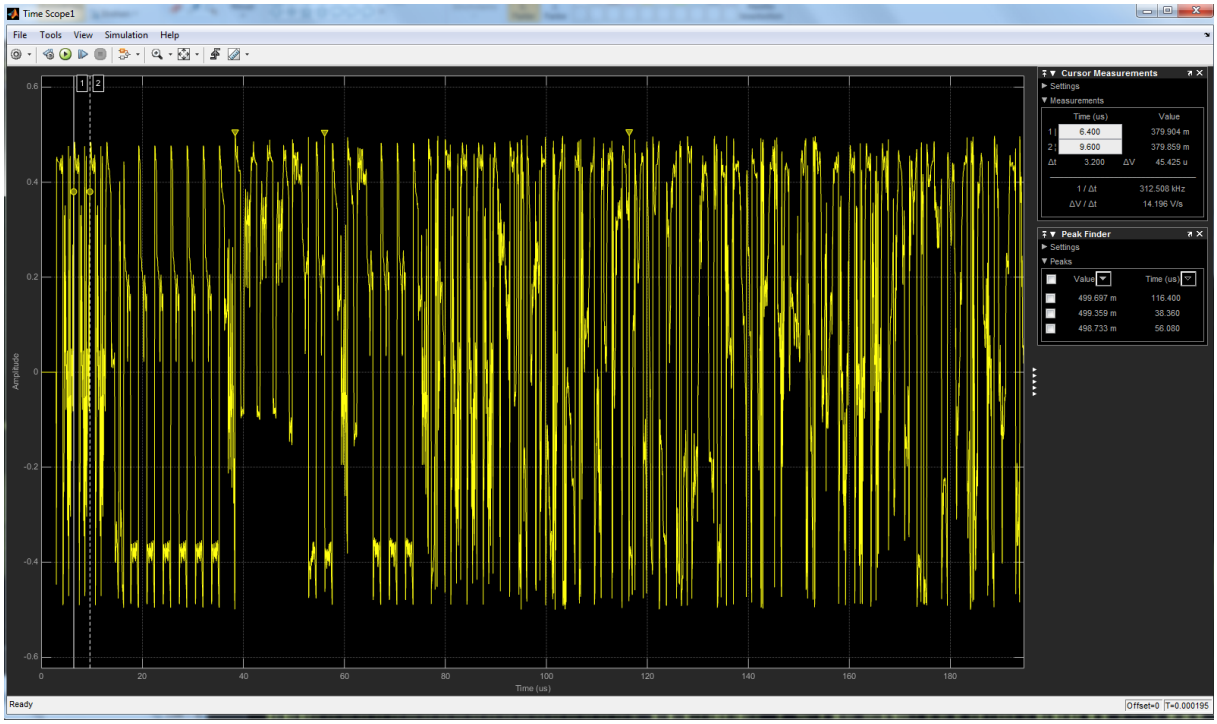

Figure A.5: ML Frequency Estmimation Signal ($N = 64,\ L_{CP} = 16$)

Appendix B

Matlab Scripts

```
1
2  function commOFDM_settings
3
4  p.M            = [ 1 2 3 4 ]; % Diversity Order
5  p.NFFT         = 64; % Number of points on FFT
6  p.NcyclicPrefix = 16; % Cyclic prefix length
7  p.guardBands   = [6; 5]; % Left and right guard bands
8  p.pilotIndices = [-21; -7; 7; 21]; % Pilot subcarrier indices
9  p.dataIndices  = setdiff([-p.NFFT/2+p.guardBands(1):-1, 1:p.NFFT/2-1-
       p.guardBands(2)], p.pilotIndices); % Data subcarrier       indices
10 p.NSD          = length(p.dataIndices);  % Number of data subcarriers
       per OFDM symbol
11 p.NSDD         = p.NSD./p.M;             % Number of data subcarriers
       per OFDM symbol with Frequency Diversity
12 p.NST          = p.NSD + length(p.pilotIndices);  % Number of data and
       pilot subcarriers per OFDM symbol
13 p.NFFT2 = p.NFFT + p.NcyclicPrefix;
14
15 % OFDM symbols
16
17 p.OFDMSymPerFrame    = 20; %OFDM Symbols Per Frame;
18 p.OFDMTrainPerFrame  = 4;  %OFDM Training Per Frame;
19 p.OFDMTotSymPerFrame = 24;
20
21 %Constellation symbols with diverstity M
22
23 p.numTxSymbolsD= p.NSDD * p.OFDMSymPerFrame;
24 p.numTrainingSymbols = p.NSD * p.OFDMTrainPerFrame;
25
26 % Modulator/demodulator banks
27
28 p.numModulators = 4;
29 p.txBitsPerSymbol = [1 1 2 2];
30 p.txBitsPerBlockD = [p.numTxSymbolsD(1) .* p.txBitsPerSymbol;...  %
       txBitperBlock Diversity
31                      p.numTxSymbolsD(2) .* p.txBitsPerSymbol;...
32                      p.numTxSymbolsD(3) .* p.txBitsPerSymbol;...
33                      p.numTxSymbolsD(4) .* p.txBitsPerSymbol];
```

```
34 p.modOrder = 2.^p.txBitsPerSymbol;
35 p.codeRate = [1/2 3/4 1/2 3/4];
36 p.bitsPerBlockD = [p.txBitsPerBlockD(1,:).* p.codeRate;...          %
       bitperBlock Diversity
37                   p.txBitsPerBlockD(2,:).* p.codeRate;...
38                   p.txBitsPerBlockD(3,:).* p.codeRate;...
39                   p.txBitsPerBlockD(4,:).* p.codeRate];...
40 p.bitsPerSymbol = p.txBitsPerSymbol .* p.codeRate;
41 p.maxBitsPerBlock = max(p.bitsPerBlock);
42 p.maxBitsPerBlockD = [max(p.bitsPerBlockD(1,:))...
43                       max(p.bitsPerBlockD(2,:))...
44                       max(p.bitsPerBlockD(3,:))...
45                       max(p.bitsPerBlockD(4,:))];...
46
47
48 % Frame size for variable rate source with Diversity M
49 p.nSourceD = [min( gcd( min(p.bitsPerBlockD(1,:)), p.bitsPerBlockD(1,:))
       )...
50               min( gcd( min(p.bitsPerBlockD(2,:)), p.bitsPerBlockD(2,:))
                     )...
51               min( gcd( min(p.bitsPerBlockD(3,:)), p.bitsPerBlockD(3,:))
                     )...
52               min( gcd( min(p.bitsPerBlockD(4,:)), p.bitsPerBlockD(4,:))
                     )];
53
54 % Source blocks per TX frame with Diversity M
55 p.nSD = [p.bitsPerBlockD(1,:)./p.nSourceD(1);...
56          p.bitsPerBlockD(2,:)./p.nSourceD(2);...
57          p.bitsPerBlockD(3,:)./p.nSourceD(3);...
58          p.bitsPerBlockD(4,:)./p.nSourceD(4)];
59
60 % Timing-related parameters
61
62 p.OFDMSymbolPeriod = 3.2e-6;
63 p.OFDMPilotPeriod  = p.OFDMSymbolPeriod*p.OFDMTotSymPerFrame./
       p.OFDMSymPerFrame;
64 p.blockPeriod      = p.OFDMTotSymPerFrame.*p.OFDMSymbolPeriod;
65 p.bitPeriod        = p.blockPeriod./ p.bitsPerBlock;
66 p.minBitPeriod     = min(p.bitPeriod);
67
68 % Timing-related parameters with Diversity M
69
70 p.bitPeriodD        = p.blockPeriod./ p.bitsPerBlockD;
71 p.minBitPeriodD     = [min(p.bitPeriodD(1,:));min(p.bitPeriodD(2,:));min
       (p.bitPeriodD(3,:));min(p.bitPeriodD(4,:))];
72
73 % TX indices
74
75 p.TXFFTShiftIndices = [p.NST/2+1:p.NFFT 1:p.NST/2];
76 p.TXCyclicPrefixIndices = [p.NFFT-[p.NcyclicPrefix-1:-1:0] 1:p.NFFT];
```

```
77
78 % RX indices
79
80 p.RXCyclicPrefixIndices = [p.NcyclicPrefix+1:p.NFFT2];
81 p.RXSelectFFTIndices = [p.NFFT-[p.NST/2-1:-1:0] 1:p.NST/2+1];
82
83 % Channel sample period
84
85 p.chanSamplePeriod = p.blockPeriod/(p.OFDMTotSymPerFrame * (p.NFFT +
       p.NcyclicPrefix));
86
87 % Viterbi trace back depth and link delay
88
89 vtbd=34;
90 vtbd_set = vtbd(ones(1, p.numModulators));
91 p.vtbd_set = vtbd_set;
92 p.link_delay = vtbd_set;
```

Bibliography

[1] Create a complex baseband-equivalent model. Technical report. Also available as http://www.mathworks.de/de/help/simrf/ug/create-a-complex-baseband-equivalent-model.html.

[2] Decode convolutionally encoded data using viterbi algorithm. Technical report. Also available as http://www.mathworks.de/de/help/comm/ref/viterbidecoder.html.

[3] Polynomial description of a convolutional code. Technical report. Also available as http://www.mathworks.de/de/help/comm/ug/error-detection-and-correction.html#fp7431.

[4] Signal model and system definition. Technical report. Also available as http://www.tdx.cat/bitstream/handle/10803/6886/04Hidw04de10.pdf?sequence=4.

[5] Working Group, IEEE 802.11 a et al. Ieee standard for information technology- telecommunications and information exchange between systems-local and metropolitan area networks-specific requirements-part 11: Wireless lan medium access control (mac) and physical layer (phy) specifications. *IEEE Std 802.11-1997*, pages i–445, 1997.

[6] A.Aboltins, D.Klavins. Synchronization for ofmd-based communication system: A brief overview. pages 1–5. IEEE, 2000.

[7] Alex, Sam P and Jalloul, Louay MA. Performance evaluation of mimo in ieee802. 16e/wimax. *Selected Topics in Signal Processing, IEEE Journal of*, 2(2):181–190, 2008.

[8] Alonso, Damián, Opalko, Oliver, Sigle, Martin, and Dostert, Klaus. Towards a Wireless Battery Management System: Evaluation of Antennas and Radio Channel Measurements Inside a Battery Emulator. In *IEEE 80th Vehicular Technology Conference: VTC2014-Fall*, Vancouver, Canada, 2014.

[9] Arslan, HUSEYIN et al. Channel estimation for wireless ofdm systems. *IEEE Surveys and Tutorials*, 9(2):18–48, 2007.

[10] Bossert, M, Donder, A, and Zyablov, V. Improved channel estimation with decision feedback for ofdm systems. *Electronics Letters*, 34(11):1064–1065, 1998.

[11] Bottomley, Gregory E, Ottosson, Tony, and Wang, Y-PE. A generalized rake receiver for interference suppression. *Selected Areas in Communications, IEEE Journal on*, 18(8):1536–1545, 2000.

[12] Cabrera, Margarita. *Tema 5: Modulaciones Avanzadas: OFDM*. ETSETB-UPC, 2009.

[13] Coleri, Sinem, Ergen, Mustafa, Puri, Anuj, and Bahai, Ahmad. Channel estimation techniques based on pilot arrangement in ofdm systems. *Broadcasting, IEEE Transactions on*, 48(3):223–229, 2002.

[14] Edfors, Ove, Sandell, Magnus, Beek, J-J Van de, Wilson, Sarah Kate, and Borjesson, Per Ola. Ofdm channel estimation by singular value decomposition. *Communications, IEEE Transactions on*, 46(7):931–939, 1998.

[15] Feher, Kamilo. *Telecommunications measurements, analysis, and instrumentation*. SciTech Publishing, 1997.

[16] Feng, Shi, Dengpeng, Hu, and Eryang, Zhang. A low-complexity channel estimation method for ieee802. 11a and hiperlan/2 wlans. In *Communication Software and Networks, 2010. ICCSN'10. Second International Conference on*, pages 276–279. IEEE, 2010.

[17] Goldsmith, Andrea. *Wireless communications*. Cambridge university press, 2005.

[18] Harjula, Ilkka, Mammela, A, and Li, Zhenhong. Comparison of channel frequency and impulse response estimation for space-time coded ofdm systems. In *Vehicular Technology Conference, 2002. Proceedings. VTC 2002-Fall. 2002 IEEE 56th*, volume 4, pages 2081–2085. IEEE, 2002.

[19] Heiskala, Juha and Terry Ph D, John. *OFDM wireless LANs: A theoretical and practical guide*. Sams, 2001.

[20] Hlawatsch, F. and Matz, G. *Wireless Communications over Rapidly Time-Varying Channels*. Academic Press, Amsterdam, The Netherlands, 2011.

[21] Jeon, Won Gi, Paik, Kyung Hyun, and Cho, Yong Soo. An efficient channel estimation technique for ofdm systems with transmitter diversity. In *Personal, Indoor and Mobile Radio Communications, 2000. PIMRC 2000. The 11th IEEE International Symposium on*, volume 2, pages 1246–1250. IEEE, 2000.

[22] Jianhua, Zhang and Ping, Zhang. An improved 2-dimensional pilot-symbols assisted channel estimation in ofdm systems. In *Vehicular Technology Conference, 2003. VTC 2003-Spring. The 57th IEEE Semiannual*, volume 3, pages 1595–1599. IEEE, 2003.

[23] Lee, Sang-Mun, Lee, Doo-Hee, and Choi, Hyung-Jin. Performance comparison of space-time codes and channel estimation in ofdm systems with transmit diversity for wireless lans. In *Communications, 2003. APCC 2003. The 9th Asia-Pacific Conference on*, volume 1, pages 406–410. IEEE, 2003.

[24] Li, Ye, Winters, Jack H, and Sollenberger, Nelson R. Mimo-ofdm for wireless communications: signal detection with enhanced channel estimation. *Communications, IEEE Transactions on*, 50(9):1471–1477, 2002.

[25] North, D Oo. An analysis of the factors which determine signal/noise discrimination in pulsed-carrier systems. *Proceedings of the IEEE*, 51(7):1016–1027, 1963.

[26] Ohno, Shuichi, Manasseh, Emmanuel, and Nakamoto, Masayoshi. Preamble and pilot symbol design for channel estimation in ofdm systems with null subcarriers. *EURASIP Journal on Wireless Communications and Networking*, 2011(1):1–17, 2011.

[27] Olsson, Mattias. Implementation of an ieee802. 11a synchronizer. In *Swedish System-on-Chip Conf., 2003*, 2003.

[28] Oppenheim, Alan V, Schafer, Ronald W, Buck, John R, et al. *Discrete-time signal processing*, volume 2. Prentice-hall Englewood Cliffs, 1989.

[29] Ozdemir, Mehmet Kemal, Arslan, Hüseyin, and Arvas, Ercüment. Mimo–ofdm channel estimation for correlated fading channels. In *Proc. IEEE Wireless and Microwave Technol. Conf*, volume 1, pages 1–5, 2004.

[30] Pathak, Srishtansh and Sharma, Himanshu. Channel estimation in ofdm systems. In *International Journal of Advanced Research in Computer Science and Software Engineering*, volume 3, pages 312–327. IJARCSSE, 2013.

[31] R.Steele. *Mobile Radio Communications*. Pentech Press Limited, London, 1992.

[32] Sari, Hikmet, Karam, Georges, and Jeanclaud, I. Frequency-domain equalization of mobile radio and terrestrial broadcast channels. In *Global Telecommunications Conference, 1994. GLOBECOM'94. Communications: The Global Bridge., IEEE*, pages 1–5. IEEE, 1994.

[33] Seki, Tsutomu, Itami, Makoto, Ohta, Hiroki, and Itoh, Kohji. Application of frequency diversity to an ofdm system. *Electronics and Communications in Japan (Part I: Communications)*, 85(2):17–29, 2002.

[34] Tse, David and Viswanath, Pramod. *Fundamentals of wireless communication*. Cambridge university press, 2005.

[35] Beek, Jan-Jaap Van de, Sandell, Magnus, Borjesson, Per Ola, et al. Ml estimation of time and frequency offset in ofdm systems. *IEEE Transactions on signal processing*, 45(7):1800–1805, 1997.

[36] Yan Sun Xiaowen Wang Liu, KJR. a joint channel estimation and unequal error protection scheme for video transmission in ofdm systems. *Image*, 2002.